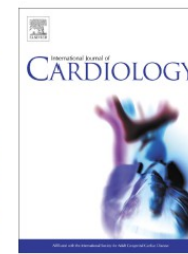


# **CARDIOMIOPATIA ARITMOGENE: WHAT'S NEW?**

**ECG e displasia aritmogena  
left-dominant**

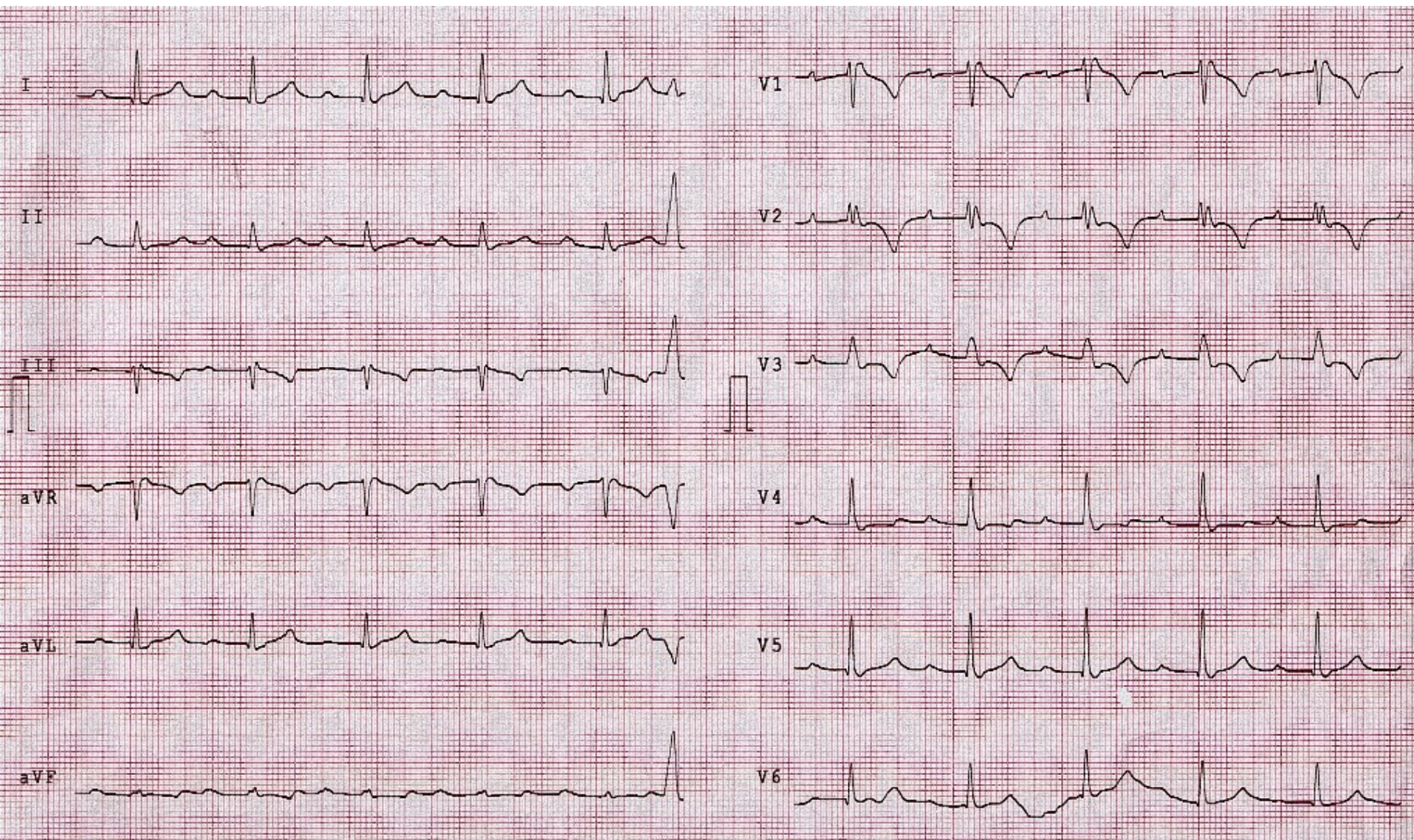
**L. Calò, Roma**

Domenico Corrado, Martina Perazzolo Marra, Alessandro Zorzi, Giorgia Beffagna, Alberto Cipriani, Manuel De Lazzari, Federico Migliore, Kalliopi Pilichou, Alessandra Rampazzo, Ilaria Rigato, Stefania Rizzo, Gaetano Thiene, Aris Anastasakis, Angeliki Asimaki, Chiara Bucciarelli-Ducci, Kristine H. Haugaa, Francis E. Marchlinski, Andrea Mazzanti, William J. McKenna, Antonis Pantazis, Antonio Pelliccia, Christian Schmied, Sanjay Sharma, Thomas Wichter, Barbara Bauce, Cristina Basso



Category	Right ventricle (upgraded 2010 ITF diagnostic criteria)	Left ventricle (new diagnostic criteria)
<b>III. Repolarization abnormalities</b>	<p><b>Major</b></p> <ul style="list-style-type: none"> <li>Inverted T waves in right precordial leads (V<sub>1</sub>, V<sub>2</sub>, and V<sub>3</sub>) or beyond in individuals with complete pubertal development (in the absence of complete RBBB)</li> </ul>	<p><b>Minor</b></p> <ul style="list-style-type: none"> <li>Inverted T waves in left precordial leads (V<sub>4</sub>-V<sub>6</sub>) (in the absence of complete LBBB)</li> </ul>
	<p><b>Minor</b></p> <ul style="list-style-type: none"> <li>Inverted T waves in leads V1 and V2 in individuals with completed pubertal development (in the absence of complete RBBB)</li> <li>Inverted T waves in V1, V2, V3 and V4 in individuals with completed pubertal development in the presence of complete RBBB.</li> </ul>	
<b>IV. Depolarization abnormalities</b>	<p><b>Minor</b></p> <ul style="list-style-type: none"> <li>Epsilon wave (reproducible low-amplitude signals between end of QRS complex to onset of the T wave) in the right precordial leads (V1 to V3)</li> <li>Terminal activation duration of QRS <math>\geq 55</math> ms measured from the nadir of the S wave to the end of the QRS, including R', in V1, V2, or V3 (in the absence of complete RBBB)</li> </ul>	<p><b>Minor</b></p> <ul style="list-style-type: none"> <li>Low QRS voltages (&lt;0.5 mV peak to peak) in limb leads (in the absence of obesity, emphysema, or pericardial effusion)</li> </ul>







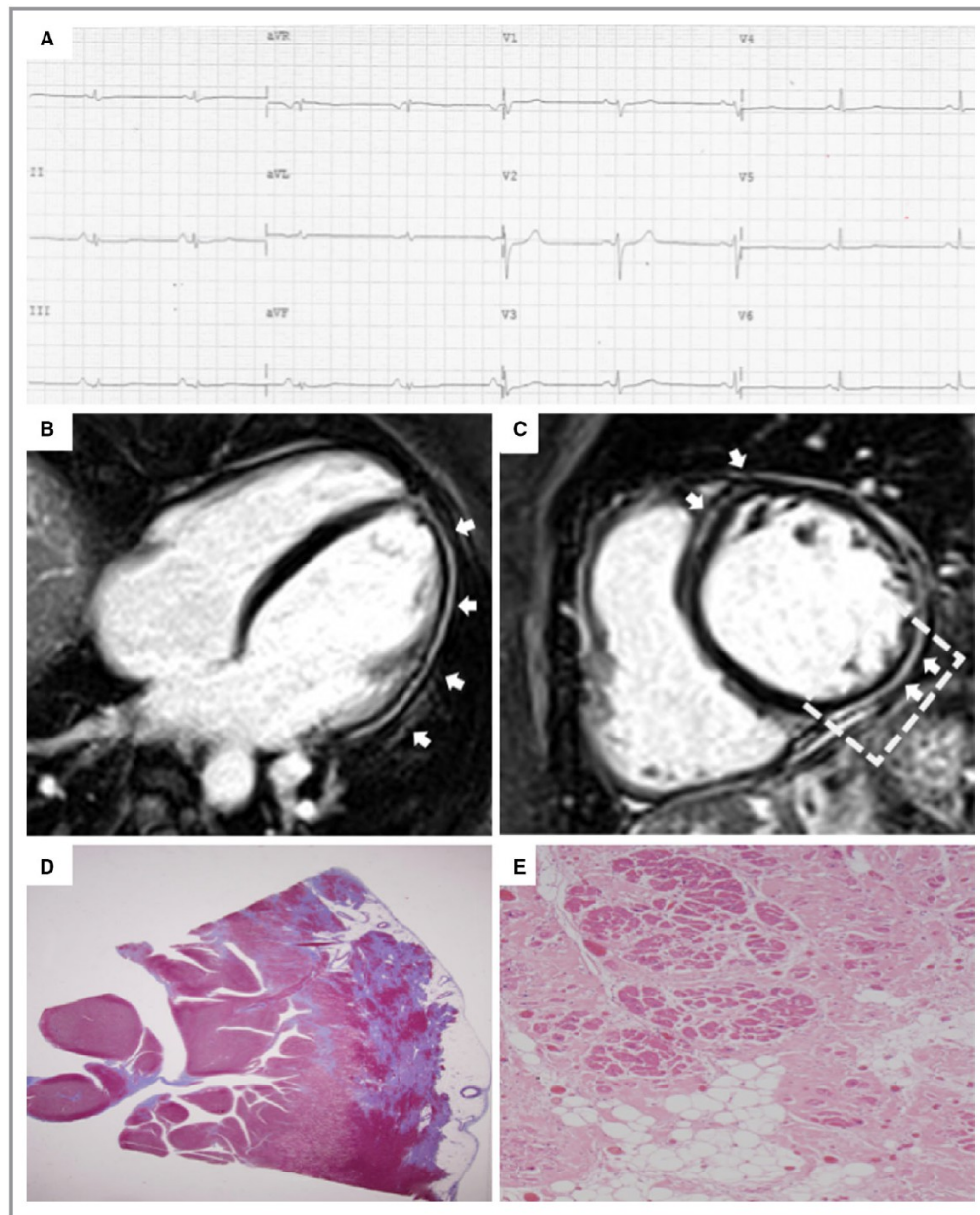
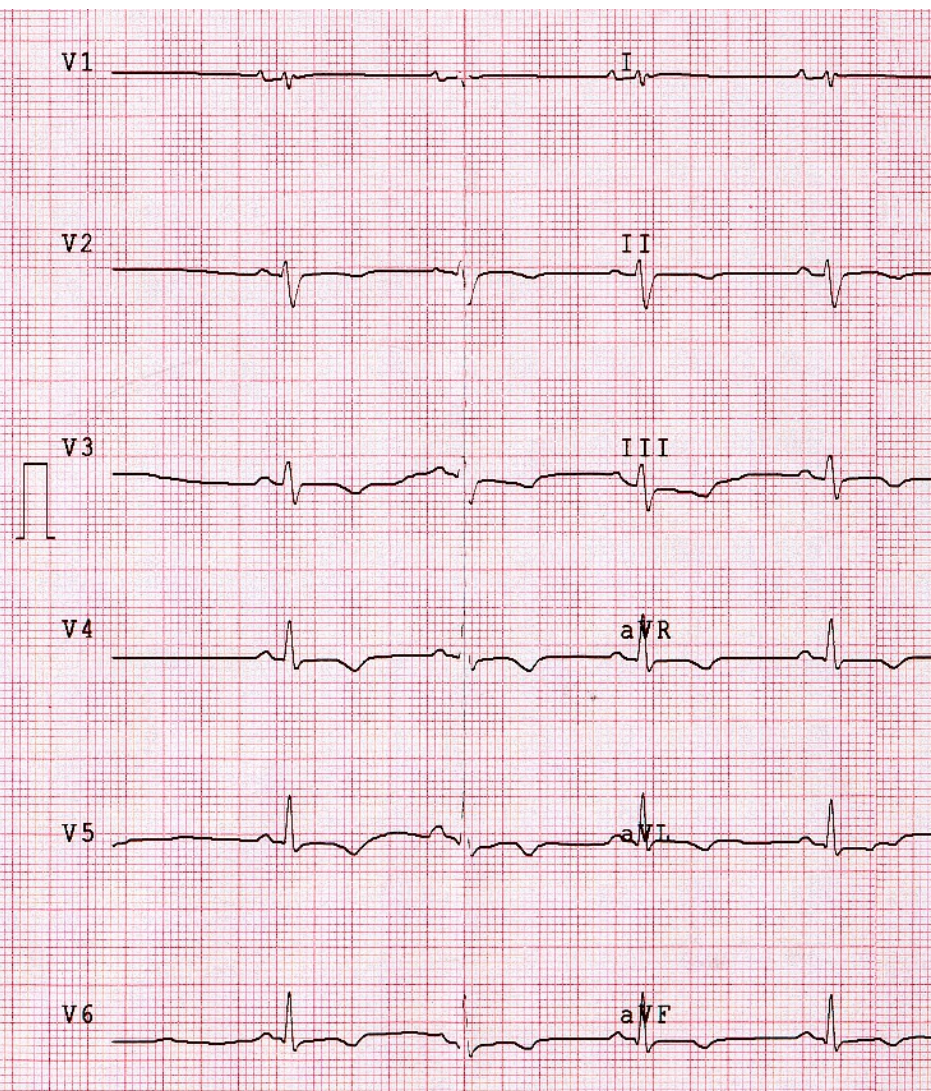
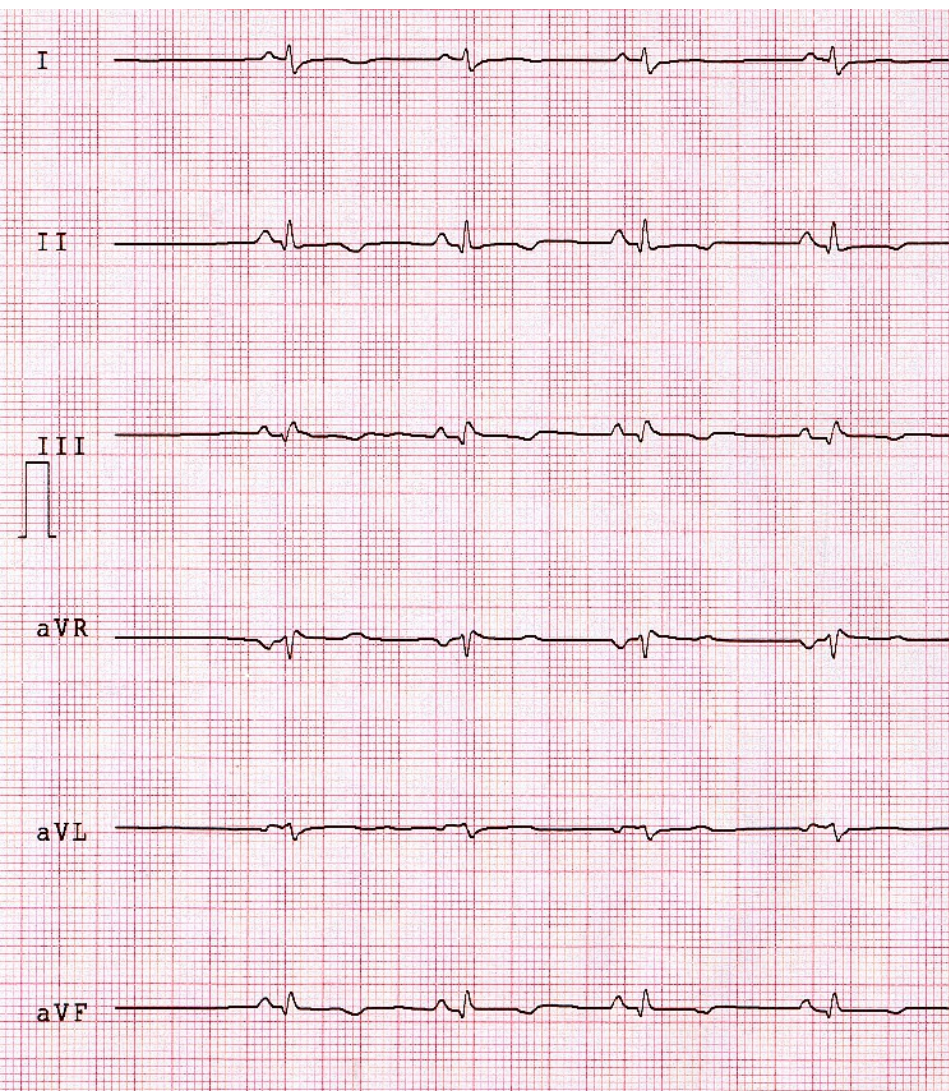


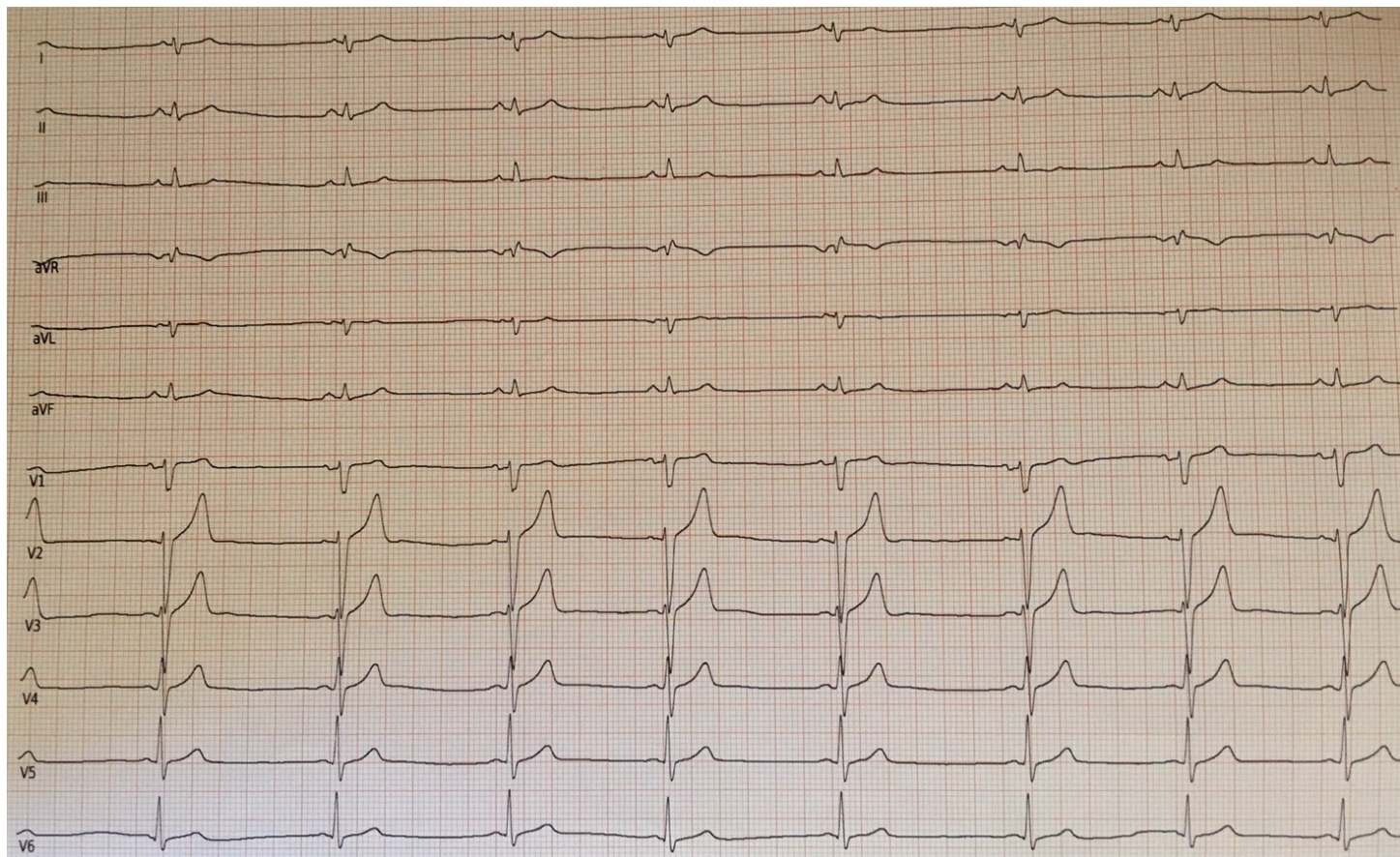
**Figure 5.** Electrocardiographic, CMR imaging, and histological features of a representative patient with ARVC undergoing cardiac transplantation. Basal ECG showing low voltages in limb leads and flattened T-waves in the inferolateral leads (A). Post-contrast CMR images in long-axis (B) and short-axis (C) views





# **OUR EXPERIENCE**



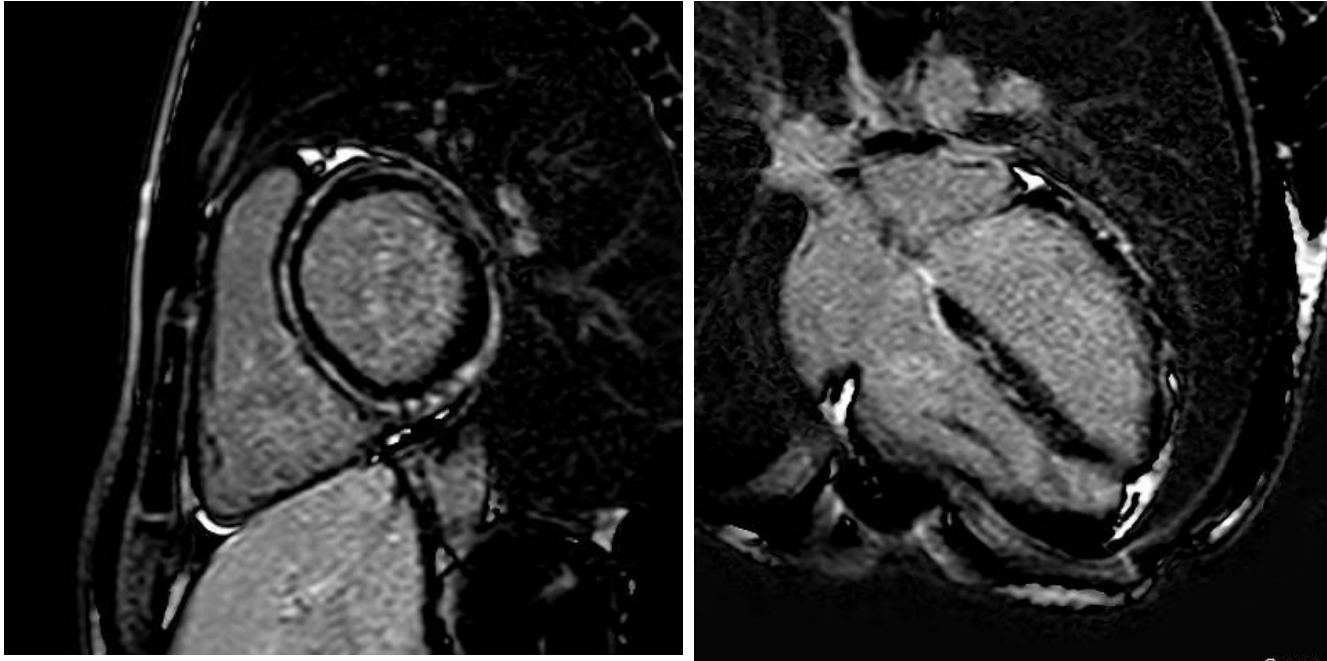


# ECG Holter monitoring

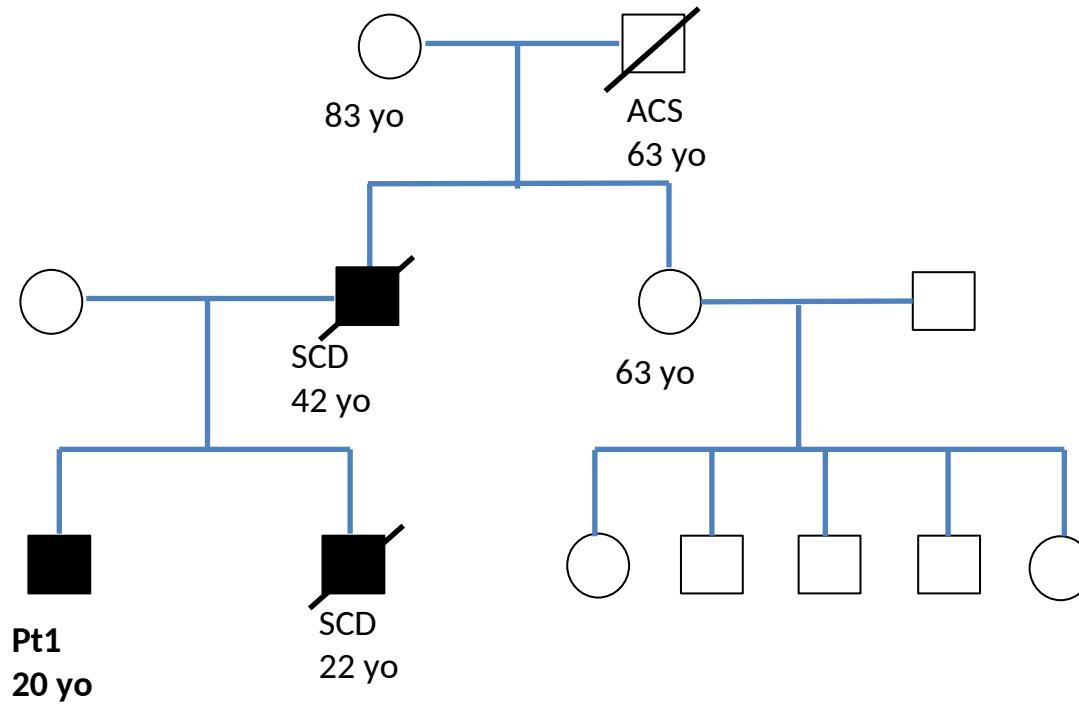




# Cardiac Magnetic Resonance

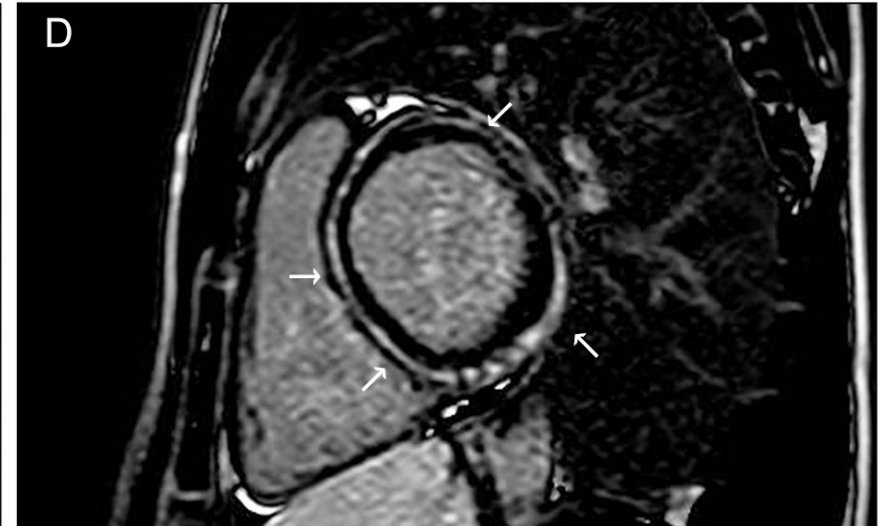
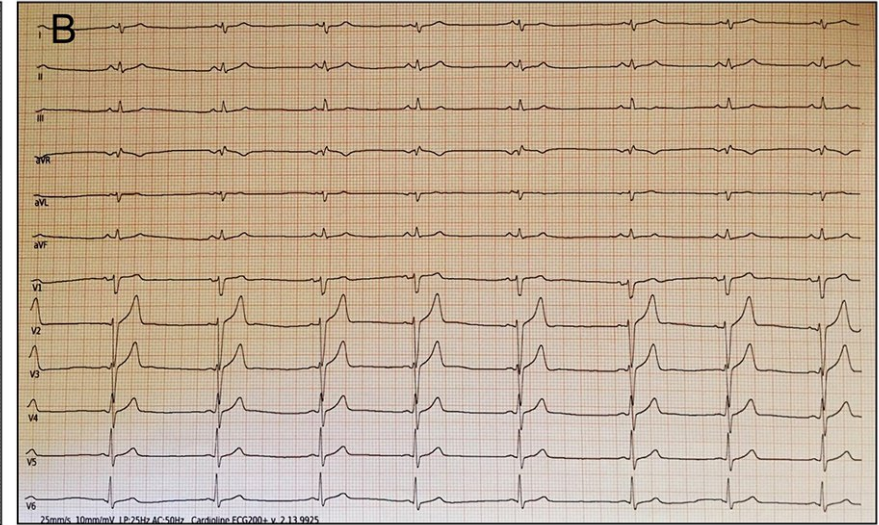
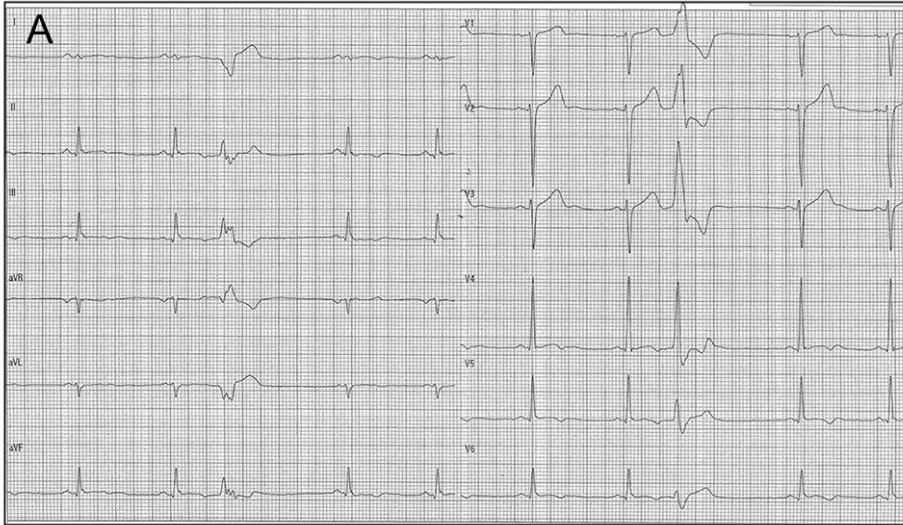


# Family history





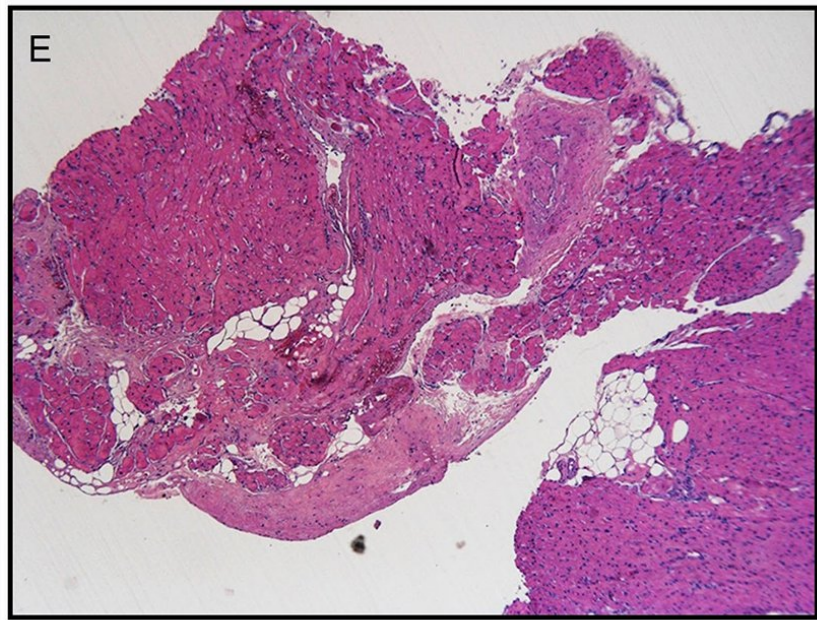
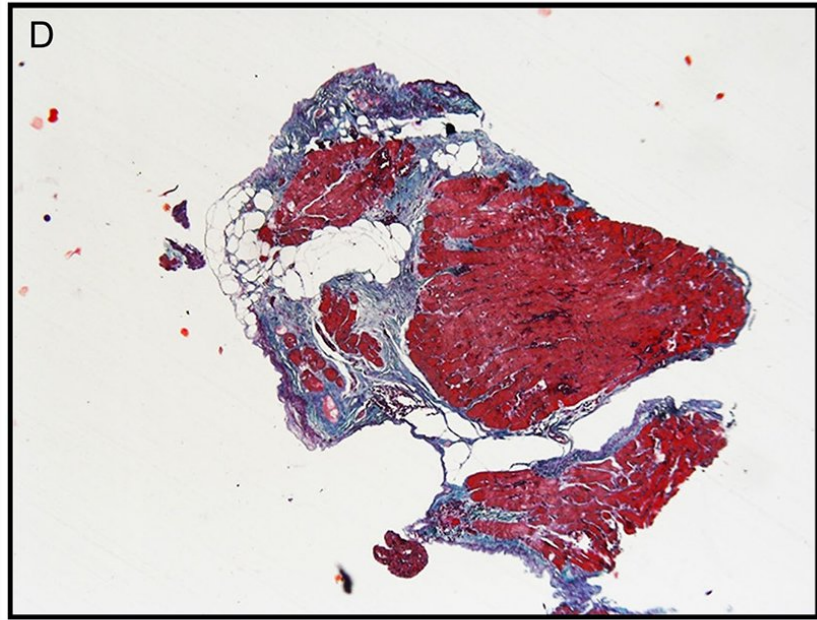
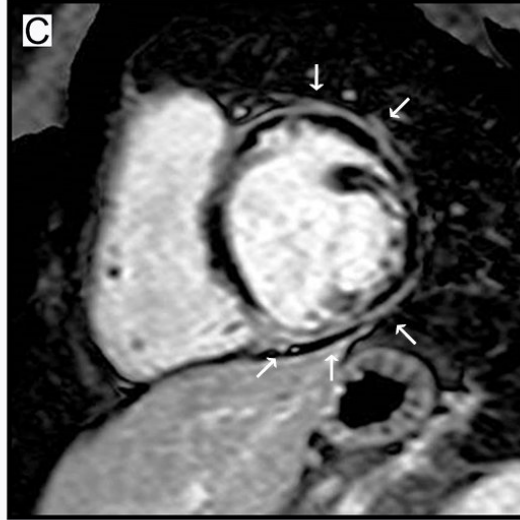
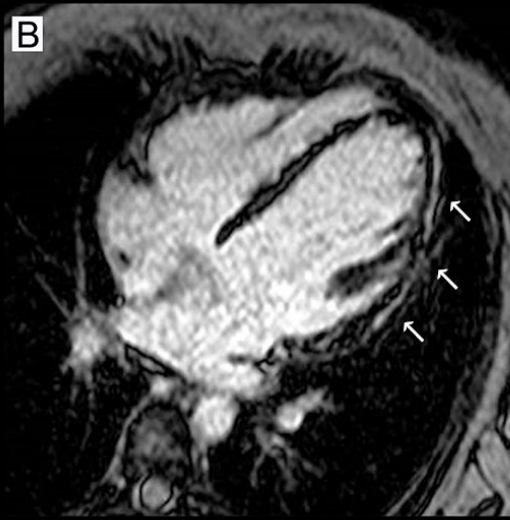
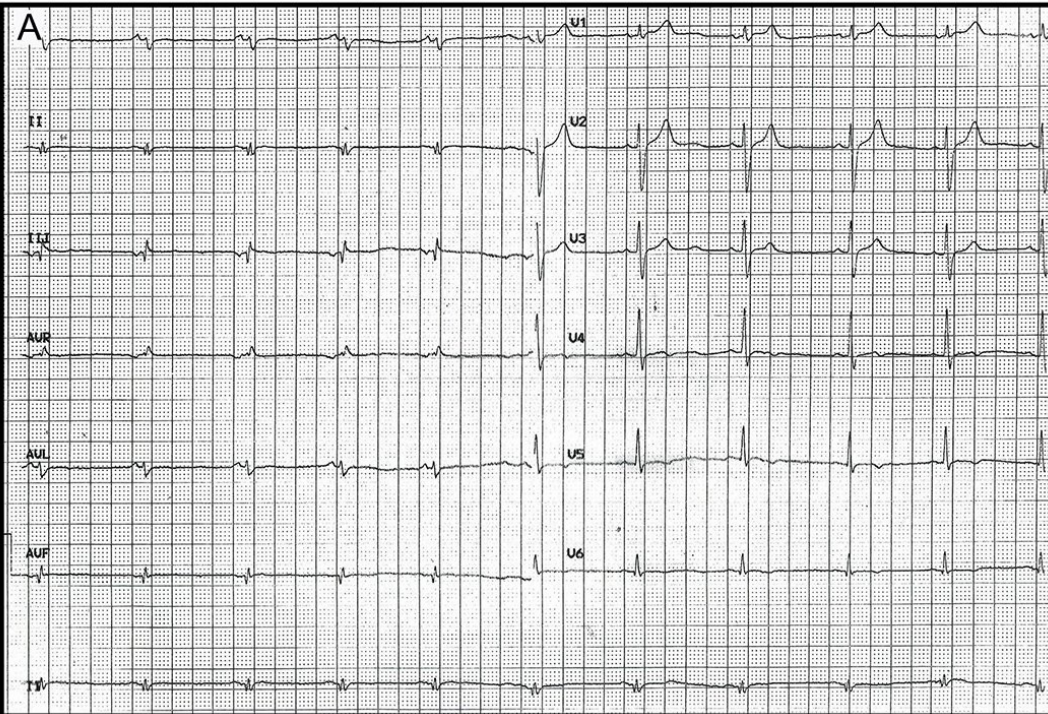
# Two brothers in comparison



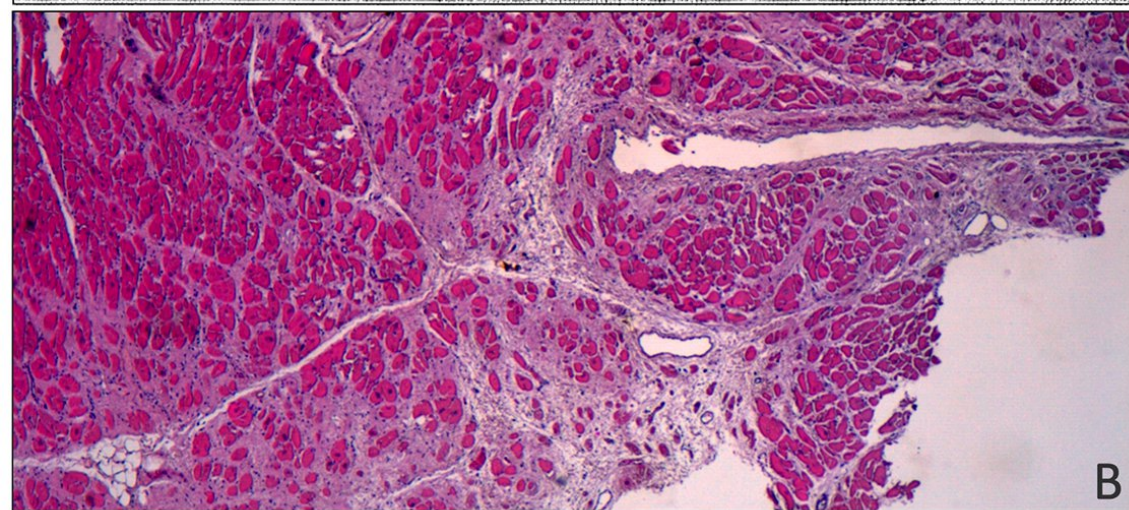
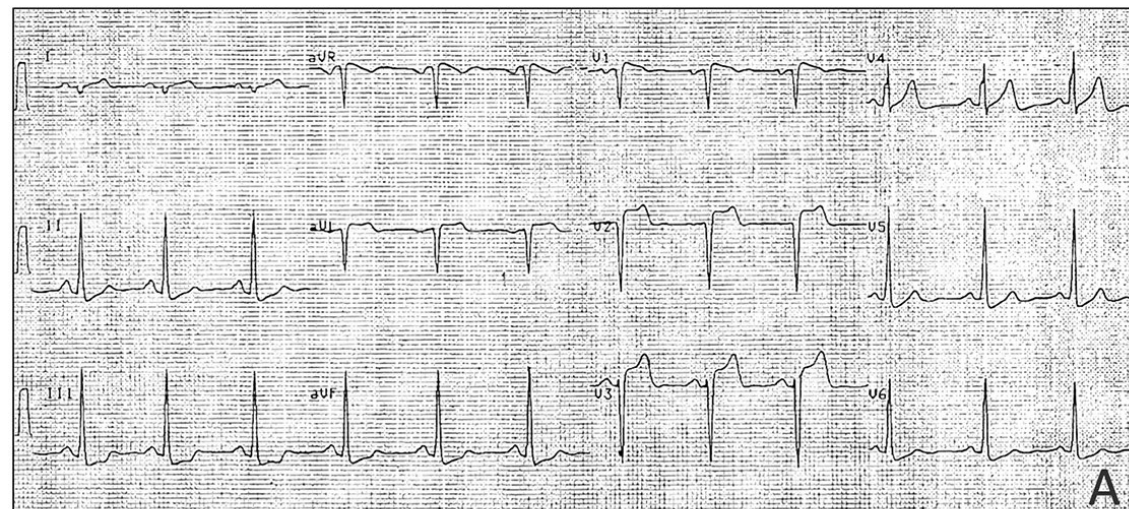
- Pt 9 CMR reveals **subepicardial/intramycardial circumferential LGE**.
- The autopsy of his brother shows the same **LV circumferential scar**, mostly located in the subepicardium, with gross features of fibroadipose myocardial replacement.



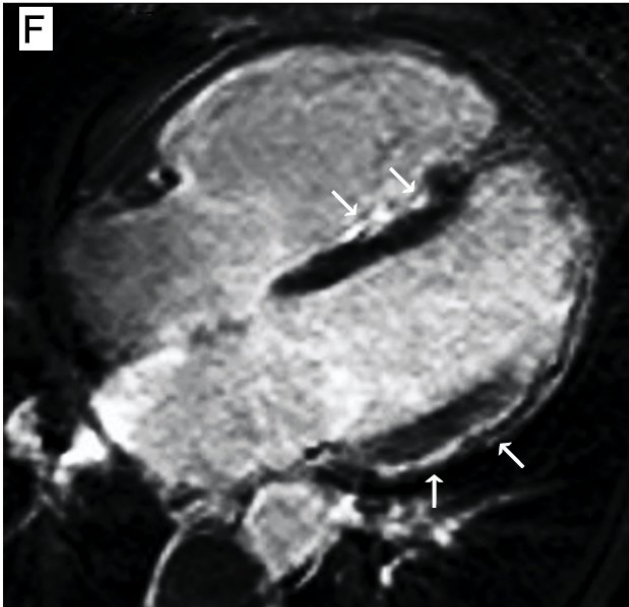
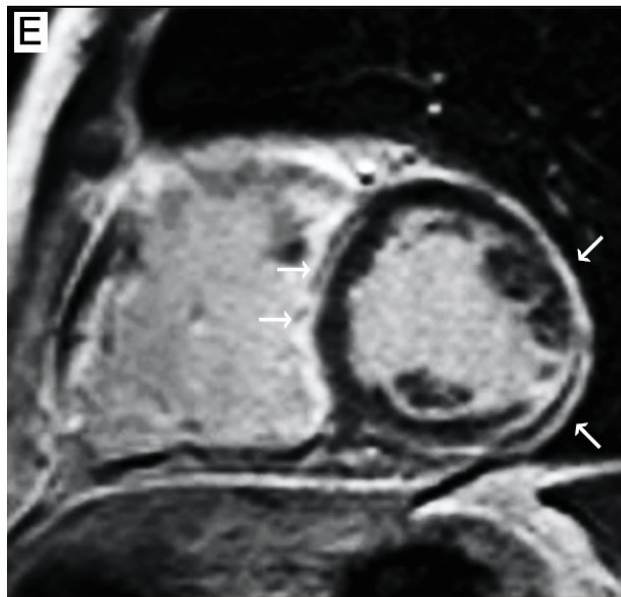
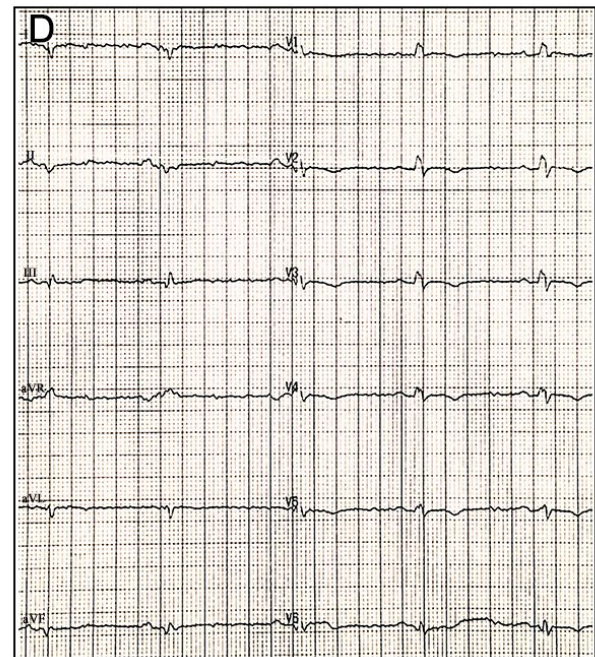
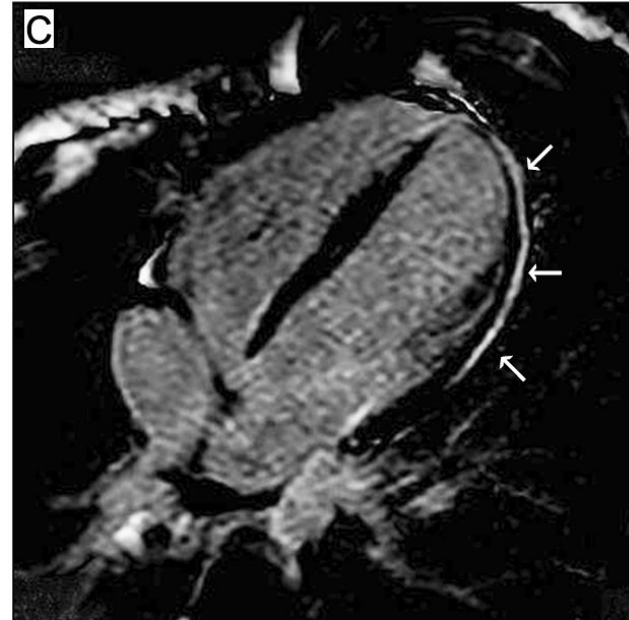
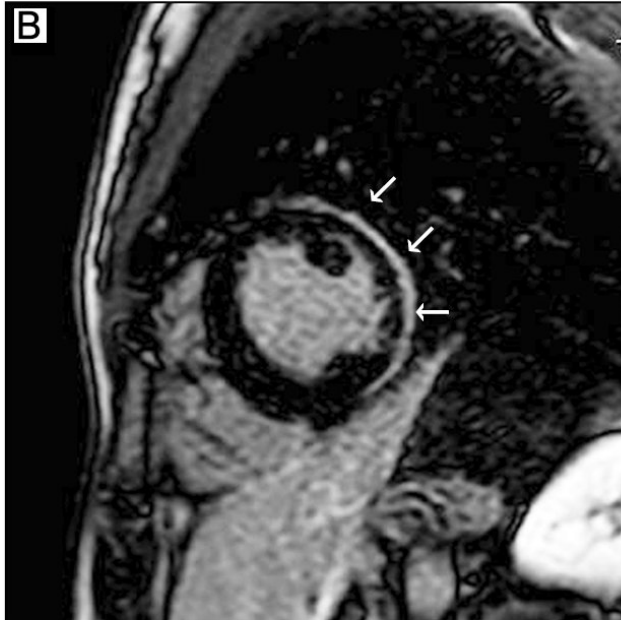
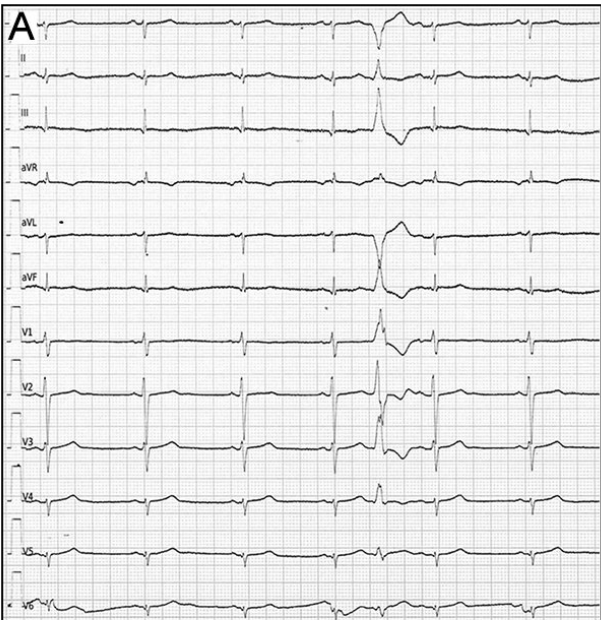




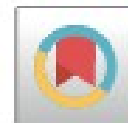








# Left Posterior Fascicular Block and Increased Risk of Sudden Cardiac Death in Young People



We retrospectively compared the clinical data for 109 consecutive individuals age  $\leq 40$  years who had ACA or SCD (86 men;  $32.3 \pm 5.9$  years [range: 17 to 40 years]) and who had at least 1 ECG in the 3 years preceding the ACA or SCD to data for 8,892 healthy individuals age  $\leq 40$  years (6,265 men;  $30.5 \pm 8.6$  years [range: 17 to 40 years]) consecutively referred to our institution for screening. LPFB was defined by the presence of all of the following: frontal axis  $100^\circ$  to  $180^\circ$ ; rS pattern in leads I and aVL; qR pattern in III and aVF; QRS duration  $< 110$  ms; and no QS pattern in I and aVL. The association of LPFB with ACA/SCD was analyzed by nominal logistic regression and was estimated with unadjusted odds ratios (ORs) and 95% confidence intervals (CIs). The study (CARITMO) was approved by our Institutional Review Board.

\*Leonardo Calò, MD

Roberta Della Bona, MD, PhD

Annamaria Martino, MD, PhD

Cinzia Crescenzi, MD

Germana Panattoni, MD, PhD

Giulia d'Amati, MD, PhD

Fiorenzo Gaita, MD

Ruggiero Mango, MD, PhD

Luigi Sciarra, MD

Mikael Laredo, MD, MSc

\*Division of Cardiology

Policlinico Casilino Rome

Via Casilina 1049

00169 Rome

Italy

E-mail: [leonardocalo.doc@gmail.com](mailto:leonardocalo.doc@gmail.com)

Twitter: [@cinzi1988](https://twitter.com/cinzi1988), [@LaredoMikael](https://twitter.com/LaredoMikael)

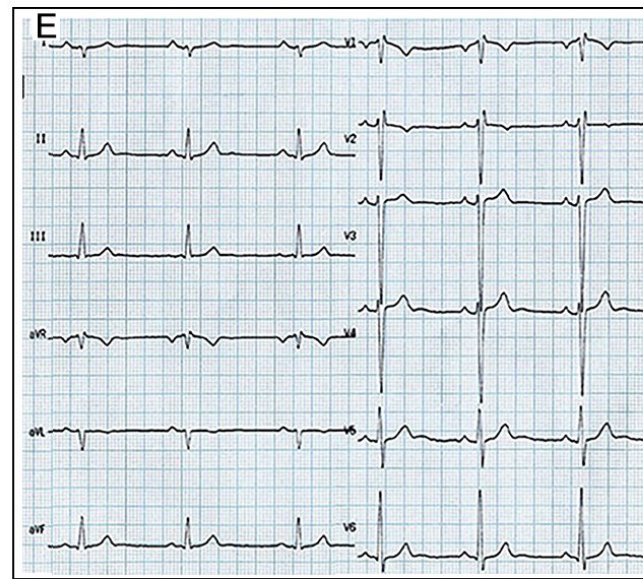
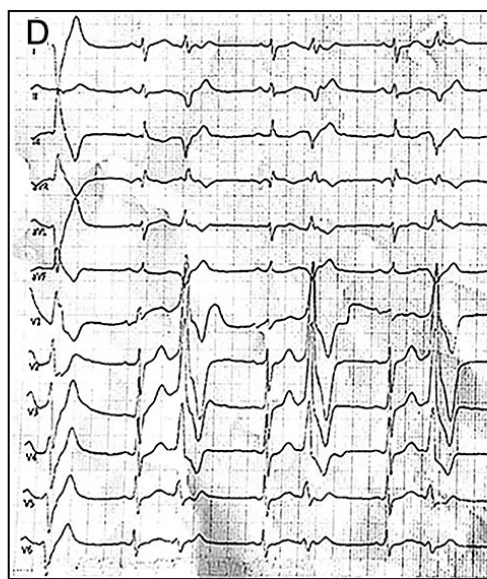
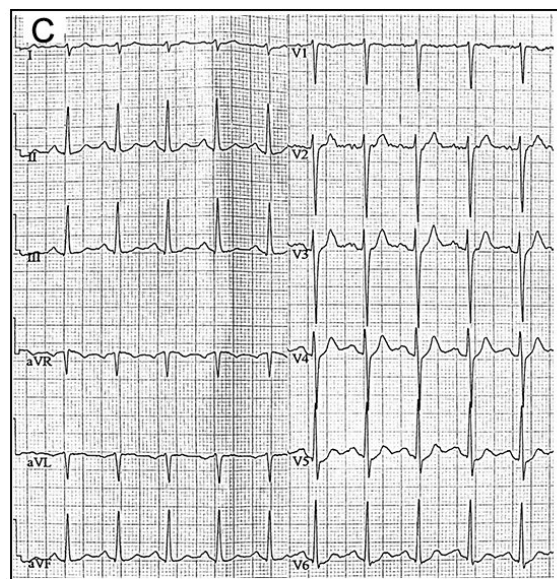
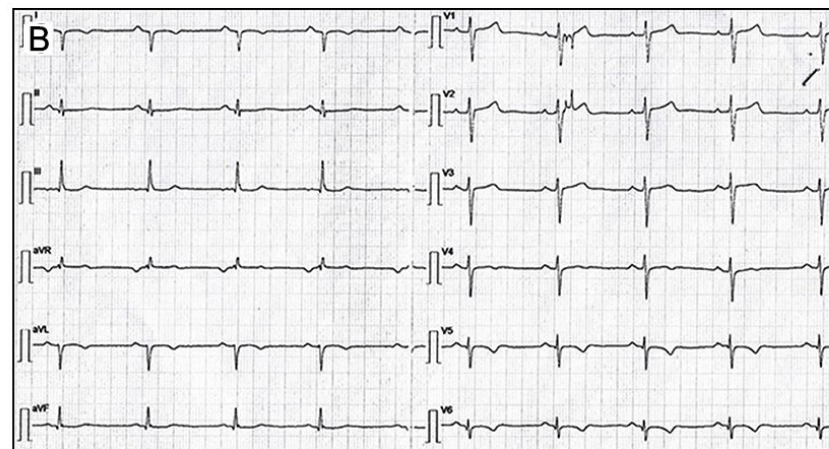
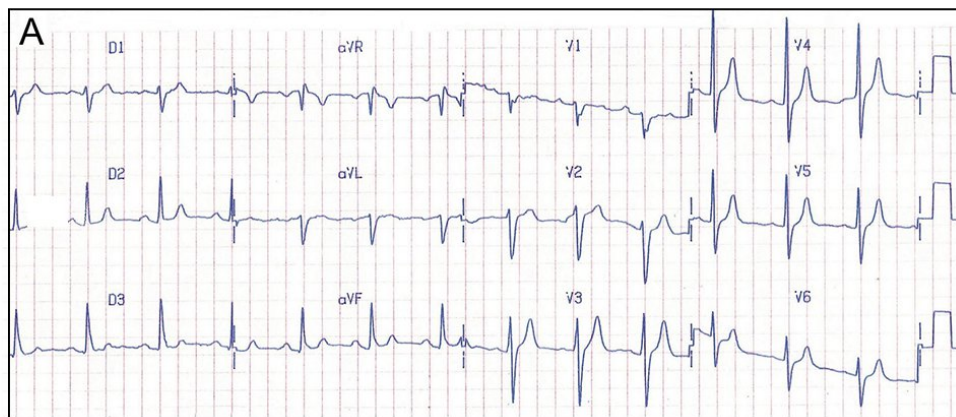
<https://doi.org/10.1016/j.jacc.2020.12.033>

© 2021 by the American College of Cardiology Foundation. Published by Elsevier.

JACC VOL. 77, NO. 8, 2021

MARCH 2, 2021:1141-8







# LPFB as a Sign for Cardiomyopathy and Increased Risk of SCD in Young People

**109** young consecutive patients with **ACA/SCD**

**Pre-ACA/SCD ECG analysis**

**LPFB in 10 (9%) patients**

**CMR in 6 patients**

**Abnormal CMR in 6 (100%)**

- **LV LGE in 6 (100%)**
  - Inferolateral LGE in 3
  - Inferior LGE in 1
  - Inferoseptal in 1
  - Diffuse in 1
- **LV systolic dysfunction in 4 (80%)**

**Autopsy in 3 patients; EMB in 1 patients**

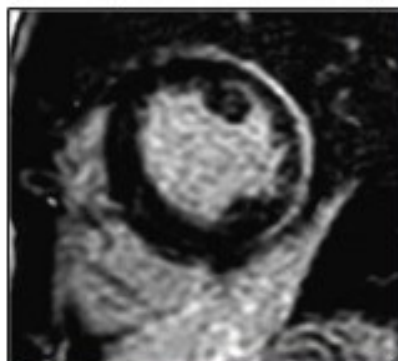
- **Abnormal histopathological findings in 4 (100%)**
  - **LV fibrosis in 4 (100%)**

**Genetic analysis in 5 patients**

- **Pathogenic variants in 2 (40%): DSG2, TTN**
  - **VUS in 1 (20%): TTN**



LPFB Odds Ratio for SCD/ACA  
**112.2** (95% CI 43.3-290.2)



**8892** young **healthy** individuals

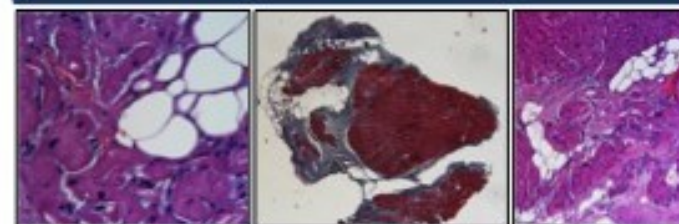
**ECG analysis**

**LPFB in 8 (0.09%) patients**

**CMR in 6 healthy subjects**

**Abnormal CMR in 4 (67%)**

- **LV LGE in 2 (33%)**
- **LV systolic dysfunction in 1 (17%)**
- **LV hypertrophy in 1 (17%)**



**Genetic analysis in 3 subjects**

- **Pathogenic variant in 1 (33%): DSP**





**54 subjects with typical LV subepicardial LGE distribution**

**5 with fibro-fatty infiltration at histological analysis (biopsy)  
and 1 autopsy with negative or presence of VUS**

**48 with positive genetic testing for pathogenic/likely  
pathogenic variants associated with ARVC with LV involvement  
affected by left dominant AC**

- 35 (72.9%) gene DSP; 7 (14.6 %) gene DSG; 3 gene PKP, 3  
JUP**



	<b>ALVC (n=54)</b>
Age at diagnosis, years	39±15
Male, n (%)	32 (59.3)
Probands, n (%)	40 (74.1)
Family history of ACM/DCM, n (%)	23 (42.6)
Family history of SCD, n (%)	18 (33.3)
NYHA class I-II, n (%)	52 (96.3)
NYHA class III, n (%)	2 (3.7)
Atrial fibrillation, n (%)	4 (7.4)
Unexplained syncope, n (%)	8 (14.8)
NSVT, n (%)	26 (48.1)
<b><i>Cardiac magnetic resonance</i></b>	
LVEDVi (ml/m2)	97.6±24.5
LVEF, %	49.5±10.0
LV WMA, %	35 (64.8)
RVEDVi (ml/m2)	85.8±18.8
RVEF, %	54.3±9.3
RV WMA, %	13 (24.1)
Intramyocardial fat signal, n (%)	22 (40.7)
Segments with LGE	6±3; 6 (4-8)
<b><i>LGE pattern</i></b>	
- Ringlike, n (%)	28 (51.9)
<b><i>LGE distribution</i></b>	
- Subepicardial, n (%)	35 (64.8)
- Midmural, n (%)	10 (18.5)
- Transmural, n (%)	9 (16.7)
<b><i>Genetic testing</i></b>	
Pathogenic/likely pathogenic variant, n (%)	48/54 (88.9)
DSP, n (%)	35/48 (72.9)
Non-DSP, n (%) *	13/48 (27.1)

	Pedigree	Gene	ACMG Variant Criteria	Deoxyribonucleic acid change	Amino acid change
1	Proband	PKP2	LP	c.1216delG	p.Val406fs
2	Proband	DSP	P	c.1707-1708insAC	p.Met571Glnfs*8
3	Proband	DSP	LP	c.7180delA	p.Arg2394fs*ter
4	Proband	DSG2	LP	c.1912G>A	p.Gly638Arg
5	Proband	DSG2	LP	c.445G>T	p.Val149Phe
6	Proband	DSC2	LP	c.977A>C	p.Gln326Pro
7	Proband	DSP	LP	c.3932_3936del	p.Gln1311Profs*13
8	Family member	DSP	P	c.5851 C>T	p.Arg1951Ter
9	Family member	DSP	P	c.5851 C>T	p.Arg1951Ter
10	Proband	DSG2	LP	c.1003A>G	p.Thr335Ala
11	Family member	DSP	LP	c.2848delA	p.Ile950Leu
12	Proband	DSP	P	c.2497 C>T	p.Gln833ter
13	Family member	DSP	LP	c.1351C>T	p.Arg451Cys
14	Proband	DSP	LP	c.2584C>T	p.Gln862Ter
15	Family member	DSP	LP	c.1351C>T	p.Arg451Cys
16	Family member	PKP2	P	c.2447_2448del	p.Thr816Argfs*10
17	Proband	DSP	LP	c.1352G>C	p.Arg451Pro
18	Proband	DSP	P	c.3203_3204delAG	p.Glu1068ValfsTer19
19	Proband	DSP	P	c.5210delG	p.Gly1737AspfsTer16
20	Proband	DSP	P	c.5210delG	p.Gly1737AspfsTer16
21	Family member	DSP	P	c.3465G>A	p.Trp1155Ter
22	Proband	JUP	P	c.2069A>G	p.Arg690Ser

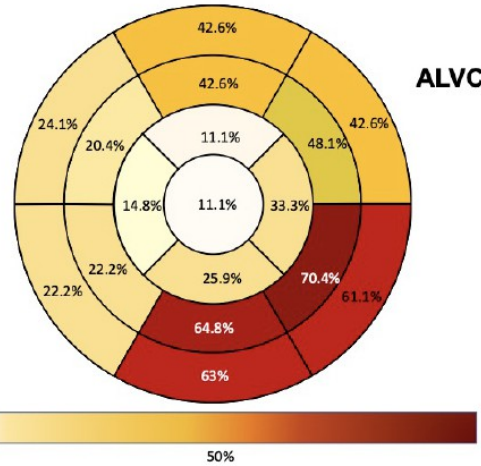
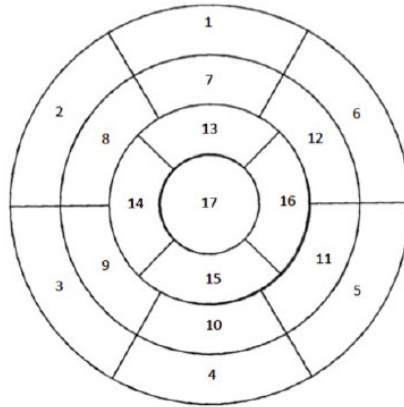
23	Proband	JUP	P	c.2069A>G	p.Arg690Ser
24	Proband	DSP	LP	c.6478C>T	p.R2160X
25	Proband	DSP	LP	c.G3793T	p.Glu1265X
26	Proband	DSP	LP	c.356dupA	p.I120Nfs*16
27	Proband	DSP	LP	c.1891C>T	p.(Gln631*)
28	Family member	DSP	LP	c.3793G>T	p.E1265X
29	Proband	DSP	LP	c.7248dupT	p.D2417X
30	Family member	DSP	LP	c.3337C>T	p.R1113X
31	Proband	DSP	LP	c.3465G>A	p.Trp1155*
32	Proband	DSP	P		6p25.1-p24.3
33	Proband	DSC2	LP	c.2078G>T	p.Gly693Val
34	Proband	DSP	LP	c.537_554del	p.Arg2334*
35	Proband	DSG2	P	c.1912G>A	p.Gly638Arg
36	Family member	DSG2	P	c.1912G>A	p.Gly638Arg
37	Proband	DSP	LP	c.448C>T	p.Arg150*
38	Proband	DSP	P	c.6852C>T	p.Arg2284*
39	Proband	DSP	LP	c.860A>G	p.Asn287Ser
40	Proband	DSP	VUS	c.212T>G	p.Ile71Ser
41	Proband	DSC2	VUS	c.907G>A	p.Val303Met
42	Proband	DSP/DSG2	LP	DSP: c.212T>G ; DSG2: c.561T>G	DSP: p.Ile71Ser; DSG2 p.Asp187Glu
43	Proband	JUP	LP	c.1359G>T	p.Glu453Asp
44	Proband	DSP	LP	c.2000delG	p.Trp667fs*0
45	Family member	DSP	LP	c.860A>G	p.Asn287Ser
46	Family member	DSP	LP	c.860A>G	p.Asn287Ser
47	Family member	DSP	P	c.1267-2A>G	
48	Proband	DSP	LP	c.448C>T	p.Arg150
49	Family member	DSG2	P	c.271G>T	p.Gly91Ter
50	Proband	DSP	P	c.4198C>T	p.Arg1400*



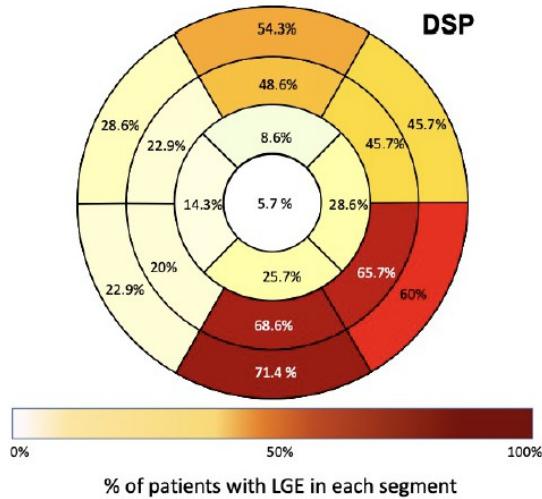
# Distribution of late gadolinium enhancement

AHA 17-segment model

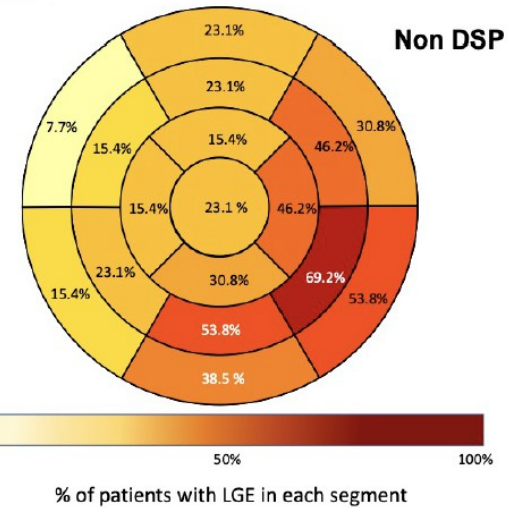
1. Basal anterior
2. Basal anteroseptal
3. Basal inferoseptal
4. Basal inferior
5. Basal inferolateral
6. Basal anterolateral
7. Mid anterior
8. Mid anteroseptal
9. Mid inferoseptal
10. Mid inferior
11. Mid inferolateral
12. Mid anterolateral
13. Apical anterior
14. Apical septal
15. Apical inferior
16. Apical lateral
17. Apex



% of patients with LGE in each segment



% of patients with LGE in each segment



% of patients with LGE in each segment





## VOLTAGES IN LIMB LEADS

	Controls (n=84)	ALVC (n=54)	P Value
Lead I QRS	7 (5-8.5)	4.5 (3-6)	<0.0001
Lead I r wave	6 (4-7)	3 (1.9-4.1)	<0.0001
Lead I s wave	0.1 (0-1.5)	1 (0-2)	0.07
Lead II QRS	10.4 (8-12.5)	6.5 (4.2-9.1)	<0.0001
Lead II r wave	9.5 (6.6-12)	4 (2-6.5)	<0.0001
Lead II s wave	1 (0-2)	1 (0-2)	0.11
Lead aVF QRS	8 (5.1-10.5)	5 (4-7.6)	0.0004
Lead aVF r wave	7 (3.3-9)	3.5 (2-6.1)	<0.0001
Lead aVF s wave	1 (0-2)	1 (0-2)	0.70
Lead III QRS	7 (5-8.5)	6 (3.5-8)	0.028
Lead III r wave	5 (2-7.4)	3 (1-5.5)	0.0055
Lead III s wave	1 (0-2.4)	0.5 (0-2.3)	0.83
Lead aVR QRS	8 (7-9.5)	5 (4-6.1)	<0.0001
Lead aVR r wave	1 (0.3-1.5)	1 (0.5-1.3)	0.35
Lead aVR s wave	0 (0-7)	0 (0-1.3)	0.0001
Lead aVL QRS	4.1 (3-6.2)	4 (2.5-5)	0.28
Lead aVL r wave	2 (1-4)	2 (0.5-3.5)	0.38
Lead aVL s wave	1 (0-2.5)	0.8 (0-2.6)	0.39

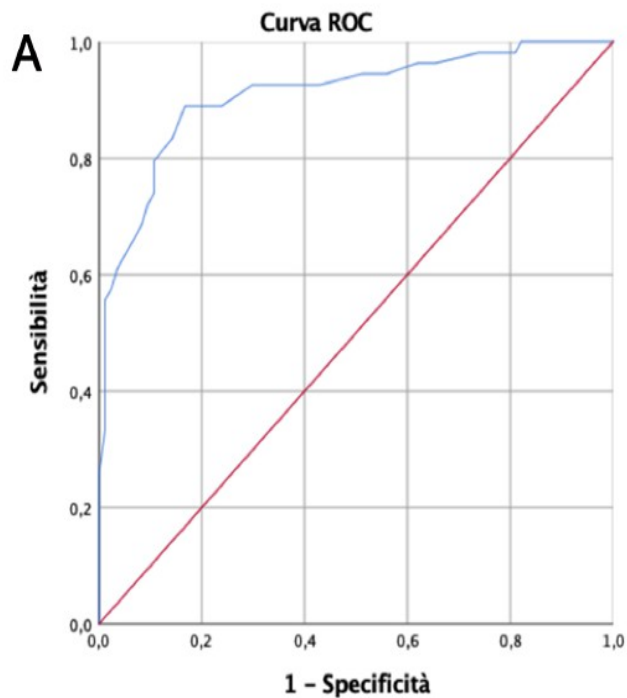
## VOLTAGES IN PRECORDIAL LEADS

	Controls (n=84)	ALVC (n=54)	P Value
Lead V1 QRS	9.3 (7-12.9)	6.8 (4.5-9)	<b>0.0007</b>
Lead V1 r wave	1.5 (1-2)	1 (1-2.6)	0.40
Lead V1 s wave	8 (6-10)	5 (3-7.1)	<b>&lt;0.0001</b>
Lead V2 QRS	13 (9-17.5)	11 (7.5-16.6)	0.24
Lead V2 r wave	2.8 (1.8-4.4)	3 (1.9-5)	0.68
Lead V2 s wave	9 (6.1-14)	8.3 (5-11.8)	0.07
Lead V3 QRS	15.3 (12-19)	11.8 (7.4-16)	<b>0.0003</b>
Lead V3 r wave	6 (4-10)	4 (2.4-6.3)	<b>0.003</b>
Lead V3 s wave	7.3 (4-11.4)	7 (4-9)	0.17
Lead V4 QRS	16 (10.6-19.8)	11.3 (9-16.6)	<b>0.0026</b>
Lead V4 r wave	11 (8-16)	8 (5.9-11.1)	<b>0.0002</b>
Lead V4 s wave	4 (1.5-5.9)	4 (2-6.3)	0.39
Lead V5 QRS	14.5 (10.6-18)	11 (8-14.3)	<b>0.0011</b>
Lead V5 r wave	12.5 (8.6-16)	8.5 (6.5-11)	<b>&lt;0.0001</b>
Lead V5 s wave	2 (0.1-3)	2 (0.9-4)	0.18
Lead V6 QRS	11.1 (9-15.5)	8.9 (6.9-11.1)	<b>0.0001</b>
Lead V6 r wave	10 (7.5-14)	7 (5-9)	<b>&lt;0.0001</b>
Lead V6 s wave	1 (0-1.9)	1 (0-2)	0.27
RI + RII	15 (13-17.5)	7 (5-10.6)	<b>&lt;0.0001</b>
SV1 + RV6	18.8 (15.5-23)	12 (9-17)	<b>&lt;0.0001</b>



**CONTROLS****ALVC**

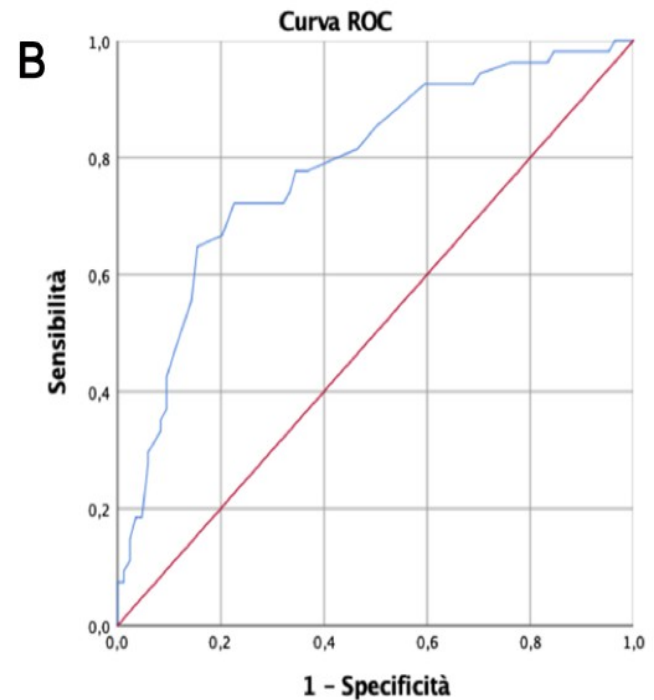
<b>RI + RII</b>	15 (13-17.5)	7 (5-10.6)	<b>&lt;0.0001</b>
<b>SV1 + RV6</b>	18.8 (15.5-23)	12 (9-17)	<b>&lt;0.0001</b>



**Sum of R-wave in I-II**

Area under curve = 0.909  
(0.856-0.962),  $p < 0.0001$ .

**Best cut-off value 8 mm**  
(sensitivity 57.4%, specificity 97.6%)

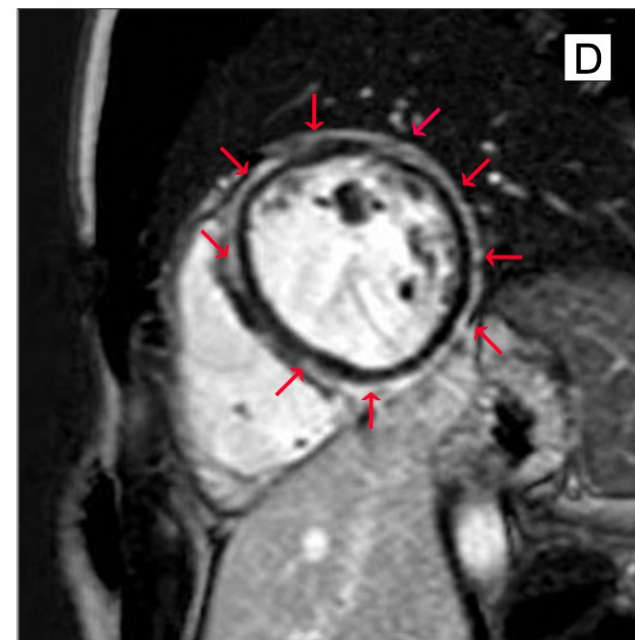
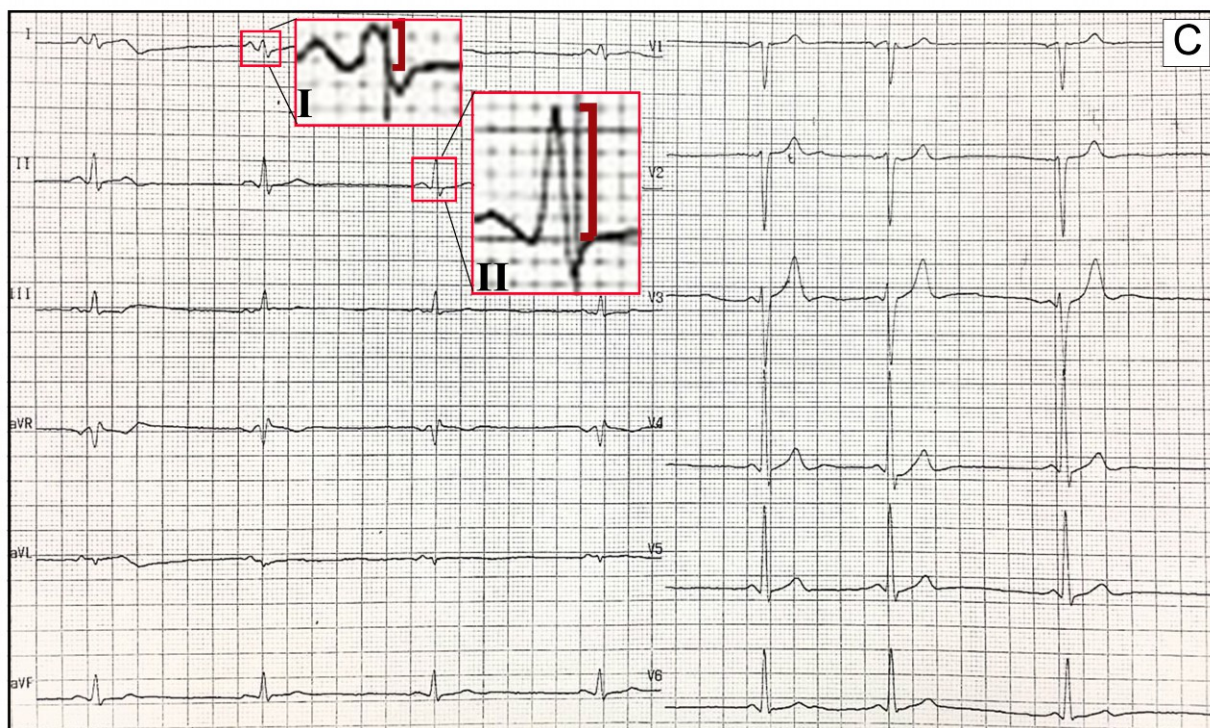


**Sum of S wave in V1 and R in V6**

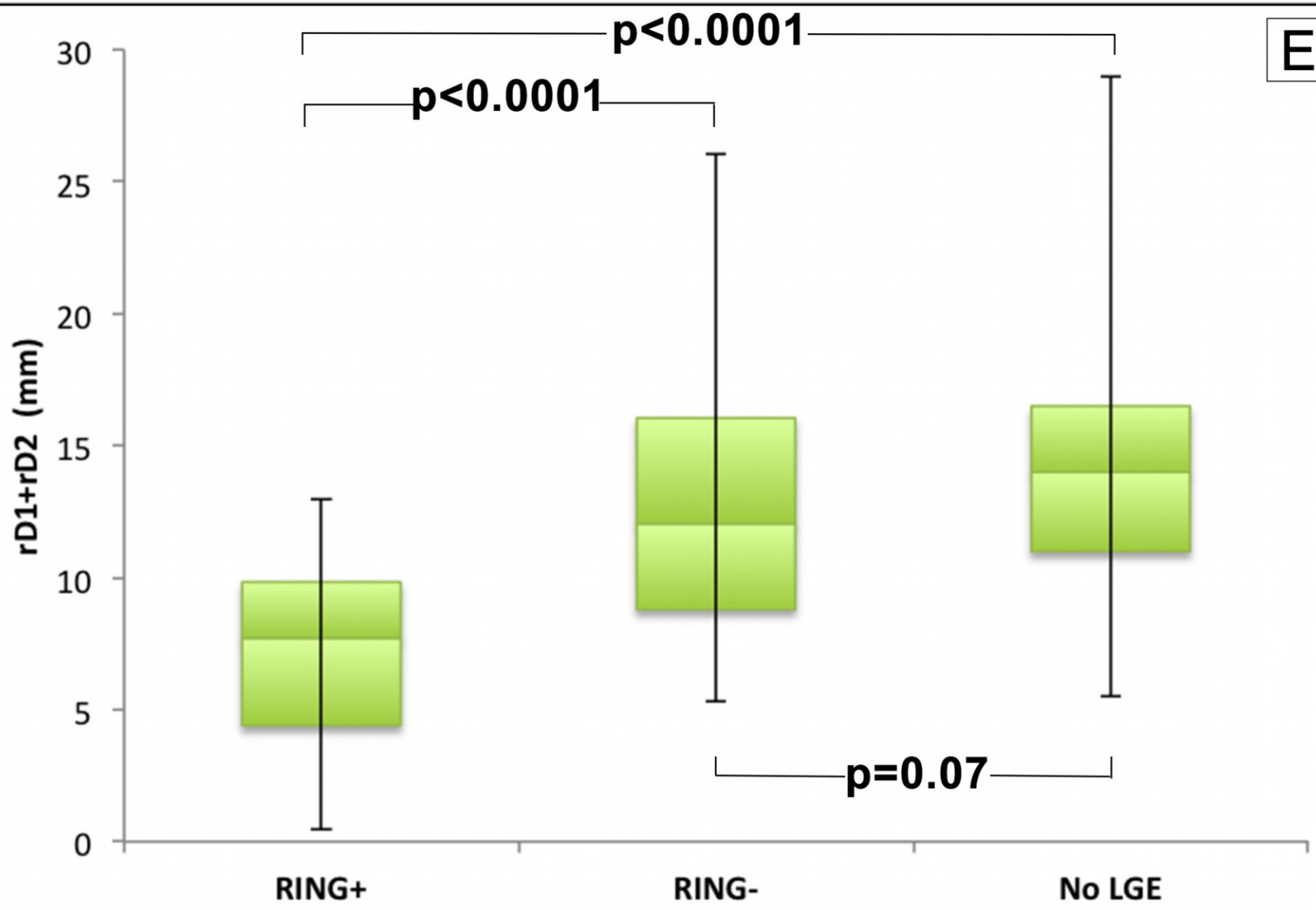
Area under curve = 0.784  
(0.704-0.863),  $p < 0.0001$ .

**Best cut-off value 12 mm**  
(sensitivity 55.5%, specificity 85.7%)

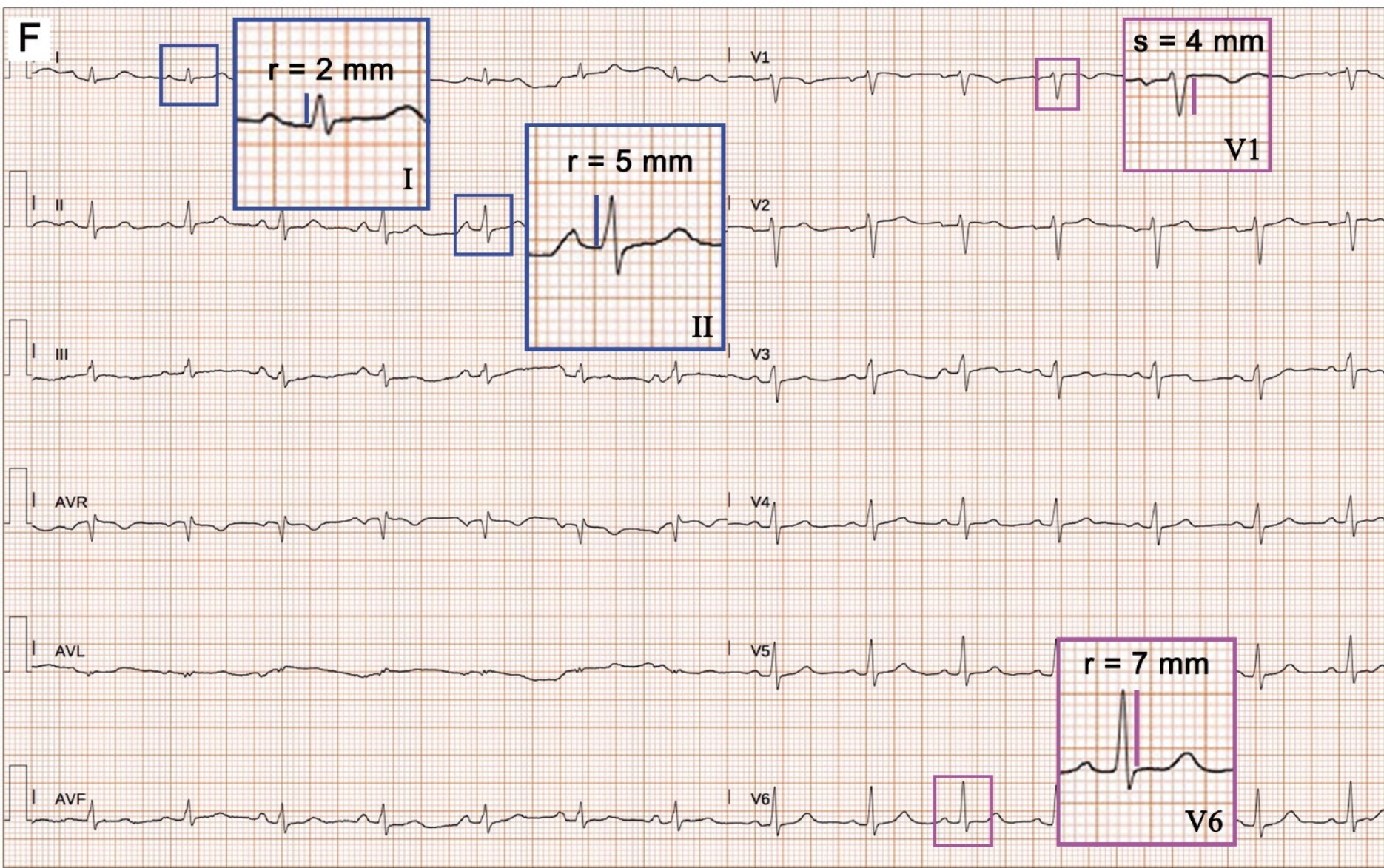




E







Patient #20, 23-year-old woman with a pathogenic variant in desmoplakin (c.5210del, p.Gly1737AspfsTer16)





# ECG characteristics of the control group and study population

	Controls (n=84)	ALVC (n=54)	P Value
QRS (msec)	91±10	95±14	0.15
First degree AV block	3 (3.6)	5 (9.3)	0.42
NSICD	0	2 (3.7)	0.30
RBBB	1 (1.2)	0	0.99
LAFB	1 (1.2)	4 (7.4)	0.15
LPFB	0	11 (20.4)	<0.0001
LBBS	0	0	0
Pathological Q waves	0	18 (33.3)	<0.0001
Lateral distribution	0	7 (13.0)	0.003
Inferior distribution	0	8 (14.8)	0.0012
Precordial distribution	0	1 (1.9)	0.82
More 2 localizations	0	2 (3.7)	0.30
Fragmented QRS	9 (10.7)	19 (35.2)	0.001
Lateral distribution	0	1 (1.9)	0.82
Inferior distribution	9 (10.7)	10 (18.5)	0.31
Precordial distribution	0	1 (1.9)	0.82
More 2 localizations	0	7 (13.0)	0.003
TWI	1 (1.2)	31 (57.4)	<0.0001
Inferolateral TWI	0	6 (11.1)	0.007
Anterior TWI	1 (1.2)	6 (11.1)	0.028
Inferior TWI	0	4 (7.4)	0.044
Lateral TWI	0	6 (11.1)	0.007
Anterolateral TWI	0	6 (11.1)	0.007
Inferior-anterior-lateral TWI	0	3 (5.6)	0.11
<b>NEW ECG CRITERIA</b>			
SV1+RV6 ≤12 (mm)	12 (14.3)	30 (55.6)	<0.0001
RI + RII ≤8 (mm)	2 (2.4)	31 (57.4)	<0.0001
SV1+RV6 ≤12 and RI + RII ≤8 (mm)	0	24 (44.4)	<0.0001

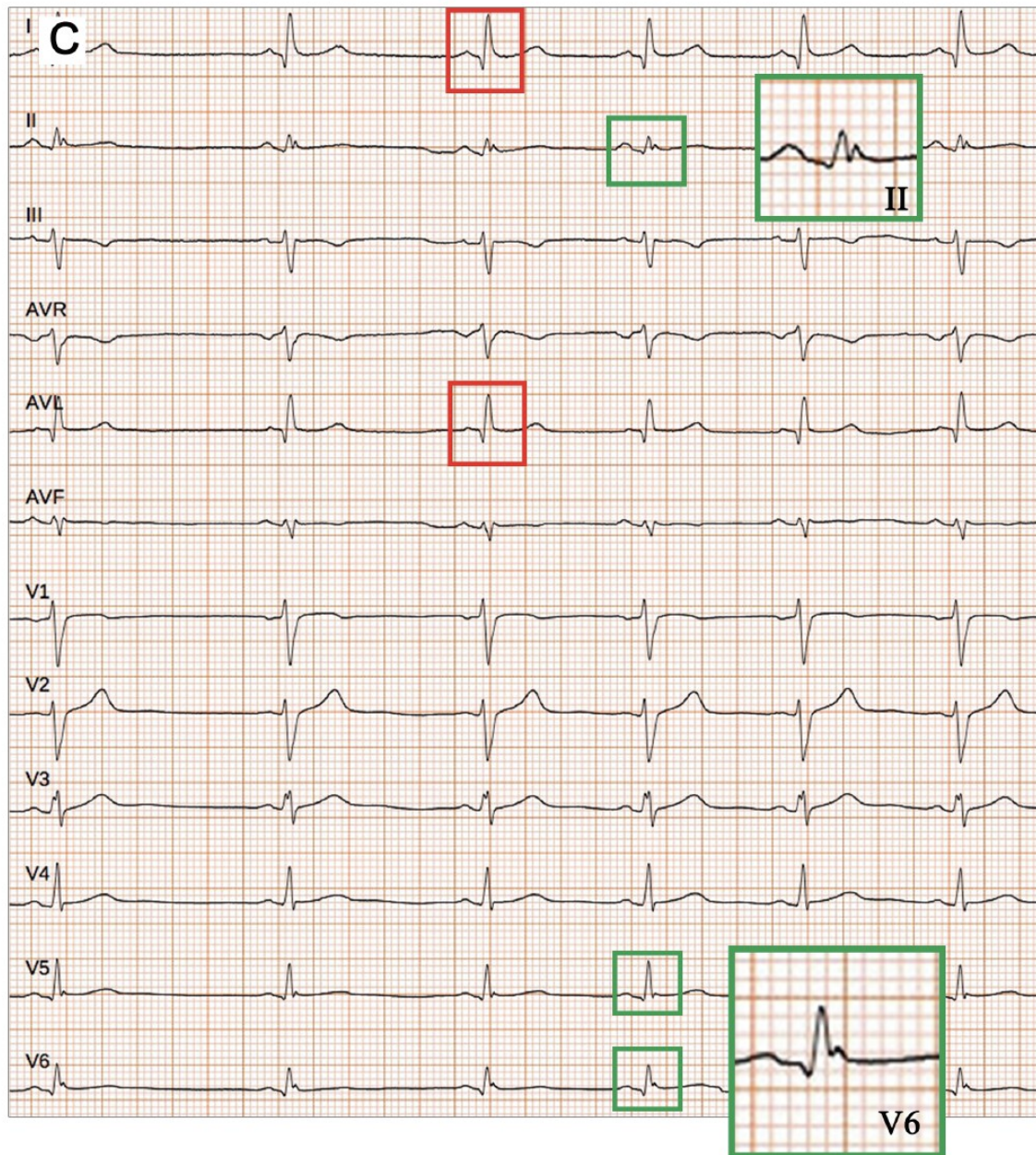
Global LQRSV	0	4 (7.4)	0.044
LQRSV in limb leads	0	8 (14.8)	0.0011
Local LQRSV			
Lateral distribution	16 (18.8)	13 (24.1)	0.52
Inferior distribution	11 (12.9)	8 (14.8)	0.75
Inferolateral distribution	0	3 (5.6)	0.11
Precordial and local distribution	3 (3.5)	8 (14.8)	0.017
Epsilon Wave	0	1 (1.9)	0.82
Epsilon-like Wave in inferior leads	0	3 (5.6)	0.11
QTc (msec)	405±19	407±26	0.49
QTc ≥440 msec	0	4 (7.4)	0.044
Tzou criteria *	15 (17.6)	10 (18.5)	0.89
R >3 mm V1	1 (1.2)	6 (11.1)	0.028
R/S ratio ≥0.5 in V1	1 (1.2)	13 (24.1)	<0.0001
R/S ratio ≥1 in V1	0	6 (11.1)	0.007
Bayés de Luna criteria †	1 (1.2)	3 (5.6)	0.33

## Sensitivity, specificity, PPV and NPV value of new and known ECG parameters for ALVC diagnosis

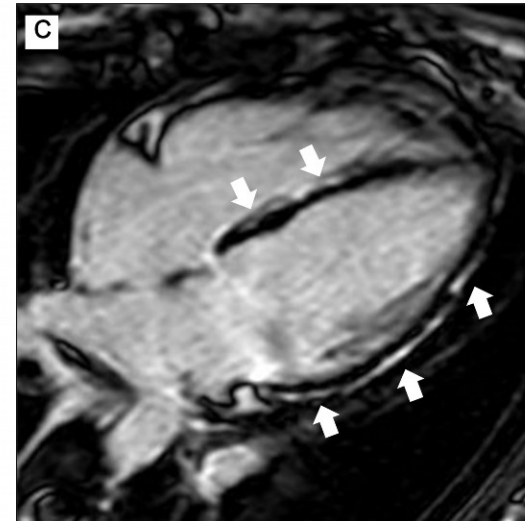
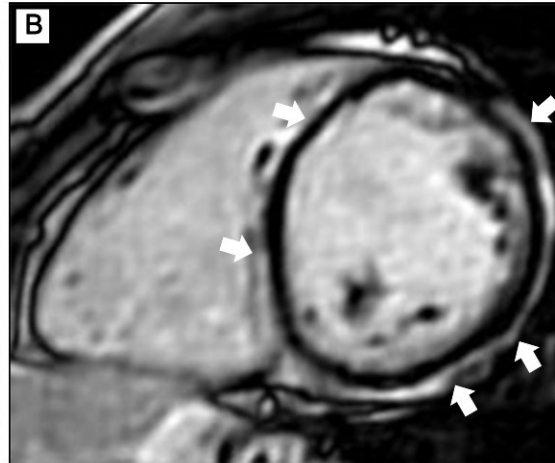
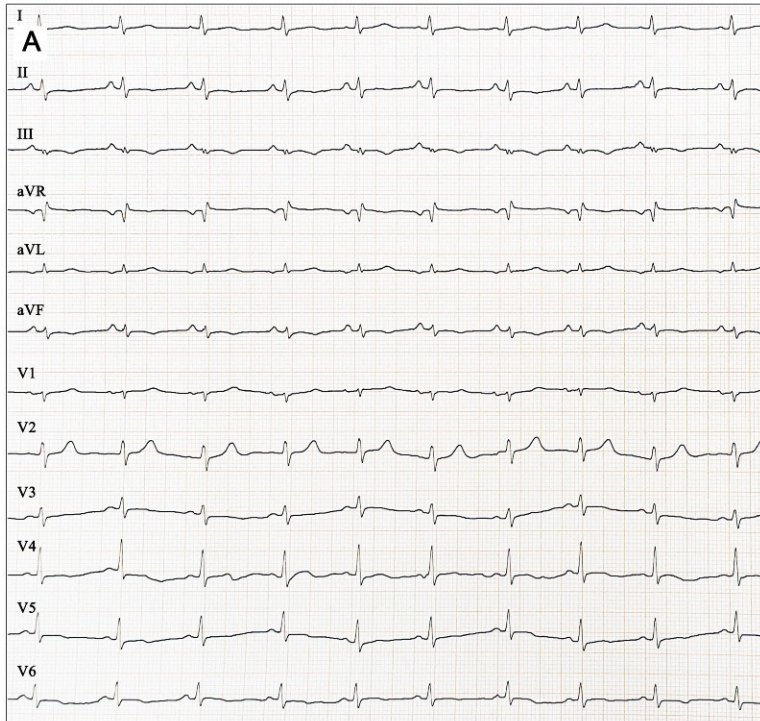
	ALVC (n=54)	Controls (n=84)	Sensitivity (%)	Specificity (%)	PPV (%)	NPV (%)	Accuracy (%)
<b>Single ECG Parameters</b>							
LPFB	11	0	20.4	100	100	66.1	68.8
Pathologic Q waves	18	0	33.3	100	100	70.0	73.9
TWI	31	1	57.4	98.8	96.9	78.3	82.6
LQRSV in limb leads	8	0	14.8	100	100	64.6	66.7
Global LQRSV	4	0	7.4	100	100	62.7	63.8
R >3 mmV1	6	1	11.1	98.8	85.7	63.4	64.5
R/S ratio $\geq 0.5$ in V1	13	1	24.1	98.8	92.9	66.9	69.6
SV1+RV6 $\leq 12$	30	12	55.6	85.7	71.4	75.0	73.9
RI+ RII $\leq 8$	31	2	57.4	97.6	93.9	78.1	81.9
<b>Combined ECG Parameters</b>							
<i>Known ECG criteria</i>							
TWI or LQRSV in limb leads	35	1	64.8	98.8	97.2	81.4	85.5
TWI or LQRSV (limb leads and global)	37	1	68.5	98.8	97.4	83.0	86.9
<i>New ECG criteria</i>							
SV1+RV6 $\leq 12$ and RI + RII $\leq 8$	24	0	44.4	100	100	73.7	78.3
LPFB or Q or R/S ratio $\geq 0.5$ in V1	30	1	55.6	98.8	96.8	77.6	81.9
LPFB or Q or R/S ratio $\geq 0.5$ in V1 or [SV1+RV6 $\leq 12$ and RI + RII $\leq 8$ ]	35	1	64.8	98.8	97.2	81.4	85.5
<i>Know and New ECG criteria</i>							
TWI or LPFB or Q	38	1	70.4	98.8	97.4	83.8	87.7
TWI or LPFB or Q or [SV1+RV6 $\leq 12$ and RI + RII $\leq 8$ ]	44	1	81.5	98.8	97.8	89.3	92.0
TWI or LPFB or Q or R/S ratio $\geq 0.5$ in V1 or [SV1+RV6 $\leq 12$ and RI + RII $\leq 8$ ] or LQRSV in limb leads	47	2	87.0	97.6	95.9	92.1	93.5





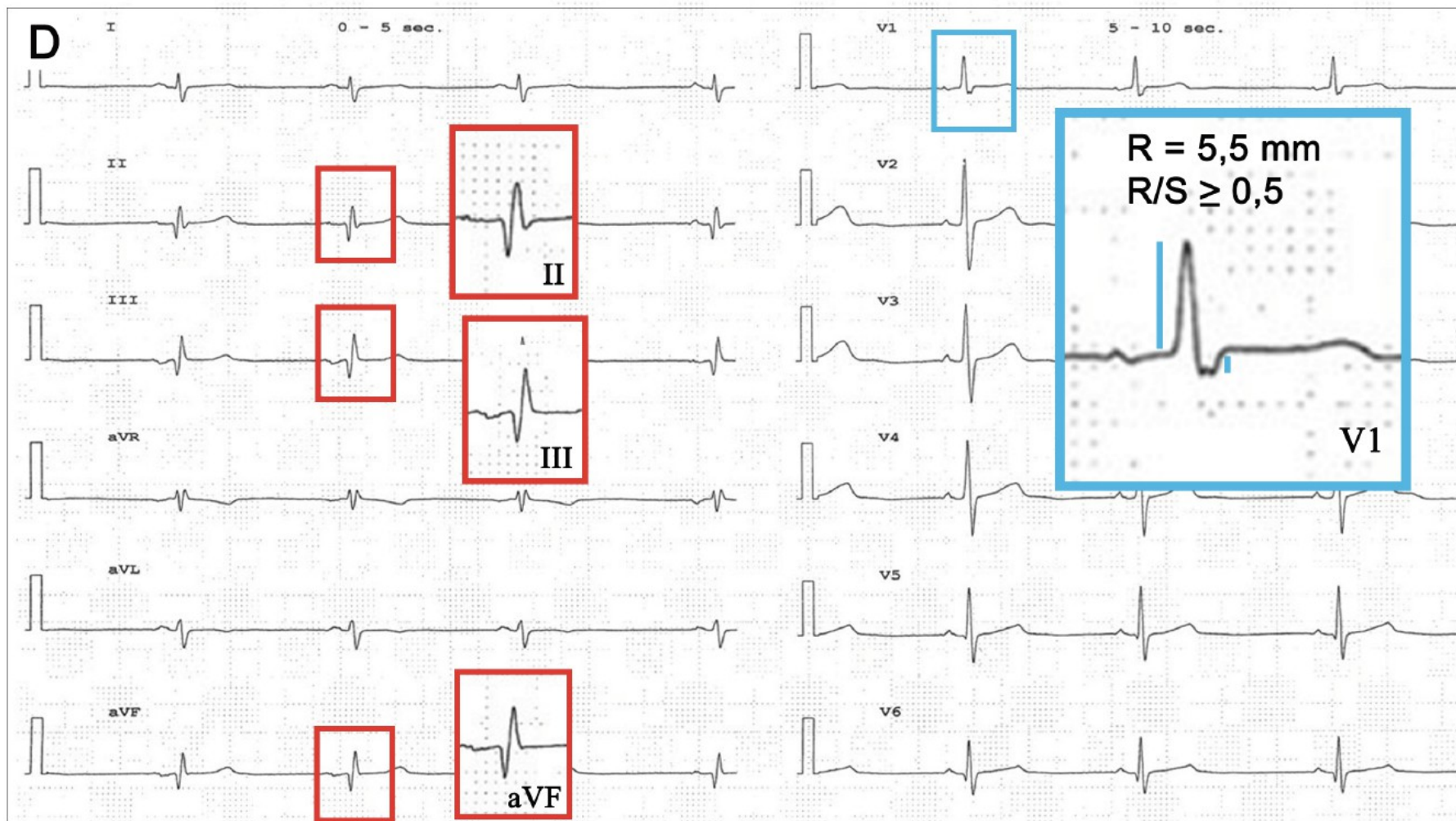


Patient #8, 20-year-old man, pathogenic variant in desmoplakin (c.5851 C>T, p.Arg1951Ter)



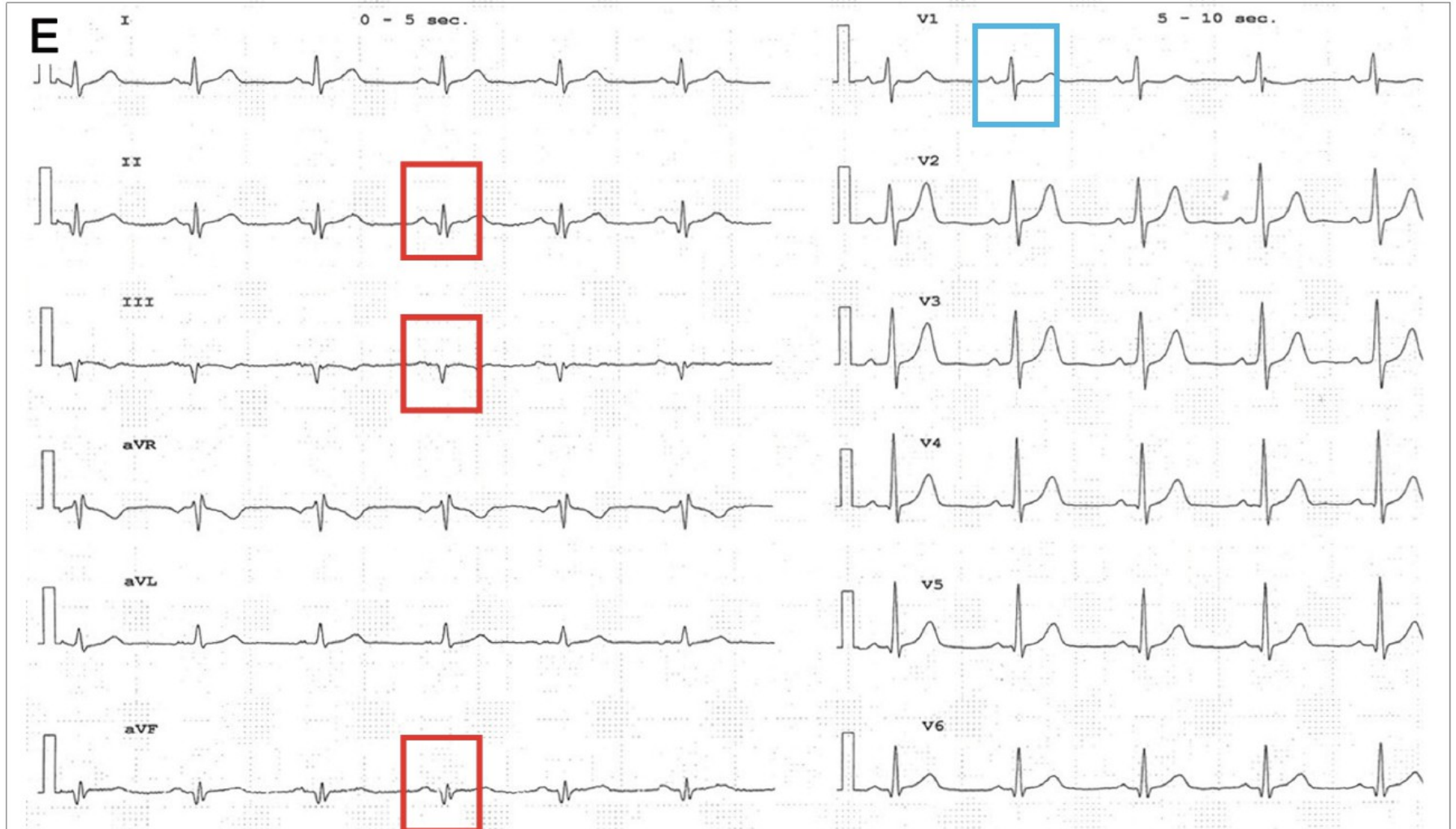
Patient #15 is a 18-year-old woman with a likely pathogenic variant in desmoplakin (c.1351C>T, p.Arg451Cys).





Patient #35, 42-year-old man), pathogenic variant in desmoglein-2 (c.1912G>A, p.Gly638Arg)





The family member (Patient #36, 37-year-old man) has the same pathogenic variant in desmoglein-2 (c.1912G>A, p.Gly638Arg)



# The Distinctive Electrocardiogram of Duchenne's Progressive Muscular Dystrophy\*

## *An Electrocardiographic-Pathologic Correlative Study*

JOSEPH K. PERLOFF, M.D.,  
Washington, D. C.

WILLIAM C. ROBERTS, M.D.,  
Bethesda, Maryland

ANTONIO C. DE LEON, JR., M.D. and DESMOND O'DOHERTY, M.D.  
Washington, D. C.

The clinical, electrocardiographic, hemodynamic and cardiac pathologic features are described in two patients with the rapidly progressive, pseudohypertrophic, sex-linked form of Duchenne's muscular dystrophy. Previous studies have shown that the electrocardiogram is distinctive enough to aid in identifying this particular type of hereditary myopathic disorder even when the clinical features of the systemic myopathy are inconclusive. Tall right precordial R waves and deep limb lead and left precordial Q waves characterize these electrocardiograms. Information thus far has not provided explanations for either the distinctive morphology of the Duchenne electrocardiogram or for the variety of rhythm disturbances that have been observed. Accordingly, an electrocardiographic-pathologic correlative study was undertaken in order to determine whether a relationship existed between the distribution of myocardial dystrophy, the presence of an unusual type of small vessel coronary arteriopathy, and the electrocardiographic abnormalities of both QRS configuration and rhythm.

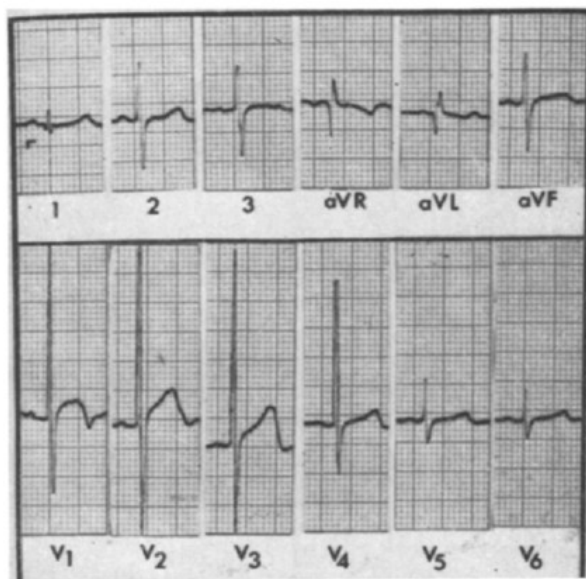


FIG. 1A. Case 1. Electrocardiogram obtained at twelve years of age shows a marked increase in the amplitude of the R wave in lead V<sub>1</sub>, but a significant Q wave only in lead aVL.

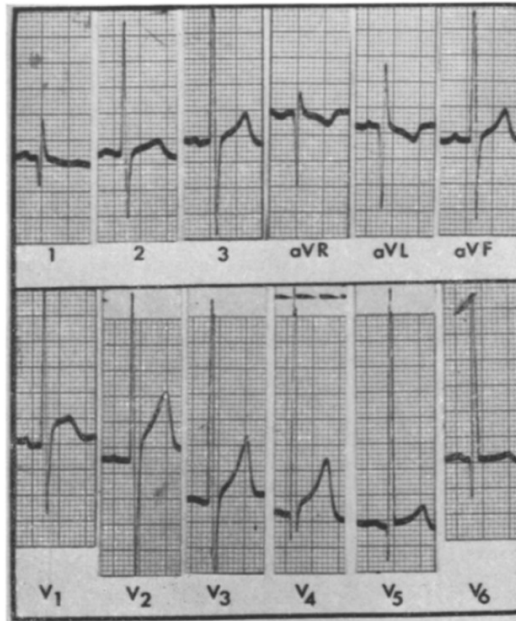


FIG. 1B. Case 1. Electrocardiogram obtained at seventeen years of age (similar to subsequent tracings except for preterminal atrial flutter). The tall R wave in lead V<sub>1</sub> persists. Deep Q waves have now appeared in leads I, aVL, and V<sub>5</sub> to V<sub>6</sub>. The amplitude of the R waves in leads V<sub>4</sub> to V<sub>6</sub> has substantially increased.

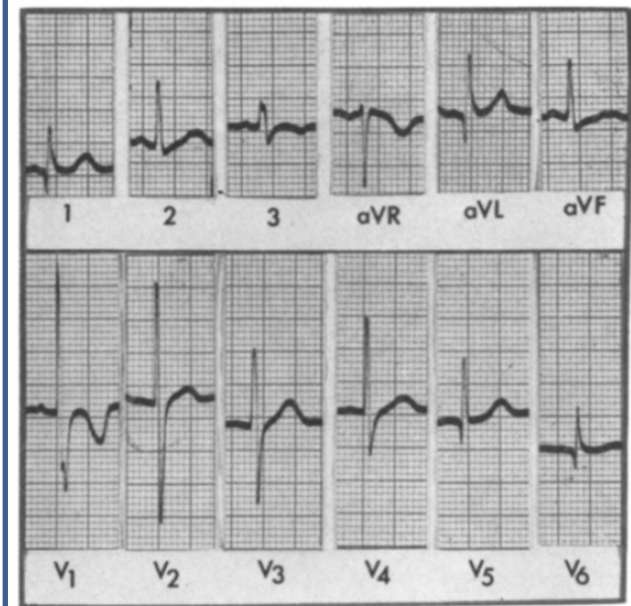
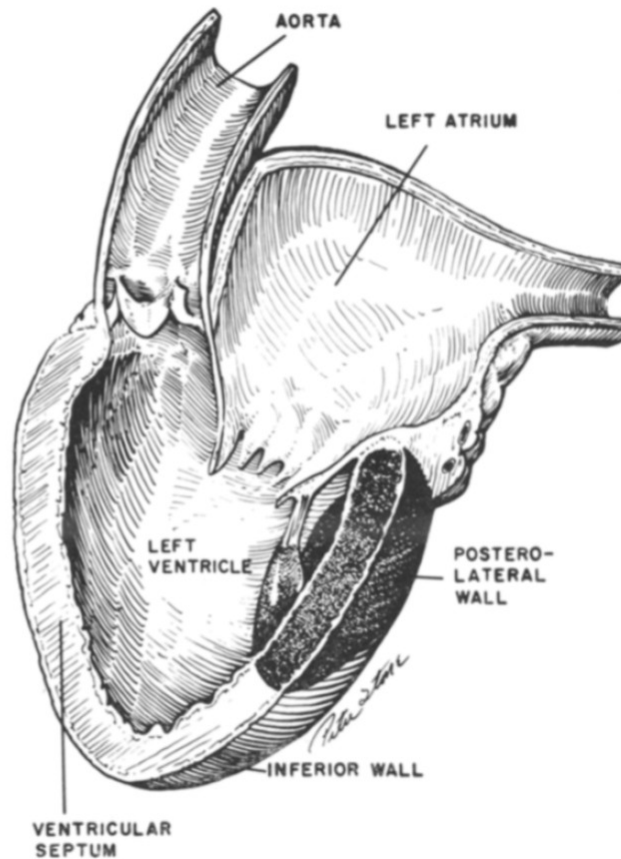


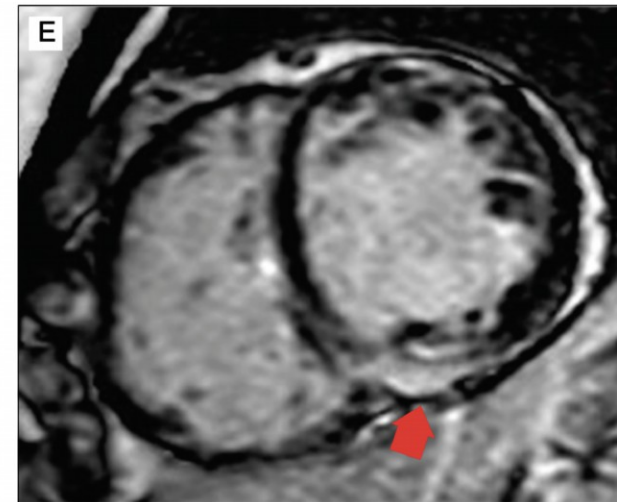
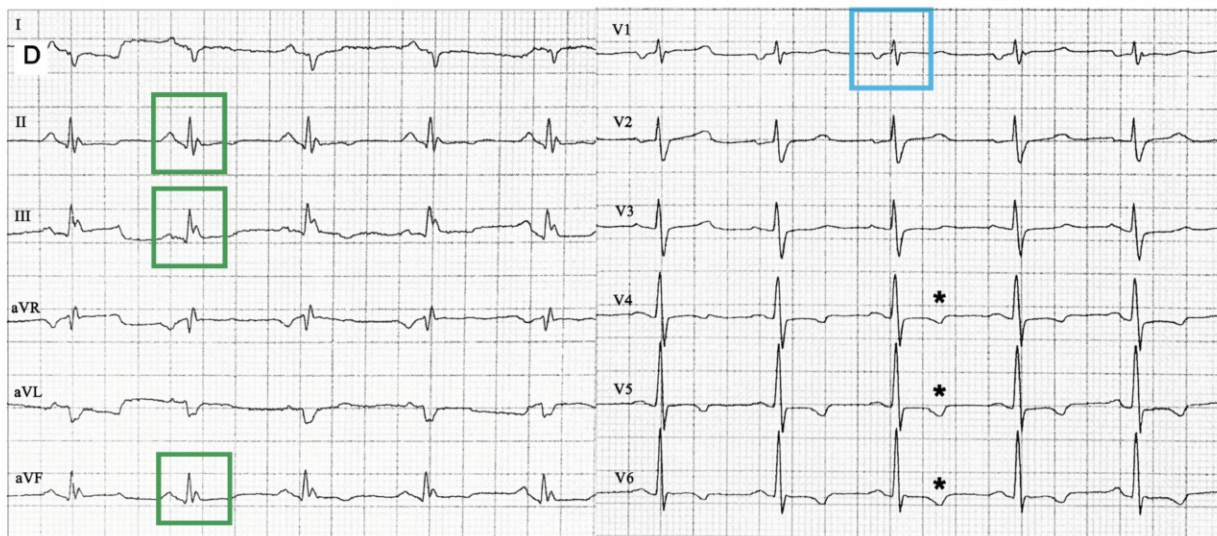
FIG. 2. Case 2. Electrocardiogram obtained at twelve years of age shows a tall R wave in lead V<sub>1</sub> in addition to deep Q waves in leads I and aVL. Leads V<sub>5</sub> to V<sub>6</sub> display moderately deep Q waves that were not present at nine years of age.



FIG. 3. Diagram of the left side of the heart illustrating the distribution of the fibrous scarring in the two patients. The scarring was focal and limited to the posterolateral free wall of the left ventricle. No scarring was observed in the diaphragmatic or inferior free wall or in the ventricular septum. A papillary muscle was involved in one patient (Case 1) who had clinical mitral incompetence.



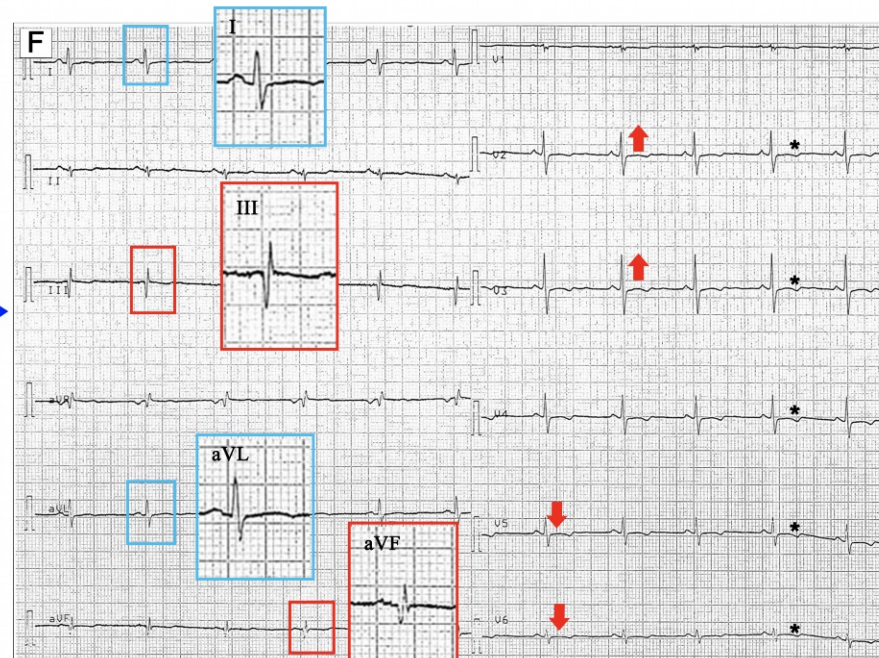
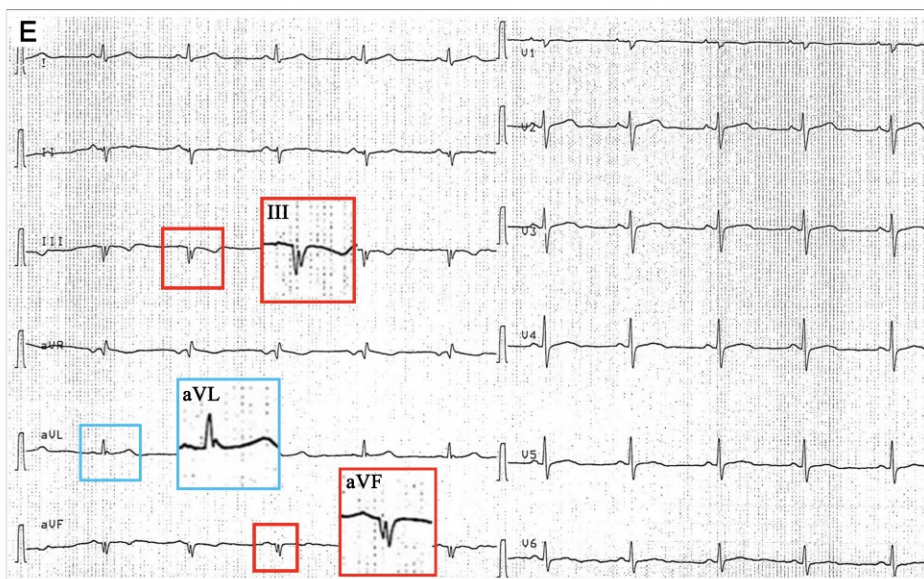
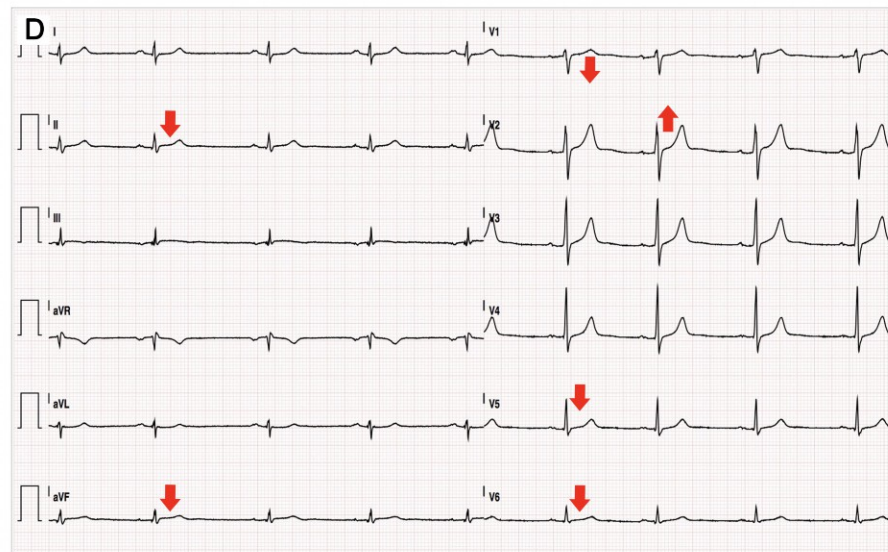
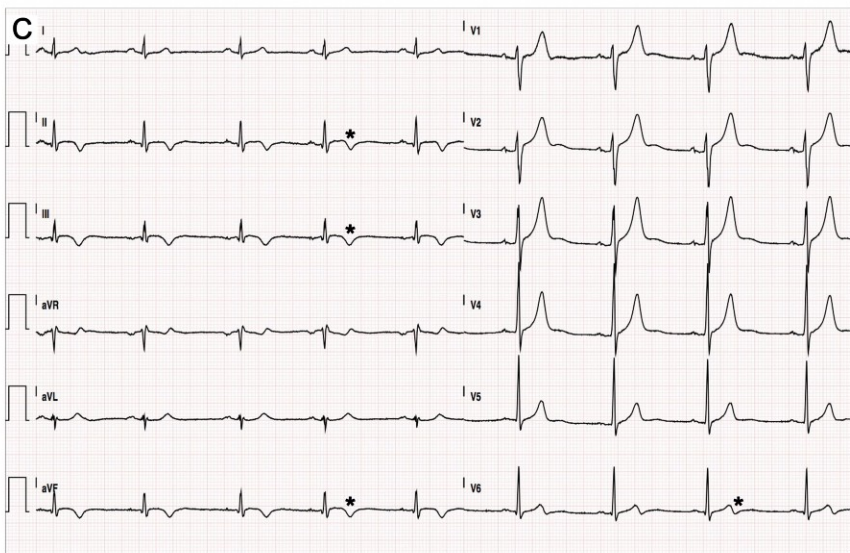




Patient #9 is a 33-year-old woman with a pathogenic variant in desmoplakin (c.5851 C>T, p.Arg1951Ter).











	Major Arrhythmic Events (n=15)	No Major Arrhythmic Events (n=39)	P Value
Age at diagnosis, years	43±15	38±15	0.28
Male gender	13 (86.7)	19 (48.7)	<b>0.011</b>
Proband	13 (86.7)	27 (69.2)	0.19
Family history of DCM	5 (33.3)	18 (46.2)	0.39
Family history of SCD	3 (20.0)	15 (38.5)	0.20
NYHA class I-II	13 (86.7)	39 (100)	0.22
NYHA class III	2 (13.3)	0	<b>0.0215</b>
Atrial fibrillation	2 (13.3)	2 (5.1)	0.31
Unexplained syncope	6 (40.0)	2 (5.1)	<b>0.001</b>
NSVT	8 (53.3)	18 (46.2)	0.64
<b>Cardiac magnetic resonance</b>			
LVEDVi (ml/m <sup>2</sup> )	99.9±19.7	96.8±26.1	0.68
LVEF, %	46.3±6.1	50.8±10.9	0.14
LVEF <50%	10 (66.7)	13 (33.3)	<b>0.0276</b>
RVEDVi (ml/m <sup>2</sup> )	87.2±20.9	85.4±18.4	0.76
RVEF, %	52.6±9.8	54.9±9.2	0.42
Segments with LGE	6±3; 6 (4-7)	6±4; 6 (4-8)	1.0
<b>LGE pattern</b>			
- Ringlike	8 (53.3)	20 (51.3)	0.89
<b>LGE distribution</b>			
- Subepicardial	7 (46.7)	28 (71.8)	<b>0.09</b>
- Midmural	2 (13.3)	8 (20.5)	0.55
- Transmural	6 (40.0)	3 (7.7)	<b>0.0047</b>
<b>Genetic testing</b>			
Pathogenic/likely pathogenic variant	12/15 (80.0)	36/39 (92.3)	0.20
DSP	6/12 (50.0)	29/36 (80.6)	0.64
Non-DSP *	6/12 (50.0)	7/36 (19.4)	<b>0.026</b>
<b>ECG</b>			
QRS (msec)	97±13	95±13	0.61
First degree AV block	1 (6.7)	4 (10.3)	0.68
NSICD	0	2 (5.1)	0.37
RBBB	0	0	-
LAFB	0	4 (10.3)	0.20
LPFB	6 (40.0)	5 (12.8)	<b>0.028</b>
LBFB	0	0	-

	Major Arrhythmic Events (n=15)	No Major Arrhythmic Events (n=39)	P Value
<b>Pathological Q waves</b>	5 (33.3)	13 (33.3)	1.0
Lateral distribution	2 (13.3)	5 (12.8)	0.96
Inferior distribution	2 (13.3)	6 (15.4)	0.84
Precordial distribution	0	1 (2.6)	0.53
More 2 localizations	1 (6.7)	1 (2.6)	0.48
<b>Fragmented QRS</b>	4 (26.7)	15 (38.5)	0.42
Lateral distribution	0	1 (2.6)	0.53
Inferior distribution	1 (6.7)	9 (23.1)	0.17
Precordial distribution	1 (6.7)	0	0.11
More 2 localizations	2 (13.3)	5 (12.8)	0.96
<b>Global LQRSV</b>	1 (6.7)	3 (7.7)	0.90
<b>LQRSV in limb leads</b>	1 (6.7)	7 (17.9)	0.31
<b>Local LQRSV</b>			
Lateral distribution	4 (26.7)	9 (23.1)	0.78
Inferior distribution	2 (13.3)	6 (15.4)	0.84
Inferolateral distribution	2 (13.3)	1 (2.6)	0.13
Precordial and local distribution	1 (6.7)	4 (10.3)	0.69
<b>QTc (msec)</b>	401±27	409±26	0.32
<b>QTc ≥440 msec</b>	0	4 (10.3)	0.20
<b>Tzou criteria †</b>	6 (40.0)	4 (10.3)	<b>0.01</b>
<b>R &gt;3 mm V1</b>	3 (20.0)	3 (7.7)	0.20
<b>R/S ratio ≥0.5 in V1</b>	9 (60.0)	4 (10.3)	<b>0.0002</b>
<b>R/S ratio ≥1 in V1</b>	6 (40.0)	0	<b>&lt;0.0001</b>
<b>Bayés de Luna criteria ‡</b>	3 (20.0)	0	<b>0.0044</b>
<b>TWI</b>	11 (73.3)	20 (51.3)	0.15
Inferolateral TWI	4 (26.7)	2 (5.1)	<b>0.025</b>
Anterior TWI	2 (13.3)	4 (10.3)	0.76
Inferior TWI	2 (13.3)	2 (5.1)	0.31
Lateral TWI	2 (13.3)	4 (10.3)	0.76
Anterolateral TWI	1 (6.7)	5 (12.8)	0.53
Inferior-anterior-lateral TWI	0	3 (7.7)	0.27
<b>NEW ECG CRITERIA</b>			
<b>SV1+RV6 ≤12 (mm)</b>	10 (66.7)	20 (51.3)	0.31
<b>RI + RII ≤8 (mm)</b>	7 (46.7)	24 (61.5)	0.33
<b>SV1+RV6 ≤12 and RI + RII ≤8 (mm)</b>	7 (46.7)	17 (43.6)	0.84

## Probability of major arrhythmic events in relation to clinical, electrocardiographic and structural parameters

	Univariate analysis			Multivariate analysis		
	OR	95% CI	<i>P value</i>	OR	95% CI	<i>P value</i>
<b><i>Clinical parameters</i></b>						
Age	1.0	0.9-1.1	0.317			
Sex	6.8	1.4-34.4	<b>0.020</b>			
Unexplained syncope	12.3	2.1-71.5	<b>0.005</b>	<b>8.9</b>	<b>1.1-70.6</b>	<b>0.037</b>
<b><i>Structural parameters</i></b>						
Transmural LGE	8.0	1.7-38.2	<b>0.009</b>			
LVEF <50%	4.0	1.1-14.1	<b>0.031</b>			
<b><i>ECG parameters</i></b>						
LPFB	4.5	1.1-18.3	<b>0.034</b>			
R/S ratio in V1 $\geq 0.5$	13.1	3.0-56.6	<b>0.001</b>	<b>6.8</b>	<b>1.4-34.4</b>	<b>0.020</b>
Inferolateral TWI	6.7	1.1-41.8	<b>0.041</b>			
SV1+RV6 $\leq 12$ mm	1.9	0.5-6.6	0.312			
RI+ RII $\leq 8$ mm	0.6	0.2-1.8	0.325			





# Unrecognized cases of prominent R-wave in V1 detected in the iconography of published papers

Case ID	References	Figure	12 lead ECG findings	Genetic analysis	CMR data	Endomyocardial biopsy data/ Histologic data
Case 1	Rubino M et al <sup>1</sup> <i>Genes</i> 2021	Fig.1	Prominent R V1 (>3mm) Inferolateral TWI Pathological Q in I-aVL	DSP (c.5428C>T, p.Gln1810Ter)	Subepicardial circumferential LGE involving the entire LV	Not available
Case 2	Zorzi A et al <sup>2</sup> <i>Circ Arrhythm Electrophysiol.</i> 2016	Fig. 4	LPFB Inferolateral TWI Pathological Q II-III-aVF Prominent R V1 (>3 mm) LQRSV in left precordial leads	Not performed	Sub/midmyocardial LGE with a stria pattern involving the inferolateral LV wall	Extensive fibrosis in the sub- and midmyocardial layers (inferolateral LV), focal and patchy fatty infiltration. Cardiomyocytes hypertrophic with dysmetric and dysmorphic nuclei, with cytoplasmic vacuolization.
Case 3	Oloriz T et al <sup>3</sup> <i>Europace.</i> 2016	Fig. 1- right panel	LPFB - R/S ratio V1 ≥0.5	Not performed	Infero-lateral scar	Not performed
Case 4	Sakamoto N et al <sup>4</sup> <i>Circ Cardiovasc Imaging.</i> 2019	Fig.1	R/S ratio V1 ≥1 Inferolateral TWI LQRSV in limb leads	DSP (c.4650delTG, p.V1551E fs74X) and MYBPC3 (c.2459G>A, p.R820Q)	LGE in the mid-myocardial septum and subepicardial anterolateral LV myocardium.	Fibrofatty replacement, mild hypertrophy, and disarrangement of the myocytes. Electron microscopy of the intercalated discs showed disarrangement of the filaments and widening of the fascia adherens gap
Case 5	Tsuruta Y et al <sup>5</sup> <i>Heart Fail.</i> 2020	Fig.1	R/S ratio V1 ≥1 Inferolateral TWI LQRSV in limb leads	Nonsense mutation in DSP (c.5212C > T, p.R1738*)	Fat signals LGE in the mid-wall to subepicardial layers in the LV myocardium	Moderate fibrofatty replacement and mild hypertrophy
Case 6	Groeneweg JA et al <sup>6</sup> <i>Heart Rhythm.</i> 2013	Fig.4	R/S ratio V1 ≥1 TWI in II and anterolateral leads	PKP2 variant c.419C4T and the PLN mutation c.40_42delAGA	LGE in the lateral wall of the LV	Normal myocardium, with locally some (<10%) subendocardial fibrosis.

Case 7	Blom LJ et al <sup>7</sup> <i>Heart Rhythm Case Rep.</i> 2018	Fig.2	LPFB TWI V5-V6, I, II, aVF R/S ratio V1 ≥1	Unclassified variant PKP2 gene and a pathogenic c.4042delAGA mutation in the PLN gene.	Not performed	Normal
Case 8	Singh SM et al <sup>8</sup> <i>JACC Case Rep.</i> 2021	Fig.3 (C)	LPFB - R/S ratio V1 ≥1	Not performed	Biventricular apical and anterolateral LGE in the epi- to mid-myocardium	Not performed
Case 9	Norman M et al <sup>9</sup> <i>Circulation</i> 2005	Fig.3	R/S ratio V1 ≥0.5 Inferolateral TWI	DSP gene identified insertion of a single adenine base (2034insA)	Not performed	Not performed
Case 10	Chen P et al <sup>10</sup> <i>Int J Cardiol.</i> 2020	Fig. 2 (A)	LPFB. TWI V1-V3. R/S ratio V1 ≥1	DSG2 p.Leu237Ter mutation	Dilation of both ventricles	Not performed
Case 11	Pilichou K et al <sup>11</sup> <i>Circulation</i> 2014	Fig.3	R/S ratio V1 ≥1	DSP c.448C>T mutation	Focal bulging on anterolateral RV apex. LGE (midepicardial stria) in the inferior LV wall	Not performed

# **The end of an electrocardiographic dogma: a prominent R wave in V<sub>1</sub> is caused by a lateral not posterior myocardial infarction—new evidence based on contrast-enhanced cardiac magnetic resonance—electrocardiogram correlations**

**Antonio Bayés de Luna<sup>1\*</sup>, Daniele Rovai<sup>2</sup>, Guillem Pons Llado<sup>1</sup>, Anton Gorgels<sup>3</sup>,  
 Francesc Carreras<sup>1</sup>, Diego Goldwasser<sup>1</sup>, and Raymond J. Kim<sup>4</sup>**

<sup>1</sup>Institut Català Ciències Cardiovasculars (ICCC), Sant Pau Hospital, S. Antoni M. Claret 167, Barcelona 08025, Spain; <sup>2</sup>CNR, Institute of Clinical Physiology, Pisa, Italy;

<sup>3</sup>Maastricht University, Maastricht, The Netherlands; and <sup>4</sup>Duke University, Durham, NC, USA

Received 6 February 2014; revised 16 October 2014; accepted 6 January 2015

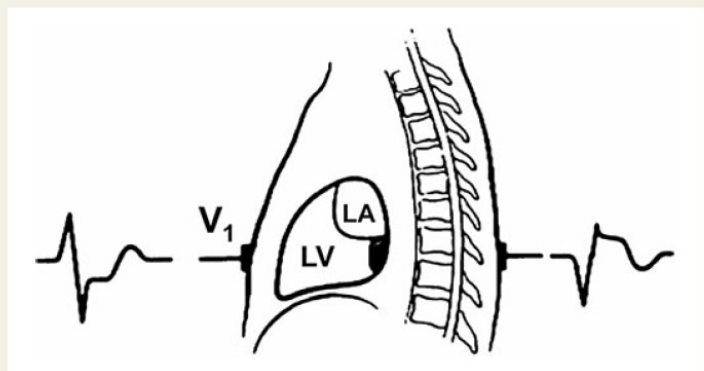


**Figure 1** Original drawing of true posterior infarction with the QRS morphology according to Perloff.<sup>1</sup>

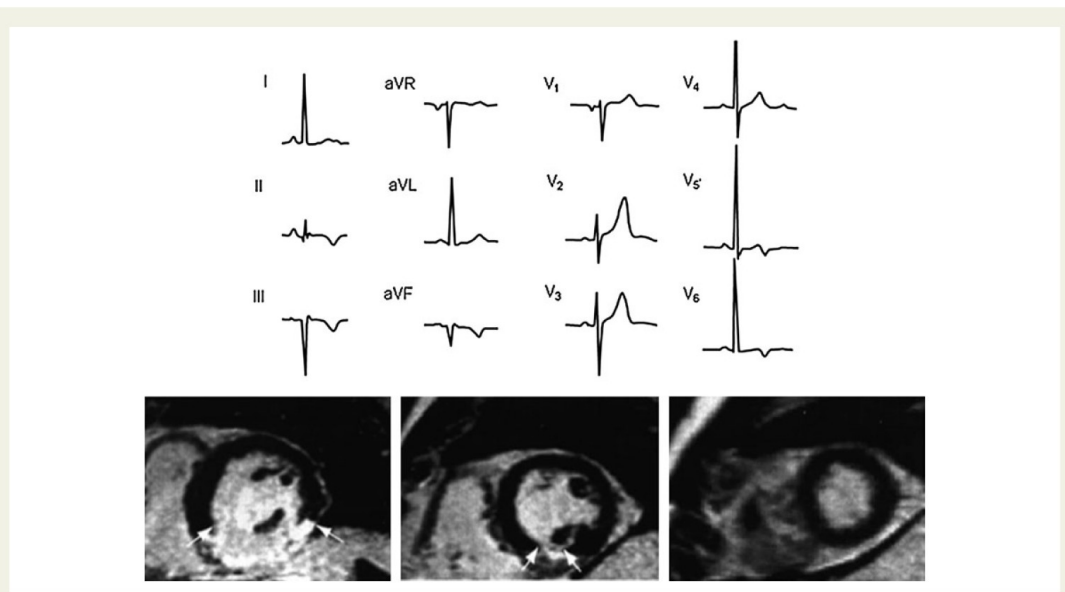


**Figure 2** Electrocardiographic and cardiac magnetic resonance images of an inferior infarct. Despite the clear infero-basal location of infarction at contrast-enhanced cardiac magnetic resonance (left-hand panel, between the white arrows), lead V<sub>1</sub> does not show a prominent R wave but an rS morphology.



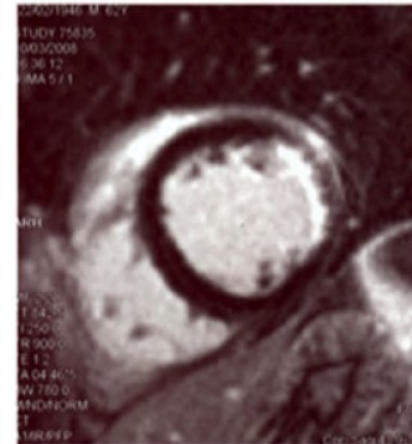
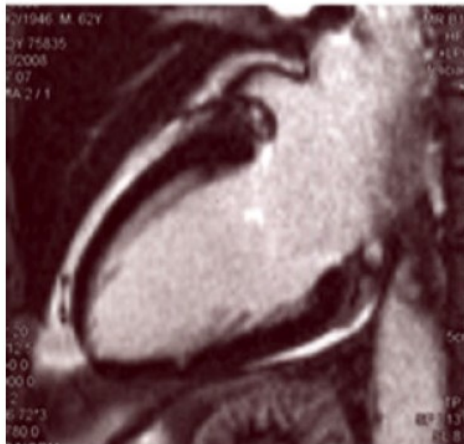
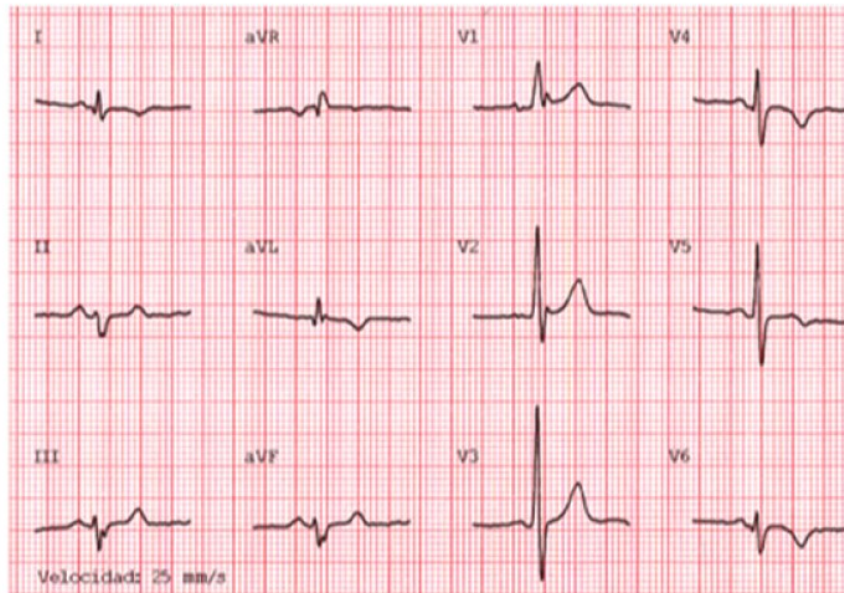


**Figure 3** Electrocardiographic and cardiac magnetic resonance images of a lateral infarct. A tall R wave in V<sub>1</sub> corresponds to a lateral infarct at contrast-enhanced cardiac magnetic resonance (lower central and right-hand panels). Of note, the infero-basal segment (segment 4) does not present any sign of necrosis (lower left and right panels).

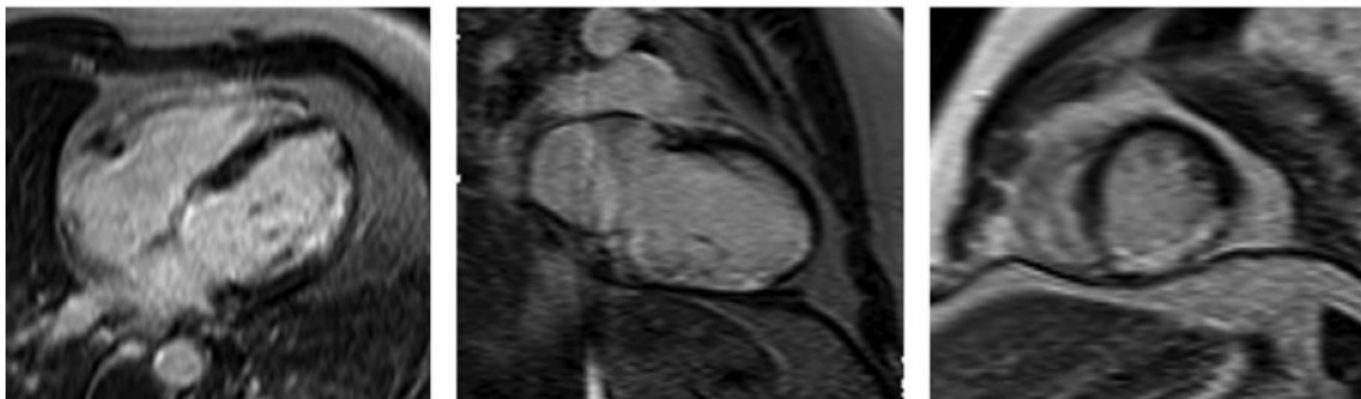
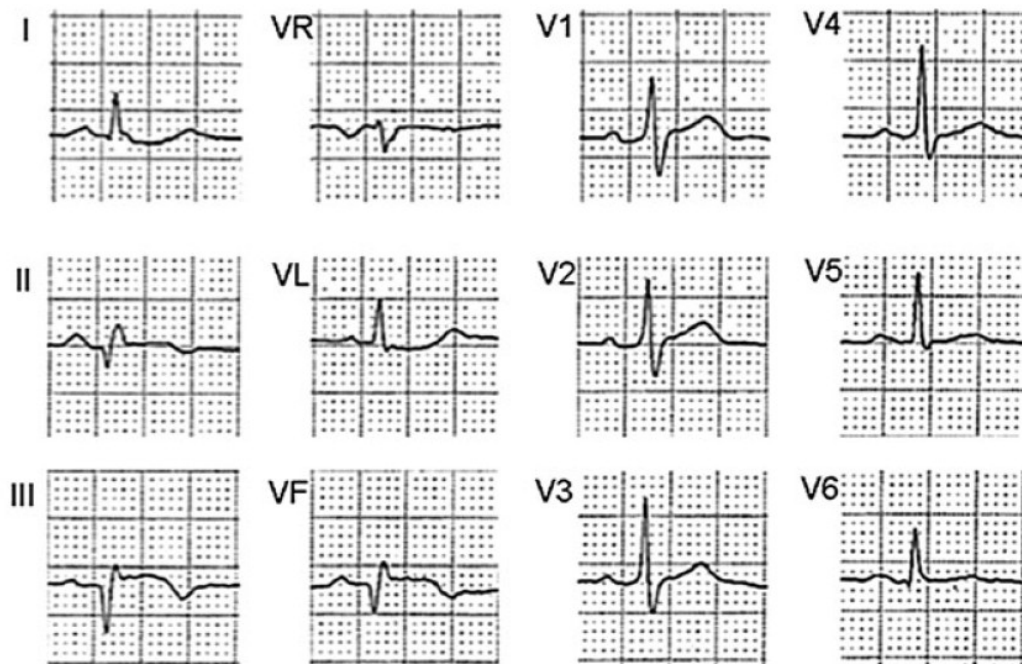
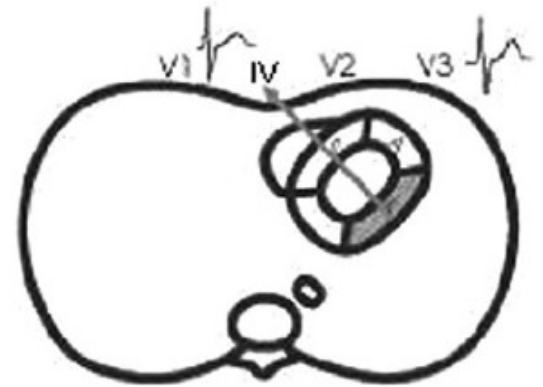
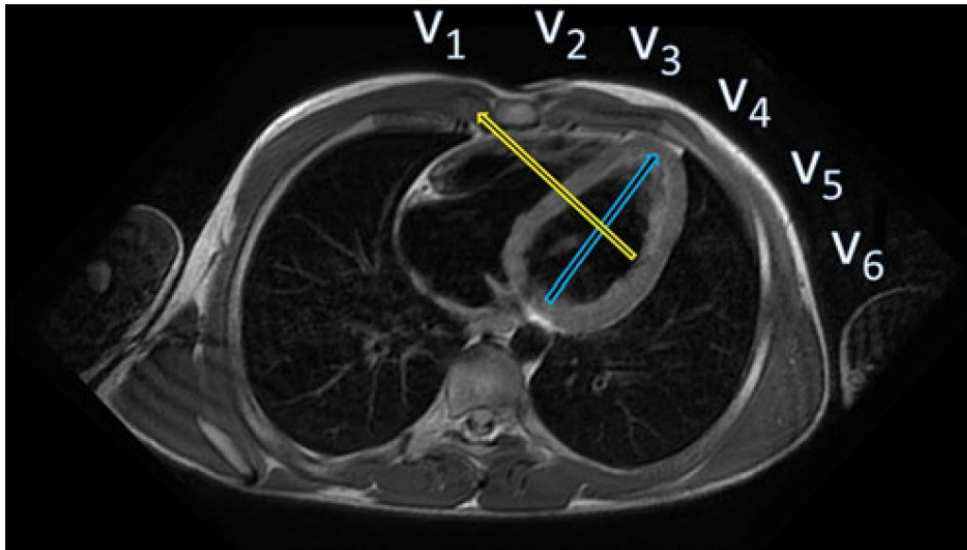


**Figure 4** Electrocardiographic and cardiac magnetic resonance images of an infero-lateral infarct. Q waves of necrosis are present in leads II, III, and aVF (inferior necrosis); an  $R \geq S$  morphology is present in lead  $V_1$  (lateral necrosis). Contrast-enhanced cardiac magnetic resonance (four-chamber, long-, and short-axis views) clearly shows an infero-lateral necrosis.

## Transverse plane of the thorax at cardiac magnetic resonance



The infarction vector produced by involvement of the wall formerly termed posterior (blue arrow) is directed towards V3–V4, while the infarction vector generated by the lateral wall (yellow arrow) is directed towards V1





# Unrecognized LPFB cases noted in the iconography of published papers

Case ID	References	Figure	12 lead ECG findings	Genetic analysis	CMR data	Endomyocardial biopsy data/ Histologic data
Case 1	Protonotarios A et al <sup>1</sup> <i>J Electrocardiol.</i> 2013	Fig. 1	LPFB, LQRSV in limb and left precordial leads, TWI V5-V6, fQRS in lead V1.	Not performed	Not performed	Fibrotic subepicardial and midwall bands on anterolateral and posterolateral LV walls and on the interventricular septum. Myocyte loss with fibro-fatty replacement and myocyte abnormalities
Case 2	Zorzi A et al <sup>2</sup> <i>Circ Arrhythm Electrophysiol.</i> 2016	Fig. 4	LPFB Inferolateral TWI Pathological Q in II-III-aVF Prominent R wave V1 LQRSV in left precordial leads	Not performed	Sub/midmyocardial LGE with a stria pattern involving the infero-lateral LV wall	Extensive fibrosis in the sub- and midmyocardial layers (inferolateral LV), focal and patchy fatty infiltration. Cardiomyocytes hypertrophic with dysmetric and dysmorphic nuclei, with cytoplasmic vacuolization.
Case 3	Oloriz T et al <sup>3</sup> <i>Europace.</i> 2016	Fig. 1 -right panel	LPFB - R/S ratio V1 $\geq 0.5$	Not performed	Infero-lateral scar	Not performed
Case 4	Miles C et al <sup>4</sup> <i>Circulation.</i> 2019	Fig. 4	LPFB – fQRS in septal leads First-degree AV block, Inferolateral TWI – LQRSV in limb leads, prolonged terminal activation duration in V1	Not performed	Extensive LV LGE, including near transmural LGE of lateral wall and midwall of anterior wall.	Myocyte degeneration and fibrofatty infiltration within the posterolateral wall of the LV (extending transmurally).
Case 5	Saguner AM et al <sup>5</sup> <i>Circulation.</i> 2015	Fig. 2	LPFB Early repolarization in the inferior leads and QRS fragmentation in aVL	Heterozygous pathogenic variant in the plakophilin-2 (c.2392A>G, p.T798A) and desmoglein-2 (c.877A>G, p.I293V) genes.	Fibrofatty infiltration involving epi- and midmyocardial layers of the inferolateral, anterolateral, and septal LV wall.	Unremarkable
Case 6	d'Amati G et al <sup>6</sup> <i>Int J Cardiol.</i> 2016	Fig. 1	LPFB	Not pathogenic mutation	Not performed	Fibro-adipose replacement (LV postero-lateral wall). Myocytes enlarged, dysmorphic nuclei

Case 7	Blom LJ et al <sup>7</sup> <i>Heart Rhythm Case Rep.</i> 2018	Fig. 1	LPFB - Intra-ventricular conduction delay, J-point elevation in inferior leads	Unclassified variant in the DSG2 gene and a p.Leu729del mutation in the gene SCN5A.	Not performed	Normal
Case 8	Blom LJ et al <sup>7</sup> <i>Heart Rhythm Case Rep.</i> 2018	Fig.2	LPFB TWI V5-V6, I, II, aVF R/S ratio V1 $\geq 1$	Unclassified variant plakophilin-2 gene and a pathogenic c.40-42delAGA mutation in the phospholamban (PLN) gene.	Not performed	Normal
Case 9	Singh SM et al <sup>8</sup> <i>JACC Case Rep.</i> 2021	Fig.3 (C)	LPFB - R/S ratio V1 $\geq 1$	Not performed	Biventricular apical and anterolateral LGE in the epi- to mid-myocardium	Not performed
Case 10	Pirou N et al <sup>9</sup> <i>ESC Heart Fail.</i> 2020	Fig.2 (B)	LPFB - TWI V4-V6 LQRSV in limb leads	Pathogenic variant in desmoplakin c.3924del	High T2 Intensity and subepicardial circumferential LGE.	Not performed
Case 11	Reichl K et al <sup>10</sup> <i>Circ Genom Precis Med.</i> 2018	Fig.1 (A)	LPFB	Heterozygous variant was identified in exon 23 of the DSP gene—c.3415_3417del TATinsG.	Epi- and midmyocardial LGE and fatty replacement in anterior, lateral and inferior LV and basal inferior RV segments.	Not performed
Case 12	Chmielewski P et al <sup>11</sup> <i>Diagnostics</i> 2020	Fig.2 (A)	LPFB TWI V1-V3 LQRSV, prolonged terminal activation duration in V1, fQRS II-III- aVF.	DSP NM_004415.4:c.3737dupA (p.Asn1246LysfsTer7) PKP2 NM_004572.3:c.2636T>C (p.Leu879Pro) NLRP3 NM_004895.4:c.1469G>A (p.Arg490Lys)	Moderate subepicardial and midwall areas of LGE with a ringlike pattern	
Case 13	Poller W et al <sup>12</sup> <i>J Am Heart Assoc.</i> 2020	Fig.3 (C)	LPFB TWI inferolateral leads	Dystrophin c.3970C>T, p.Arg1324Cys, desmoplakin c.4372C>T, p.Arg1458Ter,	Multifocal subepicardial posteroseptal and lateral LGE.	Low-level immune cell infiltration in the absence of intramyocardial virus genomes
				nexilin F-actin-binding protein c.154G>C, p.Asp52His		
Case 14	Vahidnezhad H et al <sup>13</sup> <i>Sci Rep.</i> 2020	Fig.2 (A)	LPFB, TWI V1-V3 Prolonged V3 terminal QRS duration- LQRSV limb leads	JUP mutation	Normal	Not performed
Case 15	Chen P et al <sup>14</sup> <i>Int J Cardiol.</i> 2020	Fig. 2 (A)	LPFB, TWI V1-V3. R/S ratio V1 $\geq 1$	DSG2 p.Leu237Ter mutation	Dilation of both ventricles	Not performed
Case 16	Protonotarios N et al <sup>15</sup> <i>Br Heart J.</i> 1986	Fig. 3 (A)	LPFB, QRS prolongation, LQRSV, TWI precordial leads.	Not performed (JUP mutation?)	Not performed	Not performed
Case 17	Chen V et al <sup>16</sup> <i>Eur Heart J Case Rep</i> 2022	Fig 2	LPFB	Pathogenic heterozygous DSP gene truncation variant (p.R1951X) and the pathogenic HFE variant (p.H63D).	Subepicardial basal-anterior, basal anterolateral, mid-inferior and mid-anteroseptal areas of LGE.	Mild lymphocytic myocarditis, interstitial fibrosis, and myocyte hypertrophy



Europace  
doi:10.1093/europace/euv360

Europace Advance Access published November 20, 2015

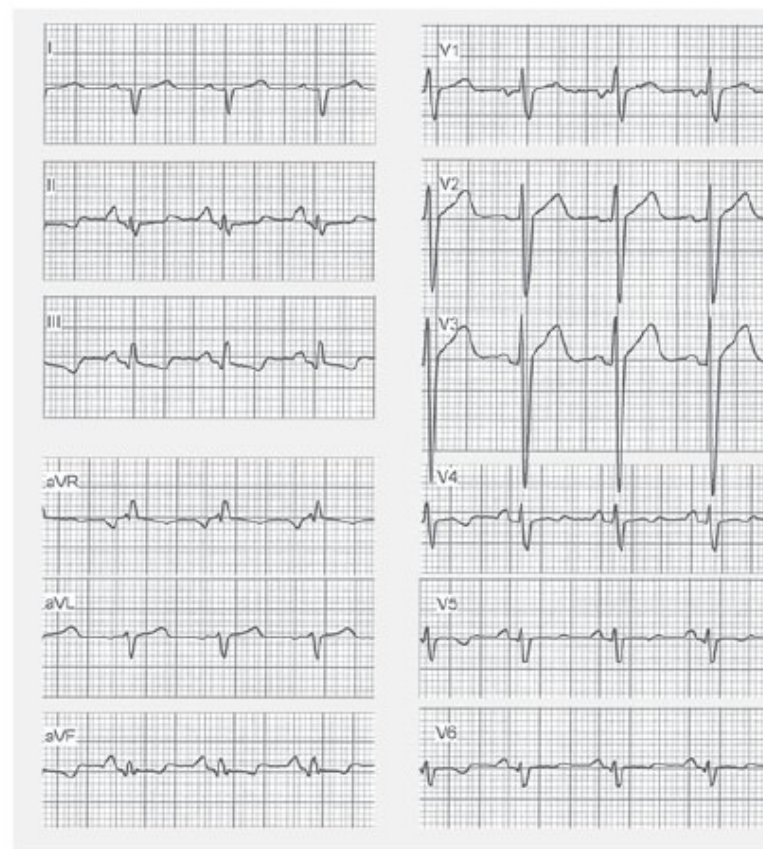
## CLINICAL RESEARCH

# The value of the 12-lead electrocardiogram in localizing the scar in non-ischaemic cardiomyopathy

**Teresa Oloriz<sup>1</sup>, Hein J.J. Wellens<sup>2</sup>, Giulia Santagostino<sup>1</sup>, Nicola Trevisi<sup>1</sup>, John Silberbauer<sup>1</sup>, Giovanni Peretto<sup>1</sup>, Giuseppe Maccabelli<sup>1</sup>, and Paolo Della Bella<sup>1\*</sup>**

<sup>1</sup>Arrhythmia Unit and Electrophysiology Laboratories, Ospedale San Raffaele, Via Olgettina 60, Milan, Italy; and <sup>2</sup>Cardiovascular Research Center, Maastricht, The Netherlands

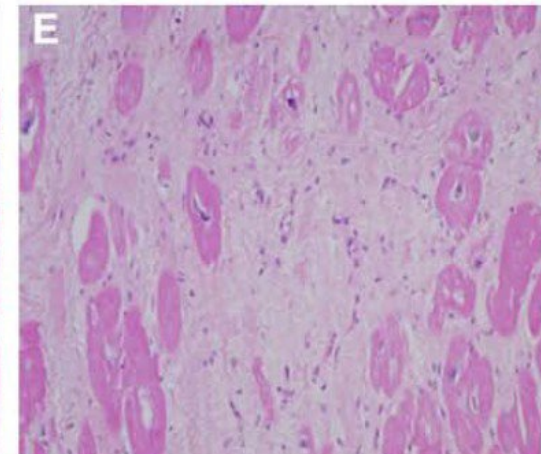
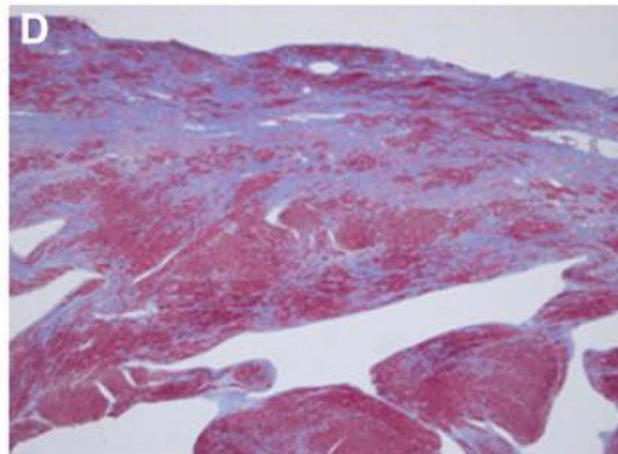
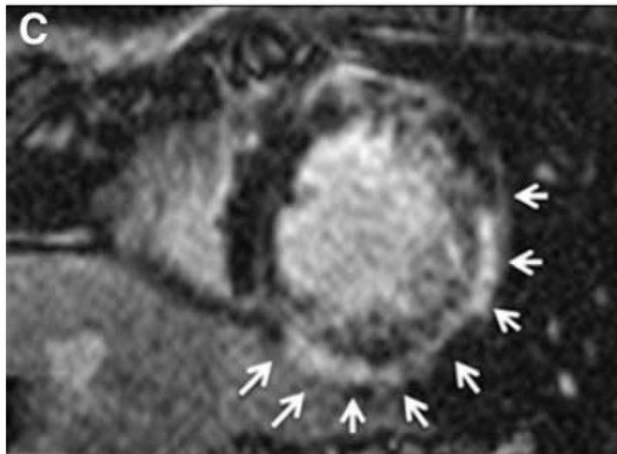
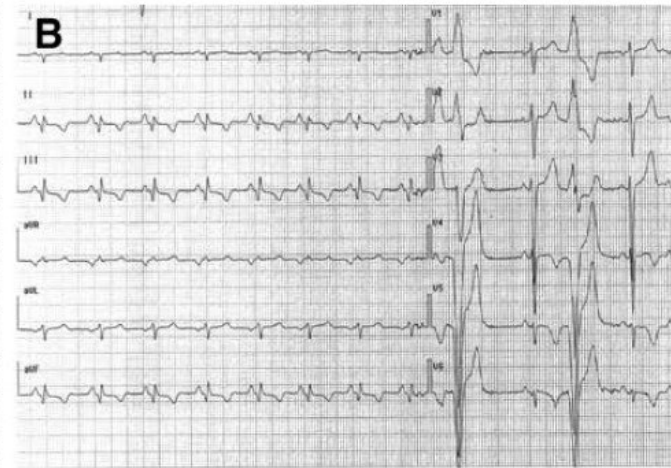
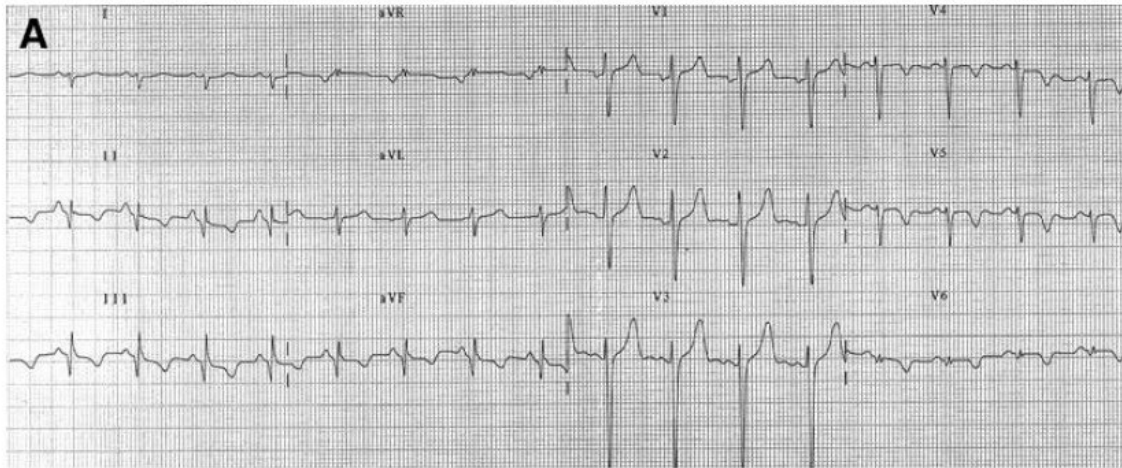
Received 16 June 2015; accepted after revision 7 September 2015





# Nonischemic Left Ventricular Scar as a Substrate of Life-Threatening Ventricular Arrhythmias and Sudden Cardiac Death in Competitive Athletes

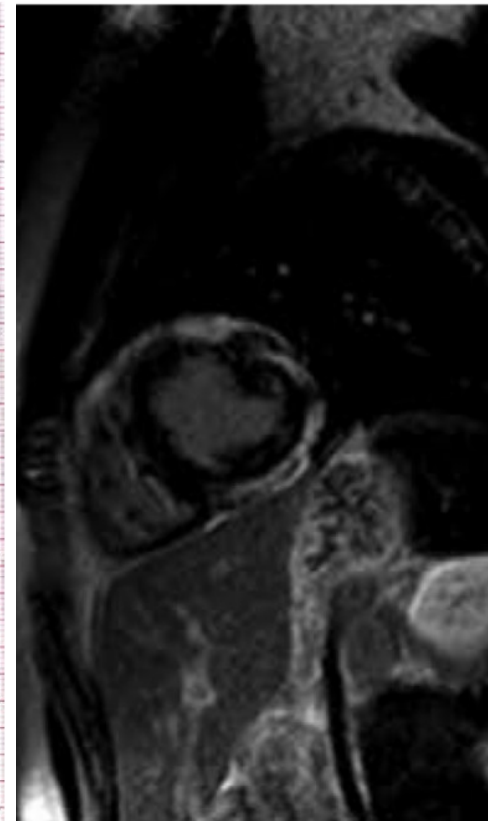
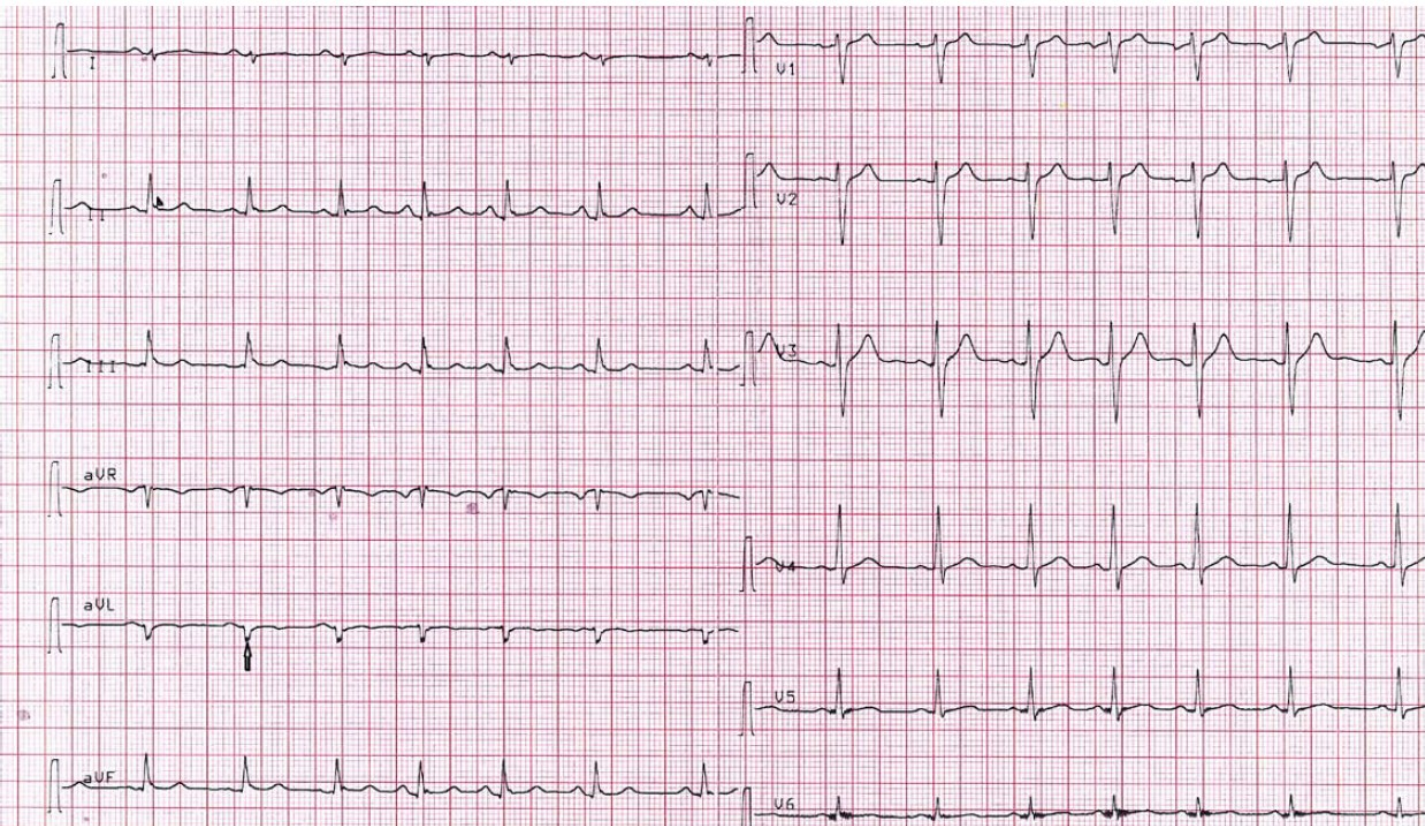
Alessandro Zorzi, MD\*; Martina Perazzolo Marra, MD, PhD\*; Ilaria Rigato, MD, PhD;  
Manuel De Lazzari, MD; Angela Susana, MD; Alice Niero, MD; Kalliopi Pilichou, BS, PhD;  
Federico Migliore, MD, PhD; Stefania Rizzo, MD, PhD; Benedetta Giorgi, MD;  
Giorgio De Conti, MD; Patrizio Sarto, MD; Luis Serratos, MD; Giampiero Patrizi, MD;  
Elia De Maria, MD; Antonio Pelliccia, MD; Cristina Basso, MD, PhD;  
Maurizio Schiavon, MD; Barbara Bauce, MD, PhD; Sabino Iliceto, MD;  
Gaetano Thiene, MD; Domenico Corrado, MD, PhD



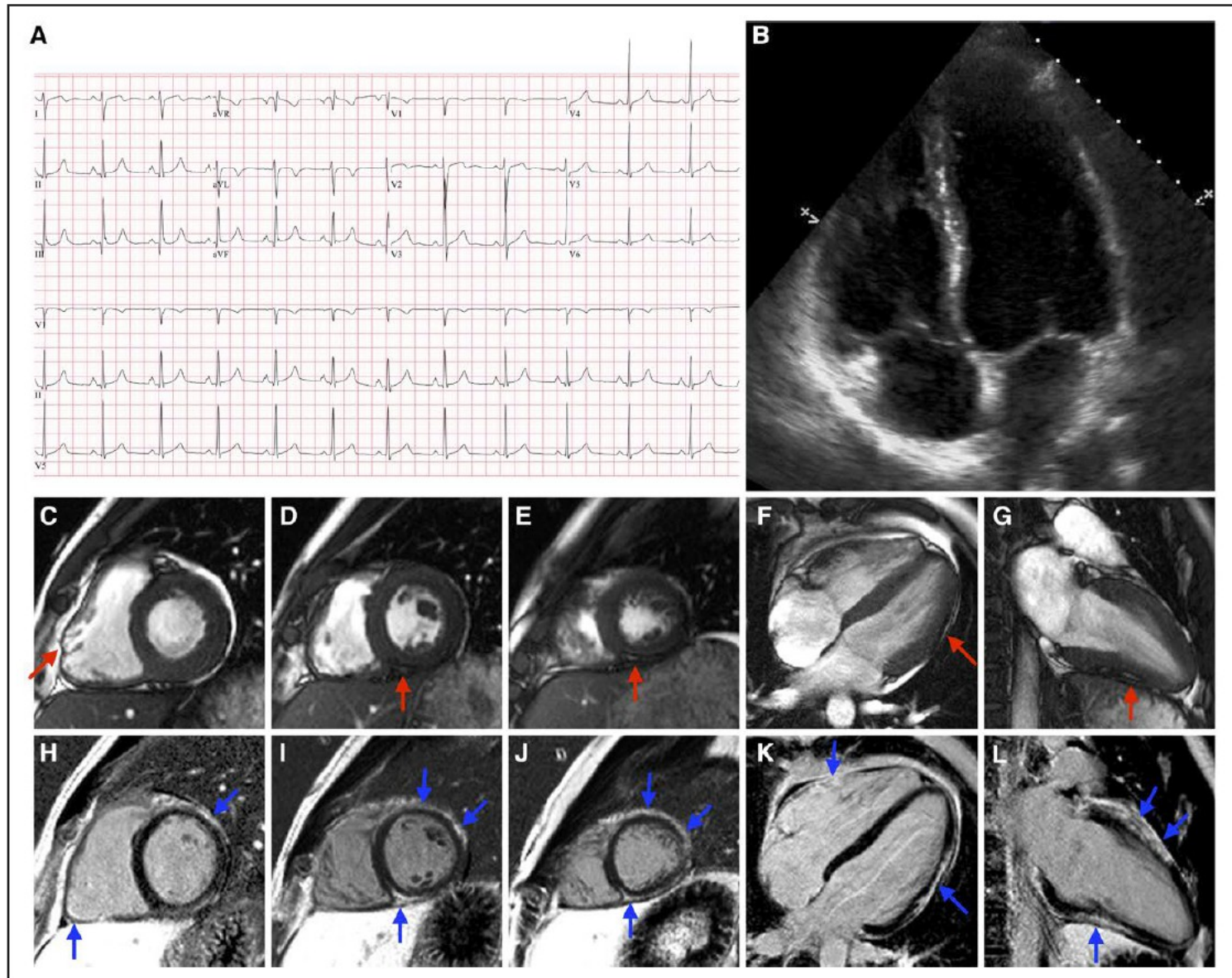


## Arrhythmogenic Left Ventricular Cardiomyopathy Suspected by Cardiac Magnetic Resonance Imaging, Confirmed by Identification of a Novel Plakophilin-2 Variant

Ardan M. Saguner, MD; Beate Buchmann, MD; Daniel Wyler, MD; Robert Manka, MD;  
Alexander Gotschy, MD; Argelia Medeiros-Domingo, MD, PhD; Corinna Brunckhorst, MD;  
Firat Duru, MD; Kurt A. Mayer, MD







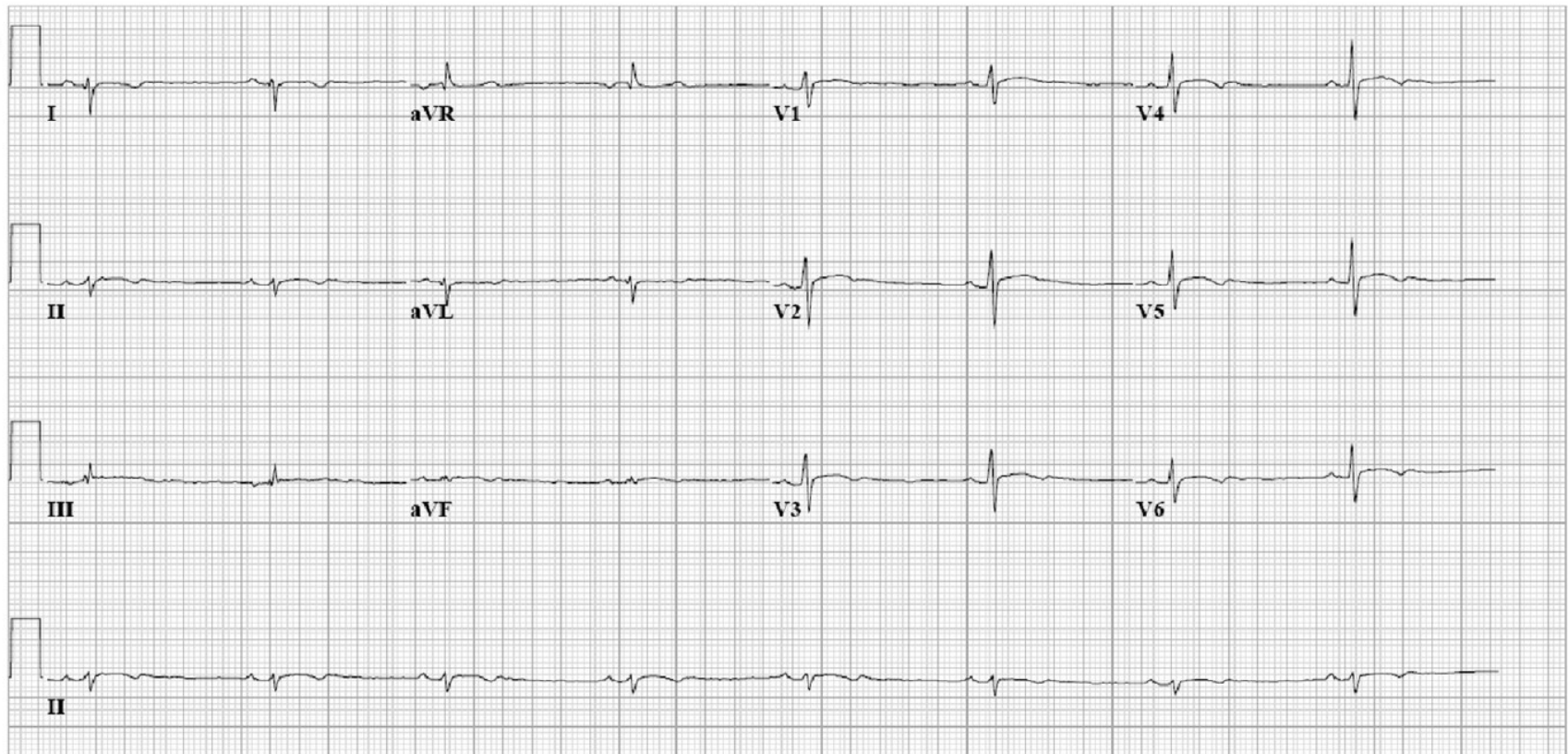


# Late evolution of arrhythmogenic cardiomyopathy in patients with initial presentation as idiopathic ventricular fibrillation

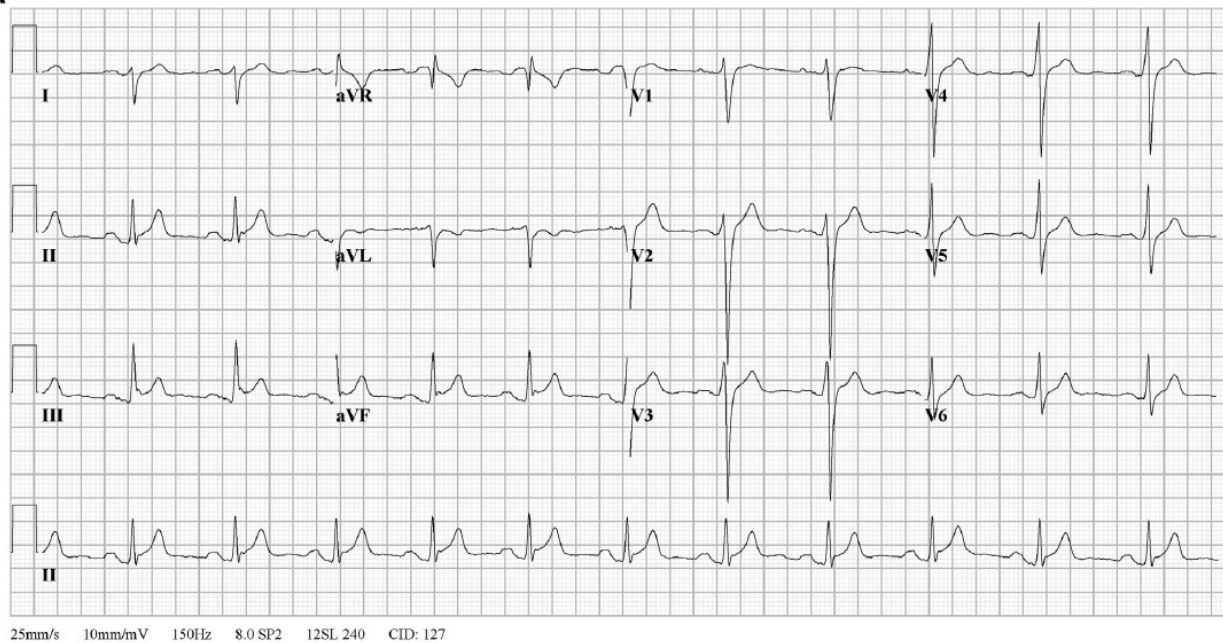
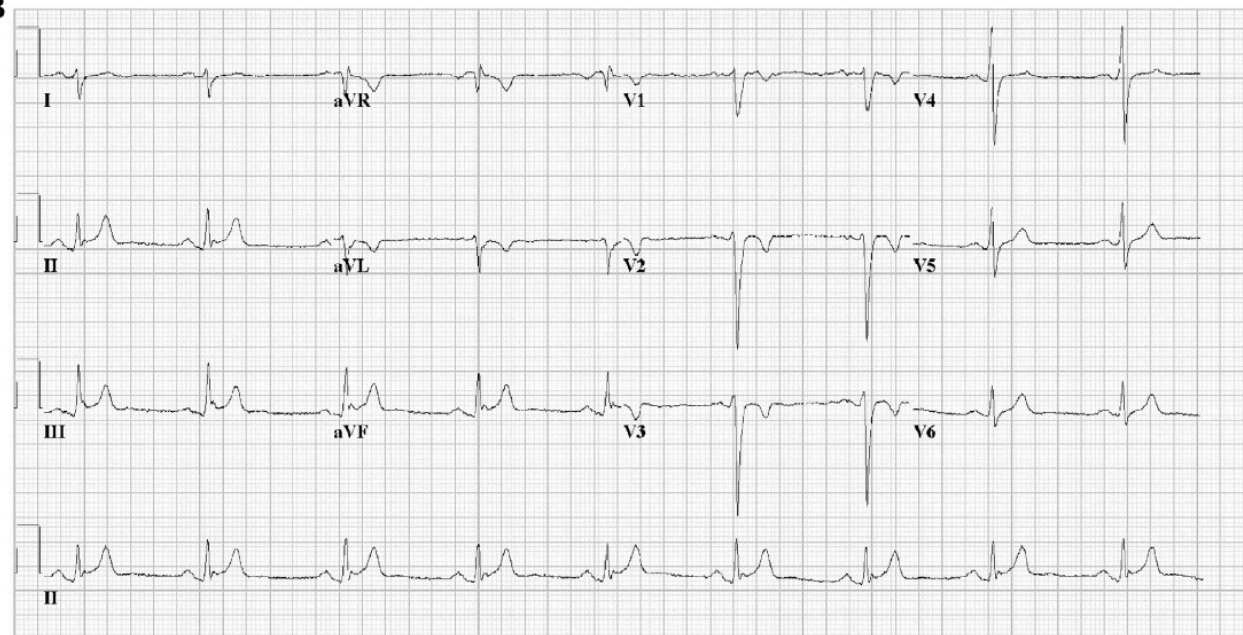


Lennart J. Blom, MD,<sup>\*</sup> Anneline S.J.M. Te Riele, MD, PhD,<sup>\*</sup> Aryan Vink, MD, PhD,<sup>†</sup>  
Richard N.W. Hauer, MD, PhD,<sup>\*</sup> Rutger J. Hassink, MD, PhD<sup>\*</sup>

**A**



25mm/s 10mm/mV 150Hz 8.0 SP2 12SL 240 CID: 127

**A****B**





## CASE REPORT

## ADVANCED

## CLINICAL CASE SERIES

## Acute Myocardial Infarction-Like Events in Related Patients With a Desmoplakin-Associated Arrhythmogenic Cardiomyopathy

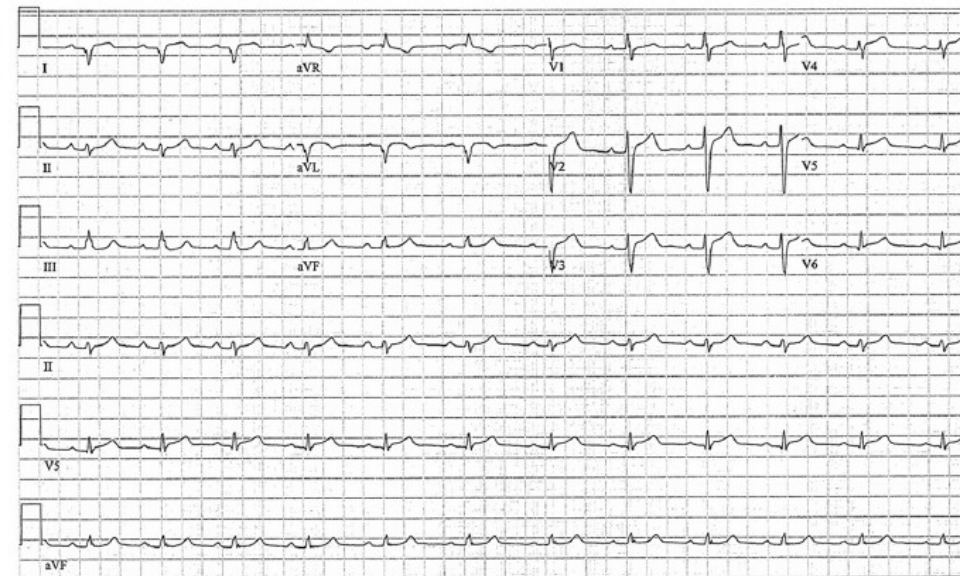
Sajya M. Singh, BS,<sup>a</sup> Scott W. Sharkey, MD,<sup>a</sup> Susan A. Casey, RN,<sup>a</sup> Kevin M. Harris, MD,<sup>a</sup> Christina M. Thaler, MD,<sup>a</sup> Mina Chung, MD,<sup>b</sup> Allison Berg, MS, CGC,<sup>c</sup> Mosi K. Bennett, MD,<sup>a</sup> Emily R. Ducanson, MD,<sup>a</sup> Shannon Mackey-Bojack, MD,<sup>d</sup> Jay D. Sengupta, MD<sup>a</sup>



B

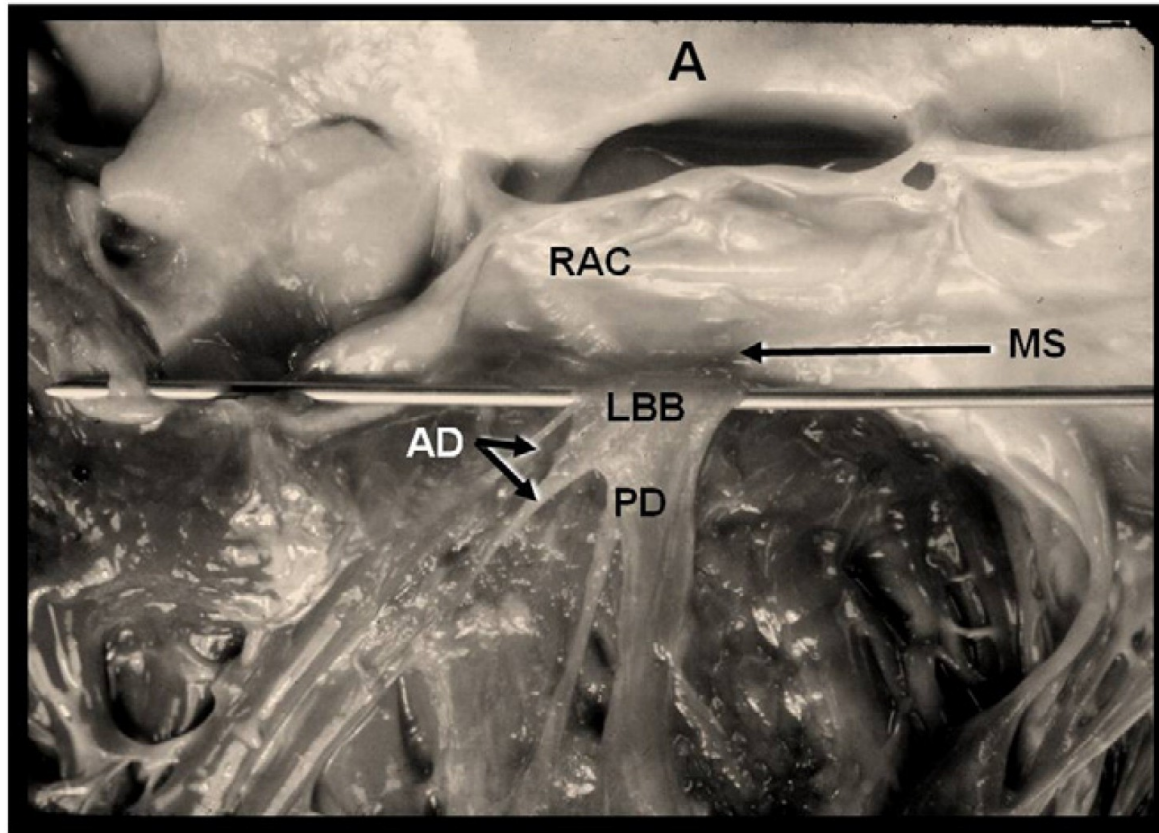


C



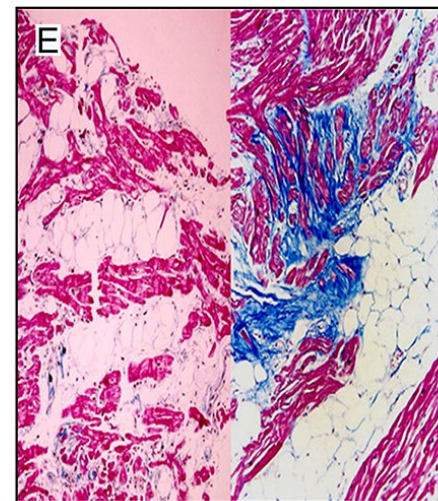
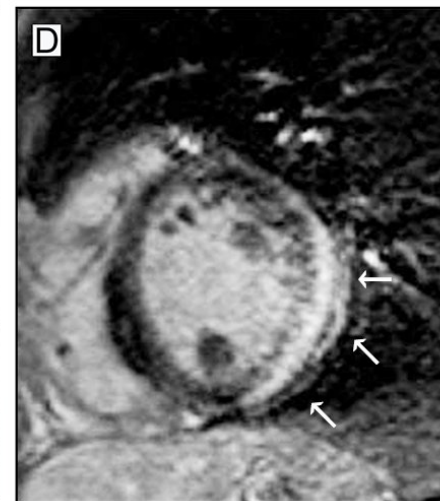
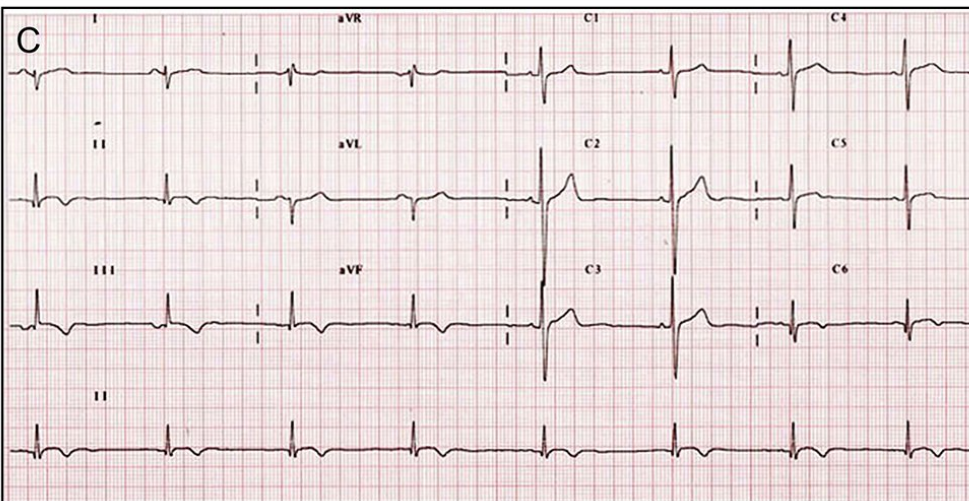
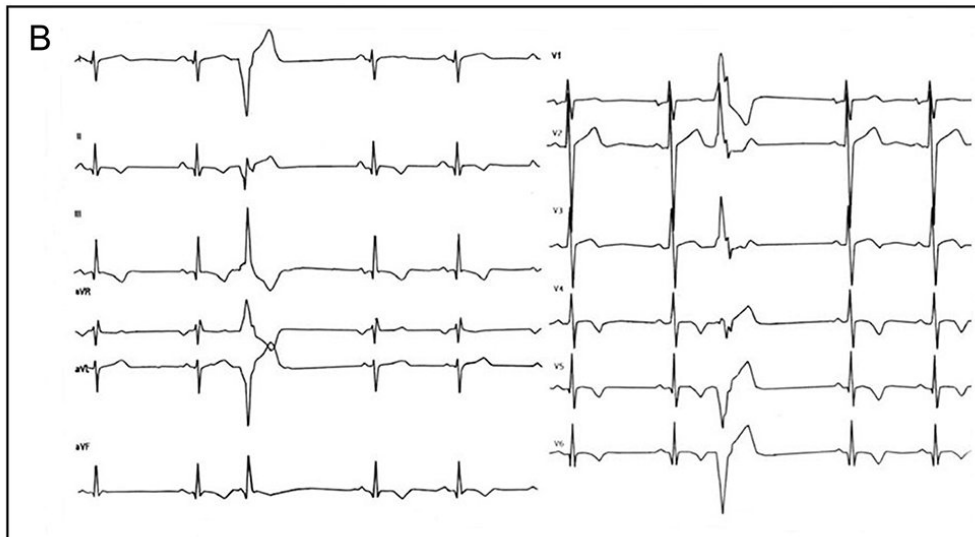
A



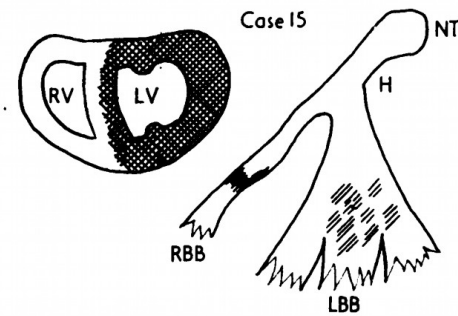
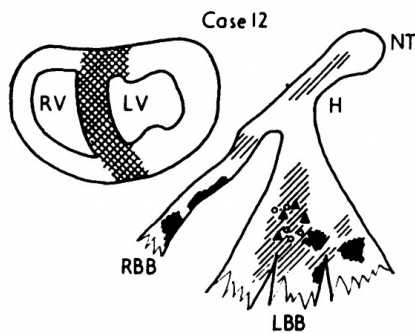
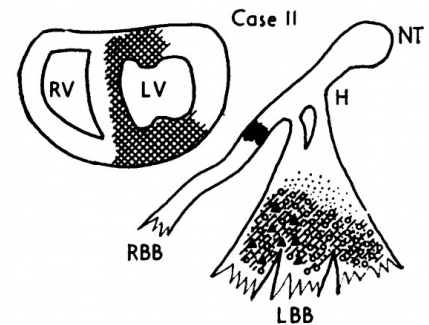
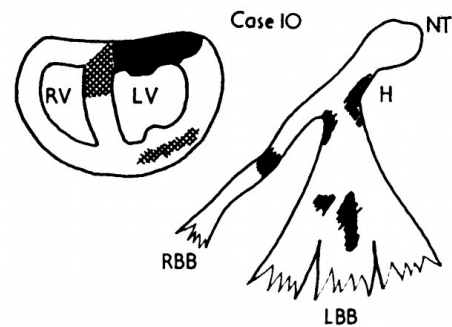
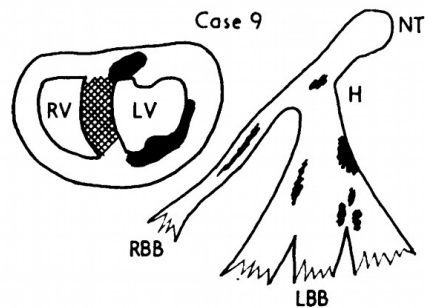
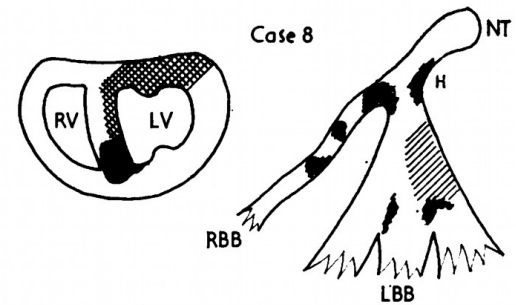
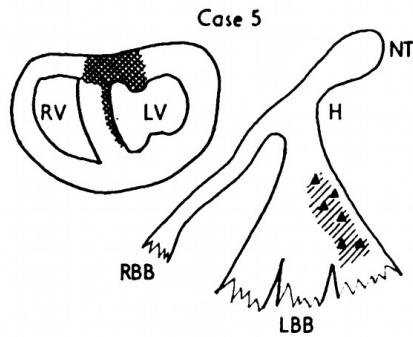
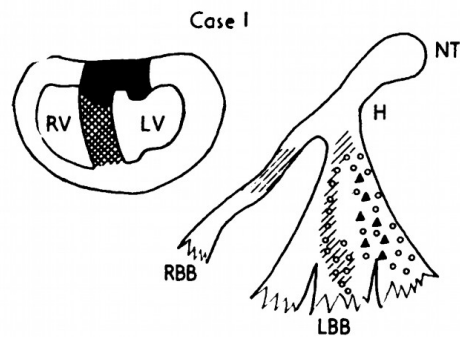


Human heart. The LBB (LBB) emerges in the subaortic region. The membranous septum (MS) is almost absent and the aortic valve lies directly over the LBB, which gives off the anterior division (AD) and posterior division (PD) from its very beginning. The membranous septum is strikingly small or practically absent in this case. The distance between the branching portion of the bundle of His from the aortic valve depends on the size of the MS. The larger the MS, the lesser the possibility that the aortic valve pathology involves this crucial part of the conducting system. A: aorta; RAC right aortic cusp.









Conduction system lesions

Cloudy swelling, vacuolization

Leucocytic infiltration

Haemorrhage

Acute necrosis

Chronic (sclerosis, atrophy)

Myocardial infarction

Acute & subacute stage

Chronic stage

RV=Right ventricle; LV=Left ventricle

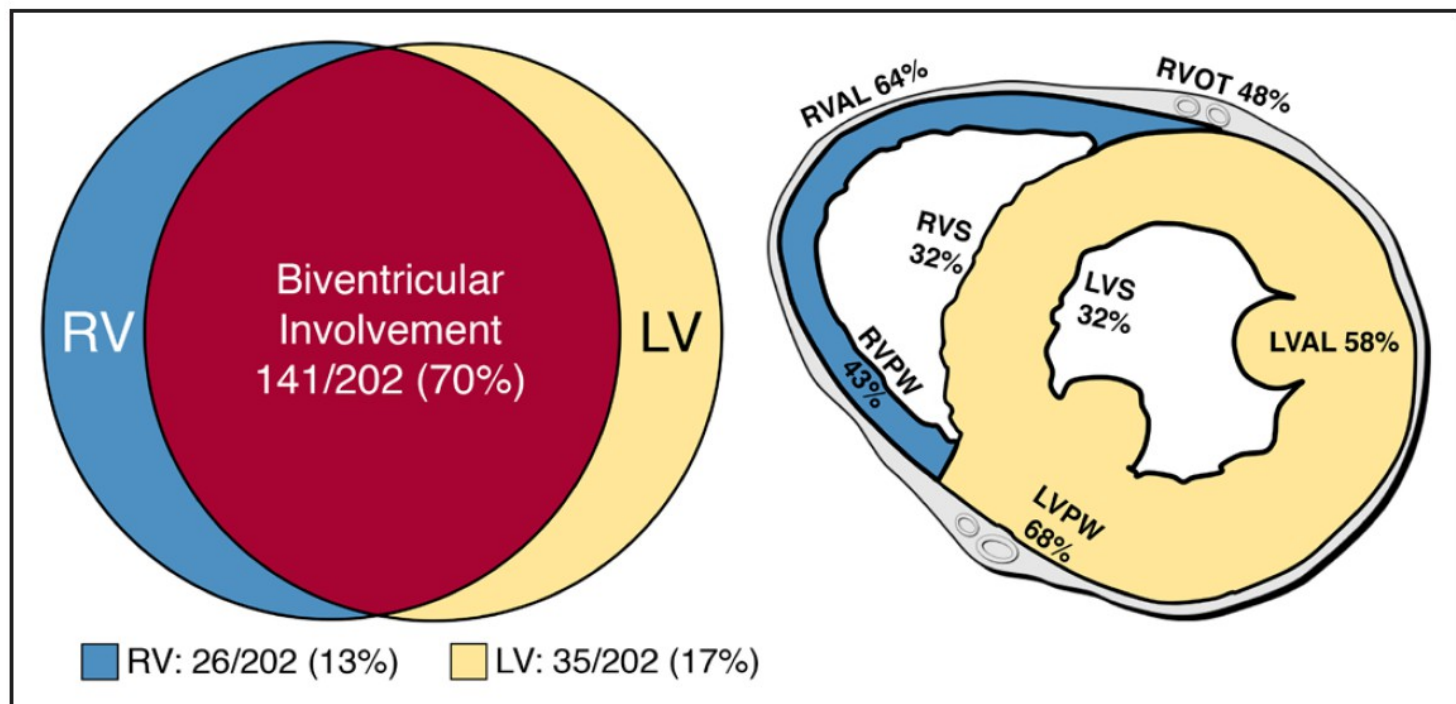
NT: Node of Tawara

H: His bundle

RBB: Right bundle-branch

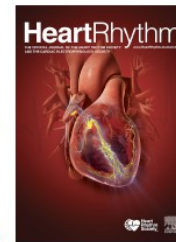
LBB: Left

## Distribution and location of disease involvement in arrhythmogenic cardiomyopathy









Fascicular heart blocks and risk of adverse cardiovascular outcomes: results from a large primary care population.

Benjamin Chris Nyholm, MD, Jonas Ghouse, MD, PhD, Christina Ji-Young Lee, MD, PhD, Peter Vibe Rasmussen, MD, Adrian Pietersen, MD, Steen Møller Hansen, MD, PhD, Christian Torp-Pedersen, MD, DMSci, Lars Køber, MD, DMSci, Stig Haunsø, MD, DMSci, Morten Salling Olesen, MSc, PhD, Jesper Hastrup Svendsen, MD, DMSci, Claus Graff, MSc, PhD, Anders Gaarsdal Holst, MD, PhD, Jonas Bille Nielsen, MD, PhD, Morten Wagner Skov, MD, PhD

PII: S1547-5271(21)02216-5

DOI: <https://doi.org/10.1016/j.hrthm.2021.09.041>

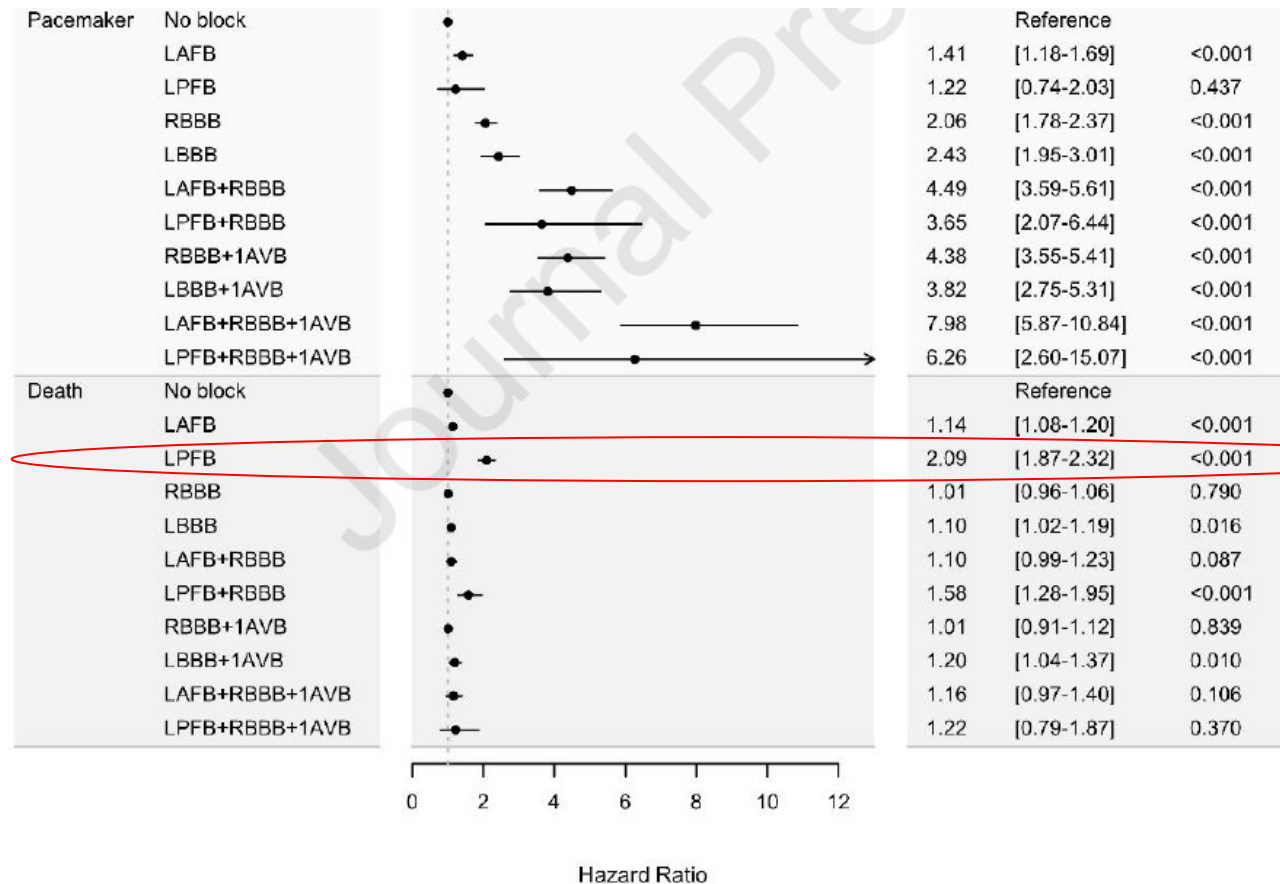


Table 1. Baseline characteristics

Fascicular block subtype n (%)	No conduction defects		LAFB		LPFB		RBBB		LBBB		RBBB + LAFB		RBBB + LPFB		RBBB + 1AVB		LBBB + 1AVB		RBBB + LAFB + 1AVB		RBBB + LPFB + 1AVB	
	345,315	(96.2)	3,526	(0.98)	2,889	(0.80)	3,910	(1.09)	1,390	(0.39)	570	(0.16)	196	(0.05)	643	(0.18)	304	(0.08)	176	(0.05)	32	(0.01)
Age, years, median (IQR)	54	(41-66)	71	(60-80)	35	(26-51)	69	(58-79)	75	(64-82)	76	(68-83)	66	(53 -78)	77	(70-84)	80	(72-86)	79	(70-86)	78	(71-84)
Women, n (%)	190,796	55	1,463	41	1,441	50	1,349	35	949	68	169	30	79	40	158	25	136	45	32	18	6	19
Medical history, n (%)																						
Hypertension	66,316	(19)	1,139	(32)	198	(7)	1,349	(35)	625	(45)	241	(42)	48	(25)	333	(52)	174	(57)	101	(57)	15	(47)
Syncope	9,355	(2.7)	135	(3.8)	83	(2.9)	148	(3.8)	60	(4.3)	26	(4.6)	6	(3.1)	37	(5.8)	13	(4.3)	16	(9.1)	<4	(<12.5)*
Atrial fibrillation	5,041	(1.5)	134	(3.8)	38	(1.3)	121	(3.1)	66	(4.8)	20	(3.5)	9	(4.6)	35	(5.4)	27	(8.9)	12	(6.8)	5	(15.6)
Valvular heart disease	1,442	(0.4)	46	(1.3)	10	(0.4)	50	(1.3)	25	(1.8)	12	(2.1)	<4	(<2)*	15	(2.3)	12	(4.0)	<4	(<3)	<4	(<12.5)*
Beta blocker therapy	52,809	(15.3)	736	(20.9)	242	(8.4)	845	(21.6)	408	(29.4)	132	(23.2)	31	(15.8)	193	(30.2)	111	(36.5)	58	(33.0)	11	(34.4)
Charlson Comorbidity Index																						
0 points	265,361	(77)	2,078	(59)	2,413	(84)	2,429	(62)	802	(58)	296	(52)	124	(63)	319	(50)	144	(47)	71	(40)	14	(44)
1 point	41,598	(12)	648	(18)	271	(9)	632	(16)	237	(17)	109	(19)	31	(16)	121	(19)	66	(22)	34	(19)	8	(25)
≥ 2 points	38,356	(11)	800	(23)	205	(7)	849	(22)	351	(25)	165	(29)	41	(21)	203	(31)	94	(31)	71	(40)	10	(31)
ECG variables																						
QRS duration, median (IQR)	92	(84-100)	102	(96-110)	96	(88-104)	136	(128-146)	146	(136-156)	144	(136-154)	140	(130-148)	144	(134-152)	154	(144-164)	151	(142-160)	150	(134-159)
PR interval, median (IQR)	156	(144-172)	168	(152-186)	154	(140-170)	162	(148-178)	168	(154 -180)	170	(156-184)	162	(146-178)	220	(208-242)	218	(208-238)	228	(211-251)	221	(207-242)
Heart rate (IQR)	69	(62-79)	72	(63-82)	71	(62-82)	70	(62-80)	73	(65-83)	71	(64-80)	74	(66-84)	68	(60-78)	70	(62-80)	69	(60-77)	76	(68-86)

TABLE 1: LAFB = left anterior fascicular block; LPFB = left posterior fascicular block; LBBB = left bundle branch block; RBBB = right bundle branch block; 1AVB = first degree atrioventricular block;

\*Due to the Act on Processing of Personal Data, we are not allowed to report any number less than four observations.



## From Argentina to Denmark—The wine is still good

Reginald T. Ho, MD, FHRS

*From the Division of Cardiology, Department of Medicine, Thomas Jefferson University Hospital, Philadelphia, Pennsylvania.*

In 1968, Dr Mauricio Rosenbaum published a book dedicated entirely to the intraventricular conduction system.<sup>1</sup> In this classic monograph and its subsequent English version, he coined the term “hemiblock” and introduced the concept of a trifascicular conduction system after analyzing electrocardiograms from a 58-year-old man who had suffered an anterior myocardial infarction and demonstrated right bundle branch block (RBBB) with alternating left anterior fascicular block (LAFB) and left posterior fascicular block (LPFB) (now called Rosenbaum’s syndrome).<sup>2</sup> He referred to the conduction system as a “detector” of the heart, showing the association between various conduction blocks and heart disease (commonly coronary artery disease and Chagas cardiomyopathy in his home country of Argentina). He described the unequal “anatomic vulnerability” of the bundle branches (right more than left; left anterior more than posterior) and the relative “immunity” of the left posterior fascicle because of its thick structure and dual blood supply (indicating that the presence of LPFB generally signified more severe heart disease). His book was followed by a flurry of studies in the mid-1970s and early 1980s evaluating the value of His-ventricular intervals in predicting impending atrioventricular block (AVB) in patients with bifascicular block—research that today remain the foundation for our current pacemaker guidelines.<sup>3</sup> Since then, however, research on the natural history of fascicular block and its progression to AVB has been relatively quiet.

In this issue of *Heart Rhythm Journal*, Nyholm et al<sup>4</sup> breathe new life into the study of fascicular blocks by providing the largest population-based study on its natural progression to AVB. Among 358,958 primary care patients in a large Danish registry (Copenhagen ECG Study), the authors studied 13,636 patients with fascicular block (3.8%) and compared them with a reference group of patients without block. Not surprisingly, RBBB and isolated LAFB were most common. With the longest follow-up approaching 16 years, they found that syncope, pacemaker implantation, and third AVB increased with increasing complexity of

fascicular block. Depending on gender and age, the 10-year absolute risk of developing third-degree AVB increased from 0% to 2% (hazard ratio [HR] 1.60) for isolated LAFB to 23% (HR 10.98) for multicomination block (first-degree AVB + RBBB + LAFB). While this dose-response relationship between worsening fascicular block and AVB is not unexpected, their data provide clearer granularity about the long-term risk of developing AVB among 10 different block subtypes. True bilateral BBB (eg, alternating BBB and Rosenbaum’s syndrome) was not represented. However, this subtype is already an established high-risk group carrying a class I indication for pacemaker implantation. While a higher burden of comorbidity occurred with increasing block complexity, LAFB was not associated with worse mortality. This has been observed in another study from the same group but not by others.<sup>5–7</sup> Curiously, isolated LPFB was associated with the youngest age group (median age 35 years) and the highest risk of death (HR 2.09). A recent case-control study of 10 young patients (median age 27.5 years) with LPFB and aborted cardiac arrest/sudden cardiac death found left ventricular fibrosis (particularly along the inferolateral wall) in all patients undergoing cardiac magnetic resonance imaging (n = 6) or histopathological analysis/autopsy (n = 4).<sup>8</sup> Further investigation is required into this small but worrisome group of young patients.

In the preface to his book, Dr Rosenbaum wrote “Like good wines, some research improves after resting for a while.” By allowing many years for their registry to mature, Nyholm et al have produced an excellent bottle of wine for a slowly aging cellar.

### References

1. Rosenbaum MB, Elizari MV, Lazzari JO. *Los Hemibloques*. Buenos Aires, Argentina: Editorial Paidós; 1968.
2. Rosenbaum MB, Elizari MV, Lazzari JO. The Hemiblocks: New Concepts of Intraventricular Conduction Based on Human Anatomical, Physiological and Clinical Studies. Oklawaha, FL: Tampa Tracing; 1970.
3. Kusumoto FM, Schoenfeld MH, Barrett C, et al. 2018 ACC/AHA/HRS guideline on the evaluation and management of patients with bradycardia and cardiac conduction delay: executive summary. *J Am Coll Cardiol* 2019;74:932–987.
4. Nyholm BC, Ghouse J, Lee CJ, et al. Fascicular heart blocks and risk of adverse cardiovascular outcomes: results from a large primary care population. *Heart Rhythm* 2021;XX:XX–XX.
5. Nielsen JB, Strandberg SE, Pietsen A, et al. Left anterior fascicular block and the risk of cardiovascular outcomes. *JAMA Int Med* 2014;174:1001–1003.
6. Mandyam M, Soliman EZ, Heckbert S, et al. Long-term outcomes of left anterior fascicular block in the absence of overt cardiovascular disease. *JAMA* 2013; 309:1587–1588.

but not by others.<sup>5–7</sup> Curiously, isolated LPFB was associated with the youngest age group (median age 35 years) and the highest risk of death (HR 2.09). A recent case-control study of 10 young patients (median age 27.5 years) with LPFB and aborted cardiac arrest/sudden cardiac death found left ventricular fibrosis (particularly along the inferolateral wall) in all patients undergoing cardiac magnetic resonance imaging (n = 6) or histopathological analysis/autopsy (n = 4).<sup>8</sup> Further investigation is required into this small but worrisome group of young patients.





# Left-Dominant Arrhythmogenic Cardiomyopathy With Heterozygous Mutations in *DSP* and *MYBPC3*

Sakamoto N. et al. Circ Cardiovasc Imaging. 2019;12:e008913

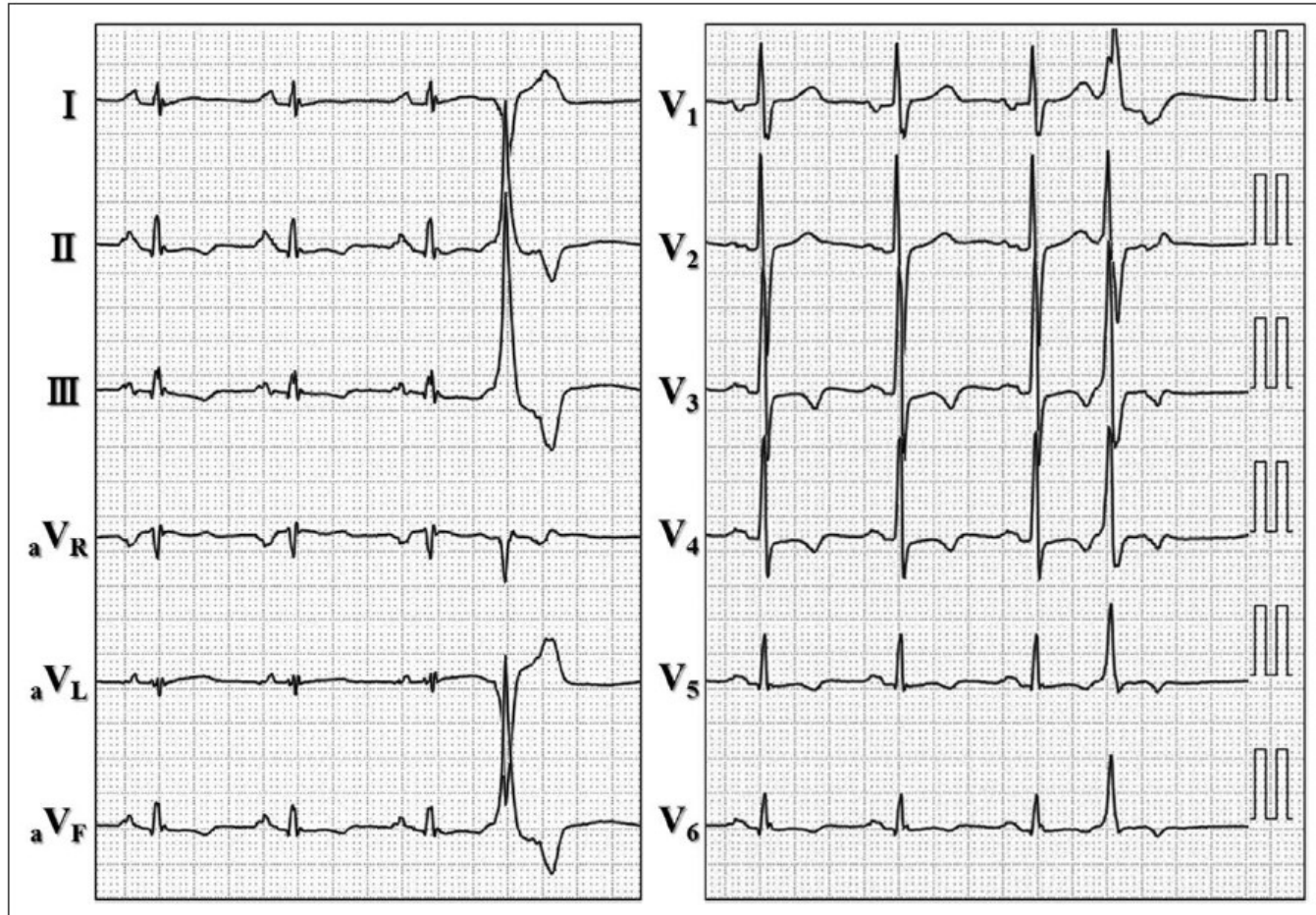


**Figure 1.** ECG showing T-wave inversion in the left-sided leads and a premature ventricular complex of left ventricular origin.

Pathogenic mutations in desmoplakin (c.4650delTG, p.V1551E fs74X) and myosin-binding protein C gene (c.2459G>A, p.R820Q)

## LETTER TO THE EDITOR

# Letter by Pérez-Riera et al Regarding Article, "Left-Dominant Arrhythmogenic Cardiomyopathy With Heterozygous Mutations in *DSP* and *MYBPC3*"

*To the Editor:*

We have read with interest the recent exceptional case report from Dr Sakamoto et al<sup>1</sup> who presented a 46-year-old woman whose main complaint was dyspnea on exertion and in whom the final diagnosis was left-dominant arrhythmogenic cardiomyopathy (ALVC). Genetic screening showed a mutation not reported previously consisting of heterozygous pathogenic mutation in the desmoplakin and myosin-binding protein C.

In their description of the 12-lead ECG, the authors wrote literally: "T-wave inversion in the left-sided leads and a premature ventricular complex of left ventricular origin." We would like to add some additional ECG features of Figure 1,

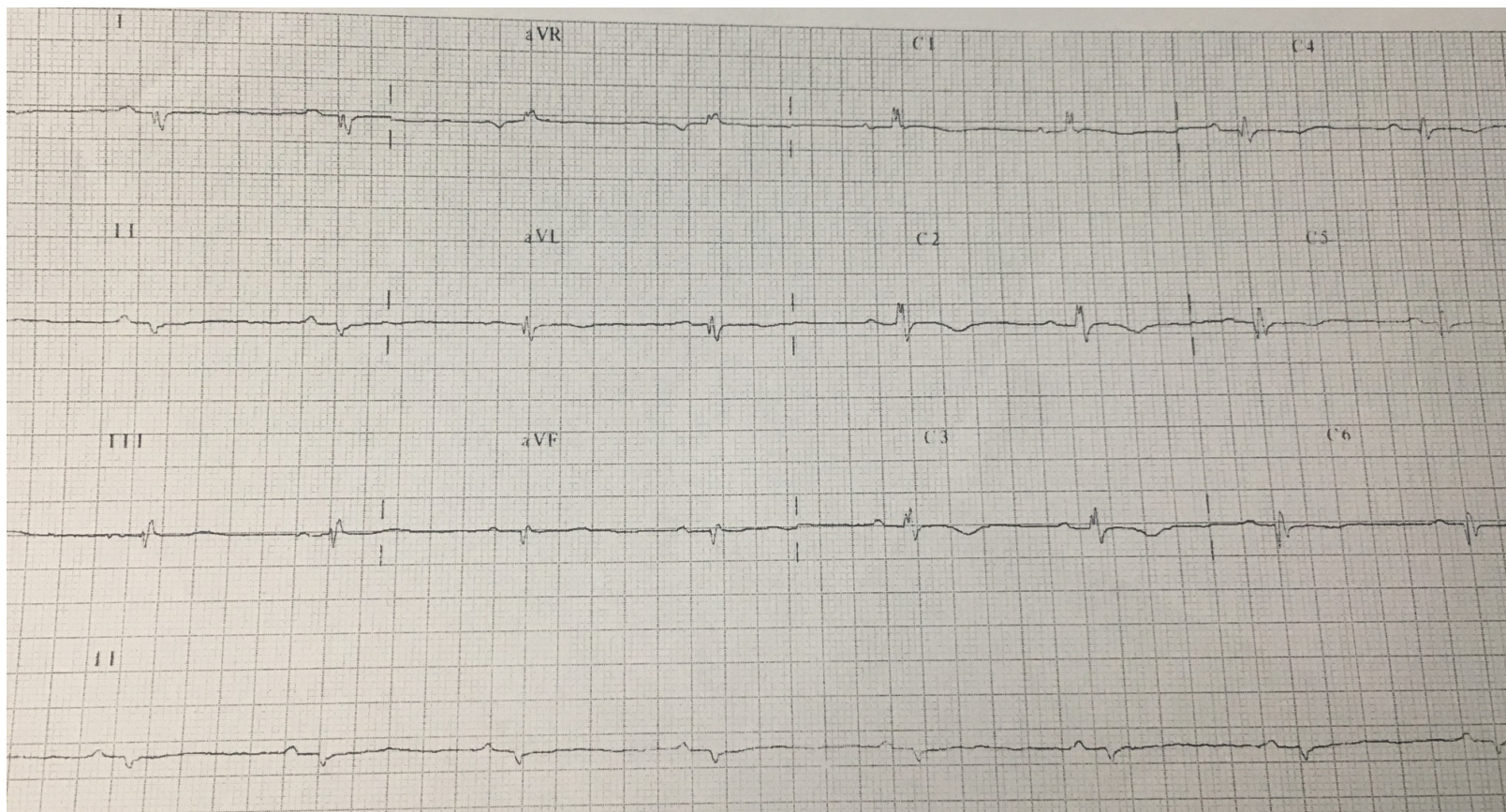
Andrés Ricardo  
Pérez-Riera, MD, PhD  
Raimundo Barbosa-Barros,  
MD  
Bernard Belhassen, MD

Finally, early precordial transition was observed in the precordial leads (R/S ratio >1 in V1-V2).

Such prominent anterior QRS forces can be observed in numerous scenarios: normal variant, athlete's heart, misplaced precordial leads, lateral myocardial infarction (previously named dorsal myocardial infarction), right ventricular hypertrophy, left ventricular hypertrophy, biventricular hypertrophy, right bundle branch block, **left septal fascicular block**, ventricular preexcitation with accessory pathway located in the posterior wall, hypertrophic cardiomyopathy, Duchenne's cardiomyopathy, endomyocardial fibrosis, dextroposition, and ALVC.

In the latter case, **early precordial transition indicates fibrosis in the basal-lateral wall of the LV.**





# The tetrafascicular nature of the intraventricular conduction system

Andrés R. Pérez-Riera<sup>1</sup>  | Raimundo Barbosa-Barros<sup>2</sup> | Rodrigo Daminello-Raimundo<sup>1</sup> | Luiz C. de Abreu<sup>1</sup> | Kjell Nikus<sup>3</sup>

<sup>1</sup>Design of Studies and Scientific Writing Laboratory, ABC Faculty of Medicine, São Paulo, Brazil

<sup>2</sup>Coronary Center of the Hospital de Messejana Dr. Carlos Alberto Studart Gomes, Fortaleza, Brazil

<sup>3</sup>Heart Center, Tampere University Hospital and Faculty of Medicine and Life Sciences, University of Tampere, Tampere, Finland

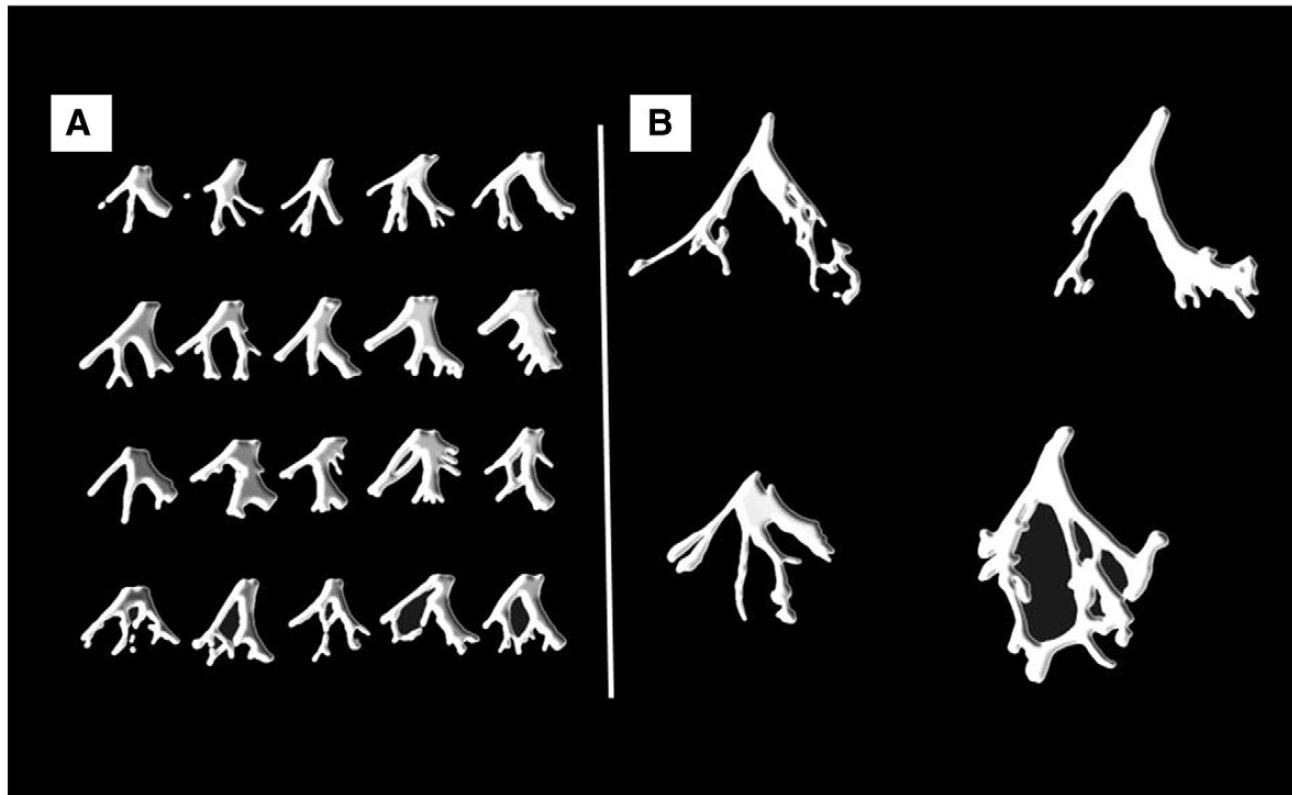
### Correspondence

Andrés Ricardo Pérez-Riera, Rua Sebastião Afonso, 885 Zip code: 04417-100 Jardim Miriam, São Paulo-SP, Brazil.  
Email: riera@uol.com.br

The existence of a tetrafascicular intraventricular conduction system remains debatable. A consensus statement ended up with some discrepancies and, despite agreeing on the possible existence of an anatomical left septal fascicle, the electrocardiographic and vectorcardiographic characteristics of left septal fascicular block (LSFB) were not universally accepted. The most important criteria requested to confirm the existence of LSFB is its intermittent nature. So far, our group has published cases of transient ischemia-induced LSFB and phase 4 or bradycardia-dependent LSFB. Finally, anatomical, anatomopathological, histological, histopathological, electrocardiographic, vectorcardiographic, body surface potential mapping, and electrophysiology studies support the fact that the left bundle branch divides into three fascicles or a “fan-like interconnected network.”

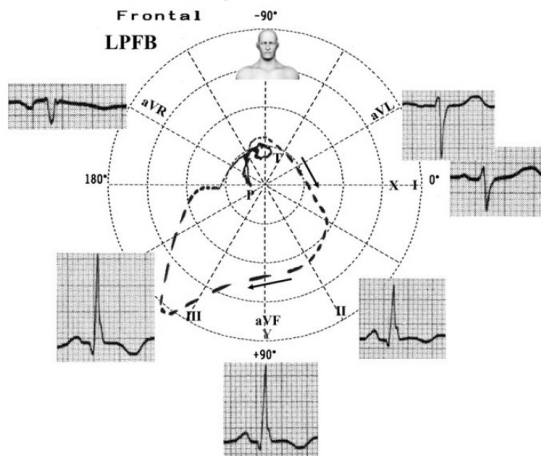
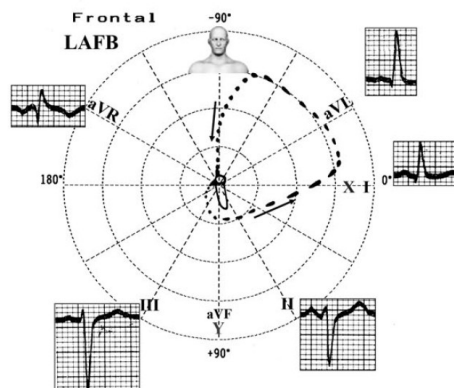
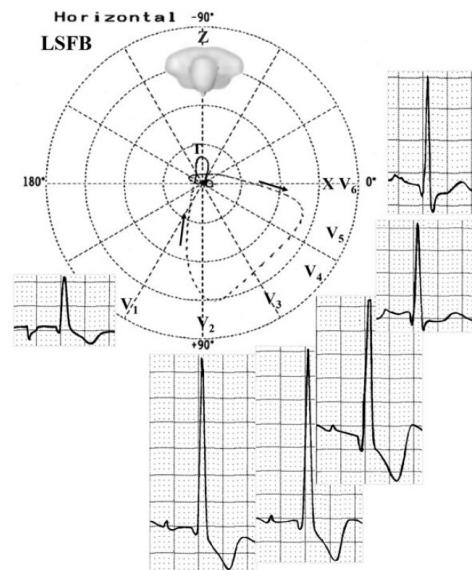
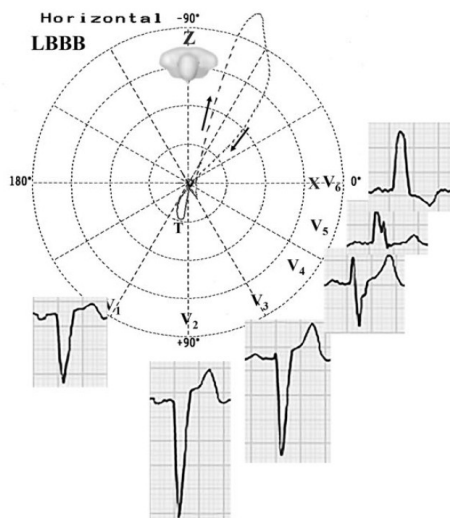
### KEYWORDS

intraventricular conduction system, left septal fascicle, left septal fascicular block



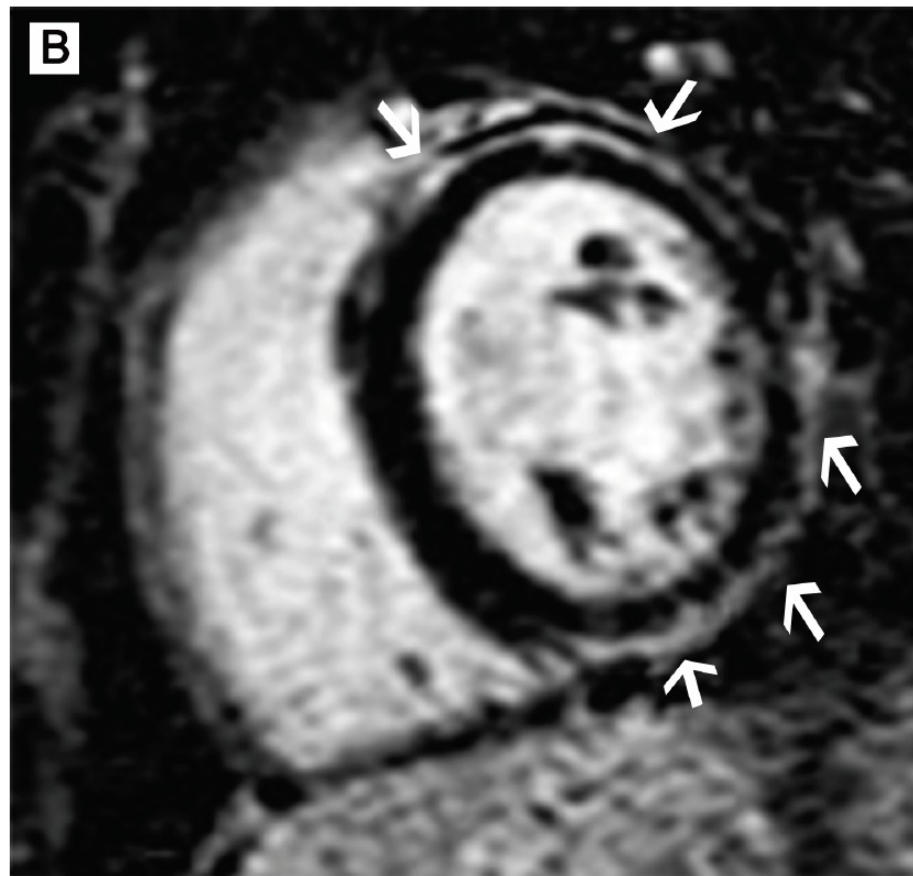
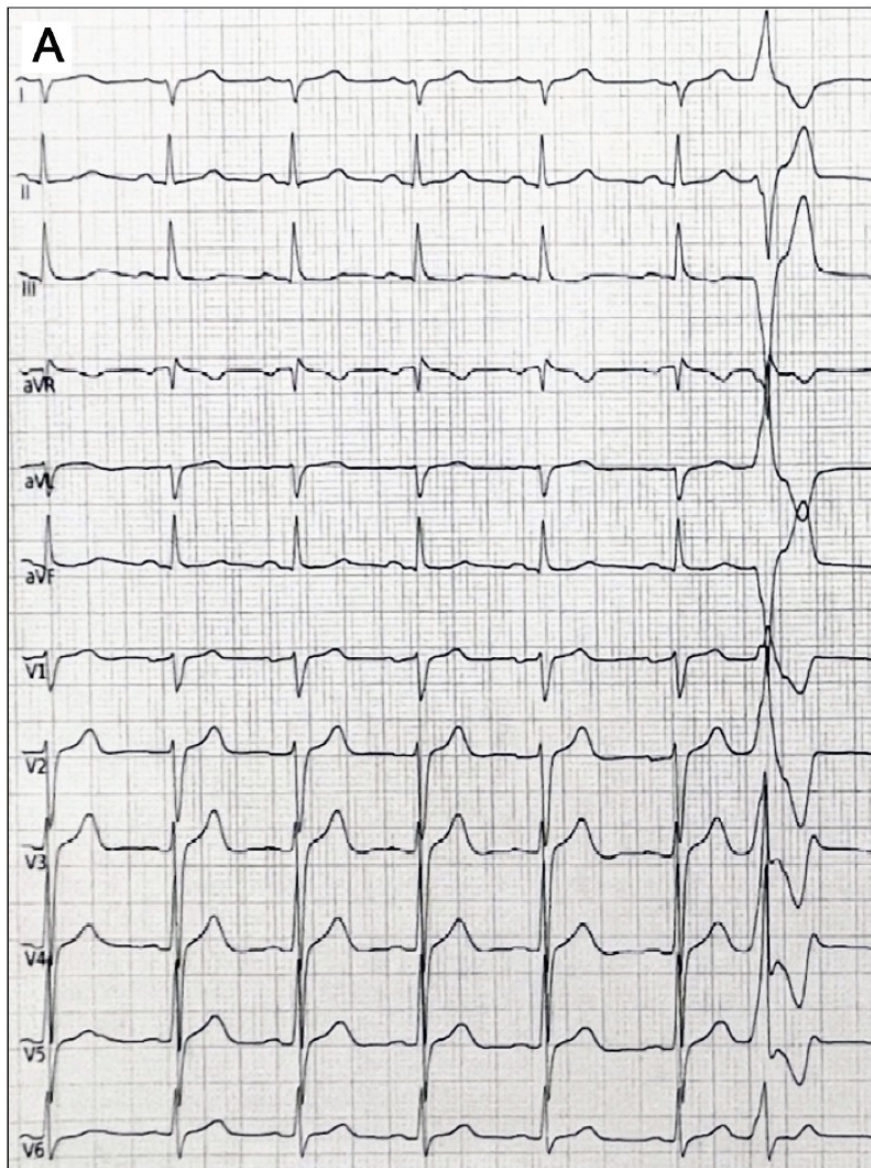
A. [Fig. 2](#) from Demoulin JC, Kulbertus HE [\[24\]](#). Diagrammatic sketches of the LBB conduction system in twenty human normal hearts. These sketches depict the anatomy from serial histologic sections of left septal myocardium. The LBB and its subdivisions were identified by their subendocardial location and histological features typical of the conducting fibers. B: Figure 28, Chapter 2 from RosenbaumMB et al. [\[13\]](#). Four human LBB systems dissected and separated from the heart considered the main prototypes observed in our material. In every case, the main LBB is short and its divisions longer depicting a wider posterior division as compared with the anterior one. The bottom left LBB shows what can be considered a medial left septal fascicle arising at the bifurcation of the LBB, although it actually emerges from a wide posterior division, a pattern that can also be observed in the examples of [Fig. 14 A](#) in most cases.







*Festina lente*



Patient #2, 19-year-old man, pathogenic variant in desmoplakin (c.1707-1708insAC,p.Met571Glnfs\*8)